Charles University in Prague

Faculty of Science

PhD programme: Developmental and Cell Biology

Veronika Tomková

Molekulární mechanismy rezistence k tamoxifenu u rakoviny prsu

Molecular mechanisms of tamoxifen resistance in breast cancer

Ph.D. Thesis

Supervisor: Mgr. Jaroslav Truksa, Ph.D

Consultant: MSc. Cristian Sandoval-Acuña, Ph.D

Laboratory of Tumour Resistance

Institute of Biotechnolgy CAS, v.v.i

Prague, 2020

Prohlášení

Prohlašuji, že jsem závěrečnou práci zpracovala samostatně a že jsem uvedla všechny použité informační zdroje a literaturu. Tato práce ani její podstatná část nebyla předložena k získání jiného nebo stejného akademického titulu.

Praha, březen 2020 Veronika Tomková

Acknowledgement

Here, I would like to thank to my supervisor Mgr. Jaroslav Truksa, Ph.D. for his valuable advices, support and very human attidude and guidance over the years I have spent in his laboratory.

I would also like to thank to all former as well as present members of the Laboratory of Tumor Resistance. Working in such friendly and supportive environment made my PhD much easier.

Special thanks belongs to my friends Piri and Nati, who genuinely supplied me not only with food and place to sleep when it was necessary, but also with unlimited optimism and encouragement in times when I felt down.

Importantly, none of this would be possible without the love and enourmous support of my parents, who never stopped believing in me.

Contents

Abstract

The resistance to tamoxifen, a drug used in the adjuvant therapy for hormone sensitive breast cancer, represents a major clinical obstacle. Although various mechanisms leading to tamoxifen resistance have been described and intensively studied, a significant number of patients still become resistant to the treatment and eventually relapse.

Tamoxifen therapy has been shown to enrich tumors with cancer stem cells (CSCs), which are naturally resistant, and have self-renewal ability and the potential to form secondary tumors. Metabolic rewiring, altered iron metabolism and upregulation of ATP-binding cassette (ABC) transporters have been shown to be important in the maintenance of CSC phenotype. Therefore, we investigated these mechanisms as possible contributors to tamoxifen resistance *in vitro* in two tamoxifen resistant (Tam5R) cell lines that we established.

We show that Tam5R cells have dramatically disassembled and less active mitochondrial supercomplexes (SCs) and higher level of mitochondrial superoxide, together with a fragmented mitochondrial network. Such dysfunction of mitochondria results in the AMP-activated protein kinase (AMPK) activation and metabolic rewiring towards glycolysis. Importantly, cells lacking functional mitochondria are significantly more resistant to tamoxifen, supporting a role of mitochondria in tamoxifen resistance.

Further, our analysis revealed significant changes in proteins participating in iron uptake, storage, export and iron sensing as well as in iron-sulfur (Fe-S) cluster assembly and hypoxia response in Tam5R cells. In addition, less incorporation of ^{55}Fe into Fe-containing mitochondrial proteins was detected. Therefore, we propose that altered iron trafficking and utilization in Tam5R cells may be linked with the resistant phenotype.

Finally, the expression profile of ABC transporters, well described contributors to multidrug resistance, was altered in Tam5R cells, with similar change in protein level of ABCC5, ABCG1 and ABCF2 in both cell lines, thereby suggesting their possible role in tamoxifen resistance.

Key words: breast cancer, tamoxifen resistance, mitochondria, iron metabolism, ABC transporters

Abstrakt

Rezistence k tamoxifenu, léčivu používaném v adjuvantní terapii při hormonální léčbě rakoviny prsu, představuje závažný klinický problém. Přestože byly popsány a intenzivně studovány různé mechanismy vedoucí k rezistenci k tamoxifenu, u značného počtu pacientů se objeví rezistence na terapii a následná recidiva.

Ukázalo se, že léčba tamoxifenem obohacuje nádory o nádorové buňky podobné kmenovým bunkám, které jsou přirozeně rezistentní a mají schopnost sebeobnovy a potenciál vytvářet sekundární nádory. Metabolická plasticita, změněný metabolismus železa a zvýšená exprese ABC transportérů jsou další factory důležité při udržování fenotypu rakovinných kmenových buněk. Z tohoto důvodu jsme zkoumali výše uvedené mechanismy v dvou *in vitro* modelech tamoxifen rezistentních buněčných linii (Tam5R), které jsme zavedli.

Ukazujeme, že Tam5R buňky mají dramaticky rozložené a méně aktivní mitochondriální superkomplexy a vyšší hladinu mitochondriálního superoxidu spolu s fragmentovanou mitochondriální sítí. Taková dysfunkce mitochondrií vede k aktivaci AMPK signální dráhy a metabolickému posunu směrem ke glykolýze. Navíc buňky bez funkčních mitochondrií (ρ0 buňky) jsou signifikantně více rezistentní k tamoxifenu, což podporuje úlohu mitochondrií v rezistenci k tamoxifenu.

Naše analýza odhalila signifikantní změny u Tam5R v proteinech účastnících se příjmu železa, jeho skladovaní, exportu, regulaci jeho vnitrobuněčné hladiny a dále proteinů podílejících se na skládání železo-sirných (Fe-S) klastrů a odpovědi buněk na hypoxii. Kromě toho jsme detekovali méně zabudovaného ^{55}Fe do mitochondriálních proteinů obsahujících železo. Naše data tak ukazují, že změny v metabolismu železa a jeho utilizaci by mohly být spojeny s rezistentním fenotypem.

Dále jsme popsali změny v expresním profilu ABC transportérů, proteinů přispívajících k mnohočetné lékové rezistenci. Popsali jsme identické změny na úrovni proteinu u ABCC5, ABCG1 a ABCF2 v obou rezistentních líniích, což ukazuje na jejich možnou roli v rezistenci k tamoxifenu.

Klíčová slova: rakovina prsu, rezistence k tamoxifenu, mitochondrie, metabolismus železa, ABC transportéry

Abbreviations

2-DG	2-deoxyglucose
2-NBDG	2-(N-(7-Nitrobenz-2-oxa-1,3-diazol-4-yl)Amino)-2-deoxyglucose
3-BrOP	3-bromo-2-oxopropionate-1-propyl ester
4-OH tamoxifen	4-hydroxytamoxifen
AAs	amino acids
ABC transporters	ATP-binding cassette transporters
Acetyl-CoA	acetyl coenzyme A
ACO1	aconitase 1 (cytosolic)
ACO2	aconitase 2 (mitochondrial)
ACS2	acetyl-CoA synthetase
ALA	aminolevulinic acid
ALDH1	aldehyde dehydrogenase 1
AMPK	AMP-activated protein kinase
AV/PI	annexin V/ propidium iodide
BCA	bicinchoninic acid
BCRP	breast cancer resistance protein
BCSC	breast cancer stem cell/breast cancer stem-like cell
BNE	blue native electrophoresis
BSA	bovine serum albumin
CCCP	carbonyl cyanide m-chlorophenyl hydrazone
CDH2	cadherin 2
CFTR	cystic fibrosis transmembrane conductance regulator
CI-CV	mitochondrial respiratory complex I - complex V
CSC	cancer stem cell/cancer stem-like cell
Ctrl	control
CXCR4	C-X-C chemokine receptor 4
CYBRD1	cytochrome b reductase 1
CYP	cytochrome P450
DCF-DA	2′,7′-dichlorofluorescein diacetate
DCYTB	duodenal cytochrome B
D-loop	displacement loop
DMEM	Dulbecco's Modified Eagle Medium

DMT1	divalent metal transporter 1
DRP1	dynamin- related protein 1
EGFR	epidermal growth factor receptor
EMT	epithelial-mesenchymal transition
EPAS1	gene coding for endothelial PAS domain-containing protein 1
ER	estrogen receptor
ERE	estrogen response element
ETC	electron transport chain
$FADH_2$	flavin adenine dinucleotide (reduced)
FBS	fetal bovine serum
FBXL5	F-Box and Leucine Rich Repeat Protein 5
Fe^{2+}	ferrous iron
Fe^{3+}	ferric iron
Fe-S clusters	iron-sulfur clusters
FPN	ferroportin
FtMt	mitochondrial ferritin
FXN	frataxin
GLRX5	glutaredoxin 5
GLUT-1	glucose transporter 1
GPER1	G-protein coupled estrogen receptor 1
GPX1	glutathione peroxidase 1
GSH	glutathione
GSSG	glutathione disulfide
HEPH	hephaestin
HER2	human epidermal growth factor receptor 2
HFE	hemochromatosis protein
HIF	hypoxia inducible factor
HKII	hexokinase 2
hr-CNE	high resolution clear native electrophoresis
HRE	hypoxia responsive element
Hsp90	heat shock protein 90
i.p	intraperitoneal
IDH2	isocitrate dehydrogenase 2

IRE	iron responsive element
IRP1	iron responsive protein 1
IRP2	iron responsive protein 2
ISCU	iron-sulfur cluster assembly enzyme
LDH-A	lactate dehydrogenase A
LDH-B	lactate dehydrogenase B
LIP	labile iron pool
LYRM4	LYR motif-containing protein 4
MDR	multidrug resistance
MFRN1	mitoferrin 1
MFRN2	mitoferrin 2
miRNA	microRNA
MRP	multidrug resistance protein
mtDNA	mitochondrial DNA
NADH	nicotinamide adenine dinucleotide (reduced)
NADPH	nicotinamide adenine dinucleotide phosphate
NBD	nucleotide binding domain
NFS1	nitrogen fixation 1 (*S. cerevisiae* homolog)
NRF2	nuclear respiratory factor 2
NTBI	non-transferrin bound iron
OCR	oxygen consumption rate
OPA1	optic atrophy 1
OXPHOS	oxidative phosphorylation
PAF	platelet activating factor
PCBP1	poly(rC)-binding protein 1
PCBP2	poly(rC)-binding protein 2
PDK1	pyruvate dehydrogenase kinase 1
PFK2	phosphofructokinase 2
PR	progesterone receptor
QSOX1	quiescin sulfhydryl oxidase 1
RFU	relative fluorescent unit
RIPA	radioimmunoprecipitation assay buffer
ROS	reactive oxygen species
RT	reverse transcription

S1P	sphingosine-1-phosphate
SC	supercomplex (mitochondrial)
SIRT3	sirtuin 3
SLC11A2	gene coding for solute carrier family 11 member 2 (DMT1)
SLC25A37	gene coding for solute carrier family 25 member 37 (MFRN1)
SLC39A14	gene coding for solute carrier family 39 member 14 (ZIP14)
SLC40A1	gene coding for solute carrier family 40 member 1 (FPN)
SOD2	superoxide dismutase 2
SOX2	SRY-box transcription factor 2
STEAP3	six transmembrane epithelial antigen of the prostate 3
SUR1	sulfonylurea receptor 1
SUR2	sulfonylurea receptor 2
Tam5R	tamoxifen resistant
TCA cycle	tricarboxylic acid cycle
Tf	transferrin
TfR1	transferrin receptor 1
TMD	transmembrane domain
TOM20	mitochondrial import receptor subunit TOM20 homolog
UTR	untranslated region
VDAC1	voltage-dependent anion-selective channel protein 1
WCL	whole cell lysate
ZIP14	zinc transporter 14

Introduction

Cancer represents the second leading cause of death globally, responsible for an estimated 9.6 million deaths in 2018 [1]. Female breast cancer is the most commonly diagnosed cancer worldwide with high incidence (24.2% of all new cases in women) and mortality rates (15%) [1]. Despite the progress in development of new screening and treatment strategies, some patients do not respond to the therapy, or some initially respond but develop resistance and relapse [2].

Emerging evidence suggests that the existence of cancer stem cells (CSCs) within the tumor may represent one of the factors limiting successful treatment [3]. CSCs form a subpopulation of cells with self-renewal capacity, undifferentiated phenotype and the propensity to drive tumor growth *de novo*. Their slow-proliferating rate makes them naturally chemo- and radio-resistant, since cancer therapies are mainly targeted to rapidly proliferating cells [4]. Another characteristic of CSCs is a high iron storage and increased labile iron pool (LIP) as a result of altered iron trafficking and reduced iron utilization [5, 6]. Similarly, overexpression of ATP-binding cassette (ABC) transporters which are able to export various types of drugs has been documented in CSCs, contributing to their resistant phenotype [7]. Moreover, the importance and role of metabolic alterations in the maintenance of the CSC phenotype is becoming appreciated [8]. Indeed, CSCs show increased metabolic plasticity that helps them respond to changing tumor microenvironment and ensure their survival [9].

The main goal of the present work was to analyze the mechanisms that may contribute to the tamoxifen resistant phenotype. The thesis is divided in four parts, each consisting of a short introduction relevant to the presented topic, results and discussion. The first part introduces tamoxifen resistant (Tam5R) breast cancer cell lines as an experimental model for studying the phenomenon of tamoxifen resistance. The second chapter discusses the role of mitochondria together with metabolic and bioenergetic changes in Tam5R breast cancer cells as possible contributors to drug resistance. The results presented in this chapter are published in my first author paper in *Free Radical Biology & Medicine*. The third part analyzes the alterations in iron metabolism and iron utilization in Tam5R cells and links these data with the resistant phenotype. Some of my results were included as a supplementary data in my *Oncotarget* co-author paper. The final part describes the gene expression profile of ABC transporters in Tam5R cells, together with the assessment of protein level of selected ABC transporters, and proposes their possible role in tamoxifen resistance (unpublished data).

Aims

The main aim of this project was to elucidate the possible roles of mitochondria, iron metabolism and ABC transporters in tamoxifen resistance.

Specific aims

1) Establishing MCF7 and T47D cell lines resistant to 5 μM tamoxifen (MCF7 Tam5R and T47D Tam5R) and evaluation of their resistance as well as cancer stem-like properties

2) Analysis of various aspects of mitochondrial function in Tam5R cells:

- Determination of the amount, assembly and enzymatic activity of mitochondrial SCs
- Assessment of the mitochondrial mass
- Analysis of the mitochondrial network
- Analysis of the mitochondrial and cellular redox systems
- Metabolic analysis (glycolytic status, respiration)
- Assessment of the tamoxifen resistance in the model of mitochondrial DNA (mtDNA) deficient MCF7 ρ0 cells

3) Determination of the iron metabolism in Tam5R cells

- Expression profiling of iron metabolism related genes and determination of the protein level of selected candidate genes
- Assessment of hypoxia-related genes in Tam5R cells
- Measurement of ^{55}Fe level and incorporation into proteins in WCL, and cytosolic and mitochondrial fractions

4) Assessment of gene expression and protein level of ABC transporters in Tam5R cells

Materials and Methods

Cell culture

Human breast cancer cell lines MCF7 (ATCC® HTB-22™) and T47D (ATCC® HTB-133™) were purchased from ATCC (Manassas, VA, USA). Both control (Ctrl) and tamoxifen resistant (Tam5R) cell lines were maintained in Dulbecco's Modified Eagle Medium (DMEM) supplemented with 10% fetal bovine serum (FBS), 2mM L-glutamine and antibiotics (streptomycin 100µg/ml; penicillin 100U/ml). In addition, Tam5R cell lines were cultivated in the presence of 5 µM tamoxifen (Sigma-Aldrich).

MCF7 ρ0 cells were prepared by long term cultivation with ethidium bromide [10]. Once established, they were cultured as Ctrl cells with the addition of 1 mM pyruvate and 50 µg/mL uridine.

Assessment of the number of viable cells

The evaluation of the effect of tamoxifen on the number of viable Ctrl and Tam5R cells was performed by crystal violet staining. Briefly, 1×10^4 cells were seeded in 96 well plates and let to attach overnight. Tamoxifen was added in increasing concentrations (1-25 µM) and cells were incubated for additional 48 hours. Afterwards, cells were fixed with 4% paraformaldehyde, washed with PBS and stained overnight with crystal violet (0.05% in water). Finally, cells were washed with PBS and crystals solubilized with 1% SDS. Absorbance was recorded at 595 nm by using a Tecan Infinity M200 microplate reader. IC_{50} values for each condition were calculated by interpolating in a dose-response curve, using the GraphPad Prism 6.0 software and a nonlinear regression of log [tamoxifen] vs. normalized response with variable slope.

Flow cytometry

Flow cytometry was performed *via* BD LSRFortessa™ flow cytometer (BD Biosciences). Each measurement contained at least 10,000 events and data were analyzed by Kaluza software.

Cell death assessment

Double staining by annexin V/propidium iodide (AV/PI staining) was used to assess the cell death after incubation of cells with increasing concentrations of tamoxifen (5-15 µM) for 48 hours. After collecting the cells, fluorescence was detected by flow

cytometry at $488nm_{Ex}/530nm_{Em}$ for AV and $561nm_{Ex}/610nm_{Em}$ for PI. Results are shown as % of dead cells (sum of AV^+/PI^-, AV^-/PI^+ and AV^+/PI^+ cells).

Mitochondrial mass measurement

Total mitochondrial mass was assessed by immunostaining with an antibody against outer mitochondrial import receptor subunit TOM20 homolog (TOM20; sc-17764, Santa Cruz Biotechnology). After fixation with 4% paraformaldehyde, cells were permeabilized with saponin and washed with PBS. Next, cells were incubated with TOM20 antibody (1:500) for 1 hour followed by incubation with the secondary antibody Alexa Fluor™ 488 (A-11001, ThermoFisher scientific; 1:500) for 1 hour. The cells were collected and fluorescence was detected by flow cytometry at $488nm_{Ex}/530nm_{Em}$.

Mitochondrial superoxide and cellular ROS determination

For the detection of the mitochondrial superoxide level we used the MitoSOX™ probe (ThermoFisher Scientific). For the determination of cellular reactive oxygen species (ROS), 2',7'-dichlorofluorescein diacetate (DCF-DA; Sigma-Aldrich) was used. Cells were incubated for 20 min with 2.5 μM MitoSOX or 5 μM DCF-DA, collected and the fluorescence was detected by flow cytometry at $488nm_{Ex}/585nm_{Em}$ and $488nm_{Ex}/530nm_{Em}$, respectively.

Glucose uptake

Glucose uptake was measured by using the 2-NBDG (2-(N-(7-Nitrobenz-2-oxa-1,3-diazol-4-yl)Amino)-2-Deoxyglucose) probe (ThermoFisher Scientific). Cells were seeded in regular DMEM medium. The next day, the medium was replaced by glucose free/phenol red free medium and cells were incubated for another 24 hours. Then, 50 μM of 2-NBDG probe was added for additional 20 min. Finally, cells were collected and fluorescence was measured by flow cytometry at $488nm_{Ex}/530nm_{Em.}$

Oxygen consumption

Oxygen consumption rate (OCR) was measured by a Seahorse Extracellular Flux (XFe96) analyzer (Agilent Technologies). In order to prevent detachment of cells during washing and measurement, culture plates were pre-coated with Poly-L-lysine. Cell seeding densities were optimized to 20,000/well for each cell line (MCF7 and T47D). The whole experiment including media supplement concentrations and washing procedures

followed the instructions from the manufacturer. The day after seeding, cells were washed with XF assay media and incubated with the same media supplemented with 10 mM glucose, 1 mM pyruvate and 2 mM L-glutamine for 1 hour in a non-CO_2 incubator. The injection protocol used was: port A: 1 µM oligomycin, port B: 0.5 µM carbonyl cyanide m-chlorophenyl hydrazone (CCCP) and port C: 1 µM rotenone and 1.8 µM antimycin A. The last injection (port D) was with Hoechst 33342 (2µg/ml; Sigma-Aldrich) in PBS in order to assess the total cell number for normalization. For this purpose, the ImageXpress Micro XLS analysis system (Molecular Devices) was utilized (available in BIOCEV core facility).

ATP measurement

Total cellular ATP was measured using the CellTiter-Glo® Luminescent Cell Viability Assay kit (Promega) and the protocol followed manufacturer's instructions. One day after seeding, cells were incubated for 4 hours with either 25 mM or 50 mM 2-deoxyglucose (2-DG, Cayman Chemicals) or normal media prior to the ATP measurement. ATP values were normalized to total protein content measured by the bicinchoninic acid (BCA) method (ThermoFisher Scientific).

Lactate production

Extracellular lactate was measured directly from the media by using the Lactate Kit (Trinity Biotech). The culture media and Lactate Standard were pipetted in triplicate in a 96 well plate. The amount of pipetted media was optimized to 5 µl in order to get a detectable signal. After the addition of Lactate Reagent (100 µl) and 10 min incubation, absorbance at 540 nm was measured by Tecan M200 infinity multiplate reader. All values were normalized to total protein content determined by the BCA method.

Animal studies

Athymic nude mice Crl:NU(NCr)-Foxn1^{nu}(Charles River) were implanted with a slow-release estradiol pellet (60-day release of 12 µg per day; Innovative Research of America). After 3 days, mice were divided in two groups and injected subcutaneously with 2×10^6 MCF7 Ctrl or Tam5R cells, respectively. When tumors reached the volume of 30–50 mm^3, each group was further divided into two subgroups and treated intraperitoneally (i.p.) with either tamoxifen (30 mg/kg weight) or vehicle (2.5% DMSO in corn oil, 100 µl per dose) twice per week for 2 weeks. Tumor volume was monitored

by the USI instrument Vevo770 (VisualSonics). All mice experiments were approved by the Czech Academy of Sciences and performed according to the Czech Republic Council guidelines for the Care and Use of Animals in Research and Teaching.

Preparation of mitochondrial lysates and blue native electrophoresis

Mitochondrial lysates were prepared by homogenization of cells with a Potter homogenizator in STE buffer (250 mM sucrose, 10 mM Tris, 1 mM EDTA) followed by differential centrifugation [11]. First, nuclei and cell debris were removed by centrifugation at 600 × g for 15 min, then supernatant was further centrifuged at 10,000 × g for 20 min in order to obtain a mitochondrial pellet. Isolated mitochondria were solubilized with digitonin for 45 min on ice (10 g of digitonin per 1 g of protein) and centrifuged at 20,000 × g for 40 min. The concentration of solubilized mitochondrial fraction was measured by the BCA method. 25 μg of mitochondrial proteins were loaded on Bis-Tris 3-12% NativePAGE™ gels (ThermoFisher Scientific). Blue native electropohresis (BNE) was used to determine the level and composition of mitochondrial respiratory complexes and ran at the following program: 25 V overnight followed by immunoblotting on PVDF membranes at 30 V for 2 hrs. Proper loading was determined by SDS-PAGE followed by immunoblotting against voltage-dependent anion-selective channel protein 1 (VDAC1). The list of used antibodies is shown in Supplementary Table 1.

In gel activity of mitochondrial complexes

For assessment of the activity of mitochondrial respiratory complexes, high resolution clear native electrophoresis (hr-CNE) was used as described in [11]. 25 μg of solubilized mitochondria were separated in Bis-Tris NativePAGE™ gels. Gels were then incubated in appropriate complex assay buffers [11] and scanned. Proper loading was determined by SDS-PAGE followed by immunoblotting against VDAC1.

Whole cell lysate preparation, SDS-PAGE and western blot

Whole cell lysates (WCL) were prepared by resuspending the collected cell pellets in radioimmunoprecipitation assay buffer (RIPA) or cell lysis buffer (20 mM Tris-HCl pH 7.5, 150 mM NaCl, 1 mM EDTA, 1 mM EGTA, 1 % Triton-X100) supplemented with protease and phosphatase inhibitors. Protein concentration was determined by the BCA method. 50 μg of the cell lysate was loaded in SDS-PAGE gel and separated at

constant voltage (100 V), followed by blotting on nitrocellulose or PVDF membrane at constant 35 V for 2 h (or 20 V overnight for ABC transporters) using a Mini blot module (ThermoFisher Scientific). Membranes were then stained with 0.05% Ponceau S solution, scanned, washed three times with TBS/Tween 20 and blocked with 5 % non-fat milk for 1 h. After blocking, membranes were again washed three times with TBS/Tween 20 and incubated with corresponding antibodies in 5 % bovine serum albumin (BSA) overnight (Supplementary Table 1). The next day, membranes were washed three times with TBS/Tween 20 and incubated with corresponding secondary antibody (Supplementary Table 1) in 1% milk for 1 h. After washing the membranes three times with TBS/Tween 20, proteins were visualized by using chemiluminiscent substrates WesternBright™ Sirius (Advansta) or Clarity™ (BioRad) and chemiluminiscence was detected by the camera Azure c600 (Azure Biosystems).

Aconitase in gel activity

The activity of aconitase was assessed in gel as described in [12]. Briefly, collected cells were lysed in buffer containing 20 mM Tris-HCl, 137 mM NaCl, 1% Triton-X100, 10% glycerol, 2 mM citrate and protease inhibitors. Protein samples (70 µg) were separated at 180 V in 8% Tris-Borate gels supplemented with 3.6 mM citrate at 4 °C. Then, gels were incubated for 2 h at 37 °C with 100 mM Tris (pH 8.0), 2.5 mM cis-aconitic acid, 5 mM $MgCl_2$, 1 mM $NADP^+$, 0.3 mM phenazine methosulfate, 1.2 mM MTT and 5 U/ml isocitric dehydrogenase, protected from light. Gels were scanned and proper loading was determined by SDS-PAGE followed by western blot and immunodetection against β-actin.

Mitochondrial to nuclear DNA ratio measurement

Mitochondrial and nuclear DNA were isolated by resuspending approximately 2×10^6 cells in DNAzol® (Molecular Research Center) according to the manufacturer's instructions. For qPCR, we used 5x HOT FIREPol® EvaGreen® qPCR Supermix (Solis BioDyne). 5 ng of total DNA per reaction were used as template. Primer sequences designed for the analysis were: for mtDNA, *MTRT1 forward: CACCCAAGAACAGGGTTTGT; MTRT1 reverse: TGGCCATGGGTATGTTGTTA*; for nuclear DNA: human gDNA ValidPrime™ assay was purchased from TATAA Biocenter. Fold changes were calculated by $2^{-\Delta\Delta Ct}$ method relative to MCF7 Ctrl. The analysis was performed *via* the GenEx software version 6.

RNA isolation and reverse transcription (RT)

Total RNA was isolated using RNAzol RT (Molecular Research Center) according to manufacturer's instructions. RNA quantity was measured with the Nanodrop spectrophotometer (ThermoFisher Scientific). Integrity of each RNA sample was assessed with the Agilent 2100 Bionalyser (Agilent Technologies). cDNA for Fluidigm qPCR was reverse-transcribed by the Maxima H minus reverse transcriptase kit (ThermoFisher Scientific) according to manufacturer's instructions. cDNA for standard qPCR was reverse-transcribed by RevertAid RT Reverse Transcription Kit (ThermoFisher Scientific) using oligodT.

Fluidigm qPCR

The Fluidigm qPCR experimental setup is described in [6]. All primers were designed in Primer BLAST. cDNA was pre-amplified (95°C for 60 s and 18 cycles of 95°C for 15 s and 4 min at 60°C) with the mix of all primers and contained 5 µl of iQ Supermix (Bio-Rad), 2 µl of diluted cDNA, 1.25 µl of pre-amplification primer mix in final concentration 25 nM and 1.25 µl of water. RT-qPCR was performed using the high-throughput BioMark HD System (Fluidigm) with 96.96 Dynamic ArrayIFC for gene expression. 5 µL of sample pre-mix contained 1 µl of 20x diluted preamplified cDNA, 2.5 µl of SsoFast EvaGreen Supermix (Bio-Rad), 0.25 µl of 20x SG sample loading reagent (Fluidigm) and 1.25 µl of water. 5 µl of assay pre-mix contained 2 µl of 10 µM primer/probe assays, 2.5 µl of 2x assay loading reagent (Fluidigm) and 0.5 µl of water. Thermal conditions for qPCR were: 98°C for 3 min, 35 cycles of 98°C for 5 s and 60°C for 5 s. Raw data were subtracted from the gDNA control and efficiencies of individual assays were calculated from the serial dilutions of a mixed cDNA sample. Assays with insufficient efficacy or very high Cq values (>25) were excluded from the analysis. GenEx software version 6 was used to analyze the data. The missing values were replaced by the average value of the whole group. Normalization genes were identified by Normfinder. Data were normalized to several reference genes (*GAPDH*, *POLR2A*, *RPLP0*, *HPRT1, PPIA* and *TBP*). Statistical analysis was performed via GenEx software. The list of primers is available as Supplementary Table 2.

Standard qPCR

5x HOT FIREPol® EvaGreen® qPCR Supermix (Solis BioDyne) was used in the standard qPCR assay. 5 µl of mastermix containing EvaGreen® qPCR Supermix, water and the primer mix (10 µM forward + 10 µM reverse) was pipetted into each well, 2.5 µl of diluted cDNA (10 ng of transcribed RNA) was added and centrifuged at 1,500 × g for 5 min. Temperature profile used in the reaction was: 95 °C for 12 min, and 40 cycles of 95 °C for 10 s, 60 °C for 20 s and 72 °C for 20 s. Data were analyzed by GenEx software and normalized to Normfinder selected reference genes (*RPLP0*, *HPRT1, PPIA* and *OAZ1*)

Confocal microscopy

For confocal imaging, cells were seeded in 35 mm dishes with 20 mm glass bottom (thickness of the glass bottom 0.16-0.19 mm; Cellvis) and let to attach overnight. Afterwards, cells were incubated for 2 minutes with 20 nM MitoTracker™ Deep Red FM (ThermoFisher Scientific) and immediately before imaging with 2 µg/ml Hoechst 33342. Confocal microscopy images were aquired using a 63x water immersion lens in a Leica SP8 confocal microscopy (Leica Microsystems) equipped with a heated humidified CO_2 incubator. Fluorescence was detected at $405nm_{Ex}/450nm_{Em}$ for Hoechst and $644nm_{Ex}/665nm_{Em}$ for MitoTracker. Radial and object analyses were performed using the ImageJ software (National Institute of Health) as previously described in [13].

^{55}Fe subcellular localization and autoradiography

Cells were incubated with 50 nM ^{55}Fe complexed with citrate (1:10; total activity 0.5 µCi/ml; Lacomed) for 5 days, then collected by trypsinization, centrifuged at 300 x g for 5 min and counted. Approximately 1 x 10^6 cells were collected for WCL. The rest of the cells was resuspended in STE buffer to a concentration of 10 milion cells per 1 ml STE and homogenized by Balch homogenizer in order to obtain intact mitochondria [14]. Homogenized cells were centrifuged at 800 × g for 5 min at 4 °C to isolate nuclear fraction and the supernatant was further centrifuged at 10,000 × g for 20 min at 4 °C to separate mitochondrial and cytosolic fraction. WCL, and mitochondrial and cytosolic fractions were then used for the determination of subcellular localization of ^{55}Fe by pipetting samples into 1 ml of ROTIScint scintillation fluid, and measured on a scintillation counter (with background correction). In parallel, the isolated fractions were mixed with 4X native buffer (50 mM BisTris, 0.05% HCl, 10% w/v glycerol, 0,001% w/v Ponceau S,

pH 7.20) and 1 % digitonin together with protease inhibitors. 40 µg of total protein wwere separated by BNE overnight at 20 V using a light blue cathode buffer (0.02% Coomassie G-250). Next day, the gel was dried and exposed to a tritium Fuji imaging plate (GE Healthcare) for 2-7 days and visualized by the Typhoon instrument (GE Healthcare).

Statistics

The results are expressed as mean ± SD or ± SEM (as indicated in the figure captions) of at least 3 independent experiments. The comparison between experimental and control groups was performed by t-student test or by two-way ANOVA with Bonferroni's multiple comparisons test, using the GraphPad Prism 6.0 or the GenEx software. *$p < 0.05$ was established as the minimum significance level.

I. Breast cancer and tamoxifen

I.1 Literature overview

I.1.1 Breast cancer subtypes

Tumors of the breast tissue are classified according to the expression of immunohistochemical markers: estrogen receptor (ER), progesterone receptor (PR), human epidermal growth factor receptor 2 (HER2) and the marker of proliferation Ki67 [15].

The pioneering works of Perou *et al.* [16] and Sorlie *et al.* [17] have described unique 'molecular portraits' of breast cancer by using large scale gene expression profiling. Five subgroups of so-called 'intrinsic subtypes' of breast cancer have been identified: luminal A (ER^+, PR^+, $HER2^-$, $Ki67^-$), luminal B (ER^+, PR^+, $HER2^-$, $Ki67^+$), HER2 overexpressing (ER^-, PR^-, $HER2^+$), basal like (ER^-, PR^-, $HER2^-$) and normal-like (ER^+, PR^+, $HER2^-$, $Ki67^-$), each driven by unique transcriptional programs and different response to treatment. Luminal subtypes represent approximately 75% of all breast tumors. Their growth is usually slow and with better prognosis. On the contrary, HER2 overexpressing tumors together with triple negative basal tumors are highly proliferative with worse prognosis. Normal-like tumors share the same expression profile with luminal A tumors, but have worse predited outcome [18].

I.1.2 ER^+ breast cancer treatment

The primary systemic therapy for ER^+ tumors is endocrine therapy, usually in combination with chemotherapy [19]. Tamoxifen represents the gold standard as an adjuvant treatment for patients with ER^+ breast tumors. A 5 year duration of tamoxifen treatment is commonly used; however, 10-15 years is recommended [20, 21]. Tamoxifen is administered orally and is metabolized in the liver by cytochrome P450 (CYP) enzymes into several metabolites. Of those, N-desmethyl-4-hydroxytamoxifen (endoxifen) and 4-hydroxytamoxifen (4-OH tamoxifen) are the most abundant, and show an almost 100-fold higher affinity to ER compared to tamoxifen [22].

ERs belong to a nuclear receptor family of transcription factors regulating diverse physiological processes connected with reproductive, neuroendocrine, skeletal and

cardiovascular systems and, in the context of this thesis, are important for mammary gland development [23]. Two main ER isoforms exist, ERα and ERβ, which are often co-expressed in the cells and can form both homodimers and heterodimers [24]. In the absence of a ligand, ERs are sequestered by cytosolic chaperons such as heat shock protein 90 (Hsp90). When an estrogen ligand binds to the ER, it induces a conformational change that leads to release from chaperones and dimerization. These dimers then shuttle to the nucleus and bind to estrogen response elements (EREs) localized within the promoters of target genes. ERs bound to EREs recruit co-activator proteins which loose the chromatin structure within the DNA sequence and promote transcription. On the other hand, co-repressors that inhibit transcription are also recruited by ERs, and the net effect on transcription is dependent on cellular and promoter context. This type of ER signaling represents the 'canonical' pathway [25] (Figure 1).

Furthermore, alternative ER signaling pathways have been described and are also summarized in Figure 1. The transcription of genes which do not contain EREs may be mediated by tethering of the ER to the promoters *via* other transcription factors [26]. ERs can also be regulated in a ligand independent way by extracellular signals, resulting in their direct phosphorylation and transcriptional activation [27]. Besides nuclear ERs, a membrane ER named G-protein coupled estrogen receptor 1 (GPER1) is responsible for non-genomic ER signaling. Activation of GPER1 leads to the activation of transduction mechanisms by producing second messengers and activation of protein-kinase cascades [28, 29].

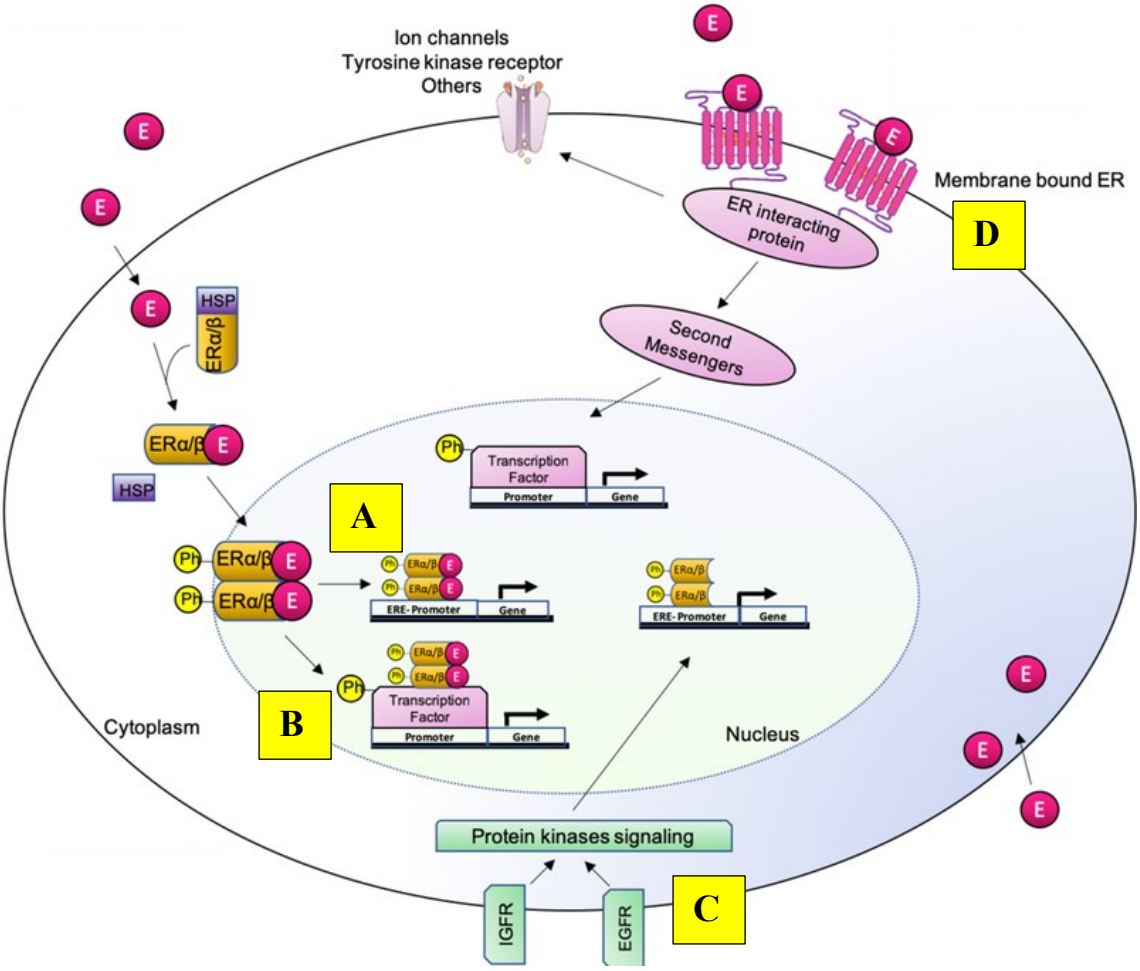

Figure 1. Genomic and non-genomic ER signaling pathways. (A) Direct binding of the ERs to EREs and transcriptional activation. **(B)** Tethering of the ER to the promoters *via* transcription factors. **(C)** Ligand-independent ER signaling mediated by growth factor receptor signaling. **(D)** Non-genomic ER signaling resulting in the production of second messengers, phosphorylation of transcription factors and thus gene transcription (adapted and modified from [30]).

The anti-cancer effect of tamoxifen is exerted mostly through ER signaling. The similarity in the structure and chemical composition between tamoxifen and the ER ligand estradiol allows tamoxifen to compete for the ER binding site. The conformational change induced by the interaction of tamoxifen with the ER results in the recruitment of co-repressors, followed by reduced transcription of the ER target genes, therefore inhibiting proliferation and survival of tumor cells (Figure 2). Such antagonist activity is observed in breast tissue; however, tamoxifen possesses also agonistic activity in uterus or bones. Due to this mixed agonist/antagonist activity, tamoxifen is referred to as a 'selective estrogen receptor modulator' [31, 32].

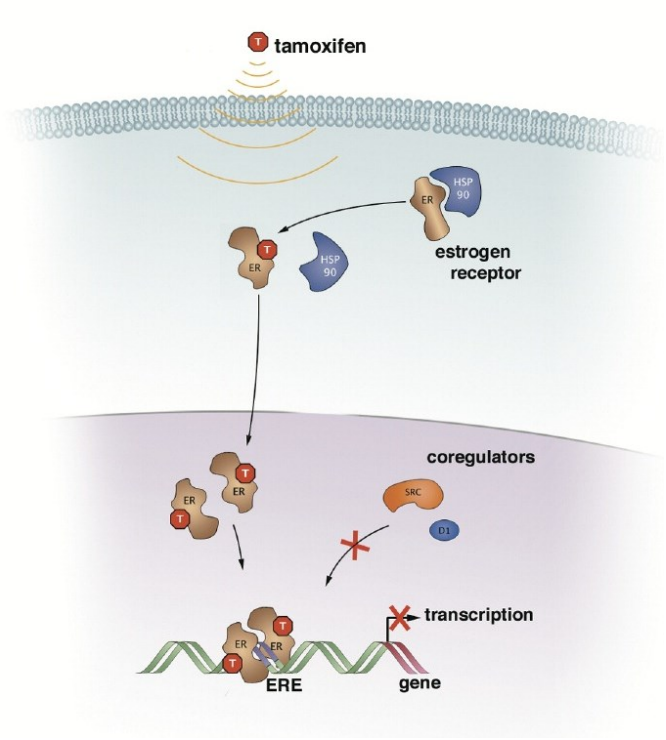

Figure 2. Mechanism of action of tamoxifen in breast tissue. When unbound, ER is sequestered in the cytosol by cytosolic chaperones such as Hsp90. After entering the cell, tamoxifen competes with estradiol for the binding site in the ER. Binding of tamoxifen to the ER induces rapid dissociation of ER from Hsp90 and its translocation into the nucleus where it binds to the EREs in the target genes. Conformational change of the ER caused by tamoxifen binding blocks the recruting of the transcription machinery, including coactivators such as the steroid receptor coactivator-1 (SRC-1) or cyclin D1, which results in the inhibition of transcription (adapted from [31]).

I.1.3 Mechanisms of tamoxifen resistance

Although tamoxifen has extended the life expectancy of many patients, one of the major clinical problems remains the resistance to this drug. The resistance can be classified as either *de novo*, where tumors do not respond to the first line tamoxifen treatment, or acquired, which emerges during the treatment in spite of an initial response. Indeed, 30-50% of patients experience relapse due to acquired tamoxifen resistance [33].

Various mechanism of resistance have been described so far. Since tamoxifen interferes with ER signaling, the loss of ER expression is considered to be the main mechanism of the resistance and therapeutic failure [34]. The loss of expression of ER can be caused by epigenetic modifications within the promoters of genes coding for ERs

or by ER^- cells overgrowing ER^+ cells, resulting in the switch from ER^+ to ER^- phenotype [35-37]. Mutations in the genes coding for ERs without the loss of ER expression, or alternatively spliced ER variants, may play a role in the resistance as well [34]. For example, the ERα 36 kDa isoform has been reported to confer tamoxifen resistance by increasing the CSC population in breast tumors and potentiate metastatic processes [38, 39].

Several microRNAs (miRNAs) such as miR-17, miR-221/miR-222, miR-27b, miR-21, miR-342 or miR-301a have been identified and proposed to mediate tamoxifen resistance. By interfering with ER expression and signaling, miRNAs can promote the switch from hormone sensitive to hormone insensitive tumor, therefore diminishing the response to tamoxifen treatment [40-43].

Different types of polymorphisms in tamoxifen-metabolizing enzymes can impact the therapeutic outcome as well. Polymorphisms in the genes coding for the well characterized isozyme CYP2D6 have been linked to different individual serum concentrations of tamoxifen in patient samples undergoing adjuvant therapy, leading to tamoxifen resistance [44, 45].

Another important contributor to tamoxifen resistance is the crosstalk between ER signaling and different growth factor signaling pathways, resulting in the sustained proliferative ability of cells despite their non-functional ER signaling [46]. For instance, the crosstalk between ER and epidermal growth factor receptor (EGFR)/HER2 pathways in tamoxifen resistant cells overexpressing HER2 leads to phosphorylation of both ER and HER2 in the presence of tamoxifen and activation of downstream protein-kinase pathways, highly contributing to the resistant phenotype [47]. Indeed, HER2 is often overexpressed in tamoxifen resistant tumors and its expression negatively correlates with ER expression [48].

An additional, well described mechanism of tamoxifen resistance involves overexpression of ABC transporters, and is discussed in detail in the chapter IV.

I.1.4 Cancer stem cells

The existence of CSCs, a subpopulation of cells with stem-like properties within the tumor, often underlies the failure of classical treatments. In fact, although conventional therapeutic strategies often lead to very efficient elimination of bulk tumor

cells, CSCs do not respond to the treatment and, over time, may give rise to secondary tumors [49].

CSCs possess self-renewal ability (asymmetric division) producing two daughter cells, one of which is a copy of the original CSC and the second one can differentiate into multiple tumor cell types. Furthermore, non-CSCs can de-differentiate into CSCs, thus enriching CSC subpopulation and contributing to tumor heterogeneity [50]. Importantly, CSC characteristics could be linked to epithelial-mesenchymal transition (EMT), where upregulation of N-cadherin participating in the formation of cell-to-cell adhesions is a crucial marker of ongoing EMT [51]. Indeed, CSCs derived from breast tumor – breast CSCs (BCSCs) possess the ability to transit between two phenotypic states: epithelial-like (E) which is proliferative and has high expression of aldehyde dehydrogenase 1 (ALDH1), and mesenchymal-like (M) which is quiescent, highly invasive and can be recognized by $CD44^{+}/CD24^{-}$ markers [52]. This shift is very reminiscent of the EMT program necessary for tumor dissemination and invasion, and further supports the role of BCSCs in cancer relapse and therapy failure [53]. Other markers routinely used to identify BCSCs are C-X-C chemokine receptor type 4 (CXCR4) or ABCG2 transporter (also known as breast cancer resistance protein BCRP) [54].

Tamoxifen therapy has been documented to enrich breast tumors with CSC populations with increased expression of markers such as SRY-box transcription factor 2 (SOX2) [55] or CXCR4 [56] and can increase the mammosphere forming capacity [57], which is also in line with our observations [6]. For this reason, understanding the principles which underlie the BCSCs phenotype and accompany acquisition of tamoxifen resistance is needed for a targeted and effective therapy.

I.2 Results

I.2.1 Evaluation of the resistant phenotype in established Tam5R cell lines

The experimental model of tamoxifen resistant cells was established by cultivation of parental cell lines in the presence of increasing tamoxifen concentrations for over 6 months, resulting in the selection of cells capable of growing in the presence of 5 μM tamoxifen (Tam5R cells). Prior to performing any experiment, we evaluated our model of Tam5R cells. First, we measured the number of viable cells by crystal violet staining after their incubation with increasing concentrations of tamoxifen (1-25 μM) for 48 hours. No significant differences were detected in lower tamoxifen concentrations (1-7.5 μM) but resistance became evident at 10 μM in both Tam5R cell lines (Figures 3A and 3B). A more profound effect was observed in T47D Tam5R cells at 12.5 μM tamoxifen, where the number of viable cells was almost comparable to untreated cells (93%), while the number of viable cells in parental T47D cells was greatly diminished (only 20% relative to untreated cells). The number of viable cells in the same tamoxifen concentration was around 88% in MCF7 Tam5R compared to 26% in MCF7 Ctrl cells (both relative to untreated cells). The calculated IC_{50} values for tamoxifen were approximately 10 μM in Ctrl cell lines and increased to about 15 μM in Tam5R cell lines (Figures 3A and 3B).

Since the crystal violet staining method is not able to discriminate between cytostatic and cytotoxic effects of tamoxifen, we measured cell death by AV/PI double staining after tamoxifen treatment for 48 hours. A very similar trend was observed as no difference in cell death between Ctrl and Tam5R cell lines was detected up to 7.5 μM concentration (Figures 3C and 3D). Once again, a more profound effect was documented in the T47D cell line where in 10 μM concentration the percentage of dead cells was only 7% in Tam5R cells compared to 68% in Ctrl cells. At the same concentration, MCF7 Tam5R cells showed 12% dead cells compared to 38% in MCF7 Ctrl cells.

In addition, we evaluated our experimental model of Tam5R cells *in vivo*. MCF7 Ctrl and Tam5R cells were injected into athymic nude mice resulting in tumor formation (Figure 3E). Each group was further divided into 2 groups: one non-treated and one treated with tamoxifen (i.p.). The tumor growth was almost identical for both non-treated groups. However, a difference was detected in tamoxifen-treated groups where tumors originated from MCF7 Ctrl cells responded by significantly reduced growth while tumors derived from MCF7 Tam5R cells responded less to the treatment and

continued to grow. By performing the aforementioned experiments we confirmed the tamoxifen resistance of our Tam5R model both *in vitro* and *in vivo.*

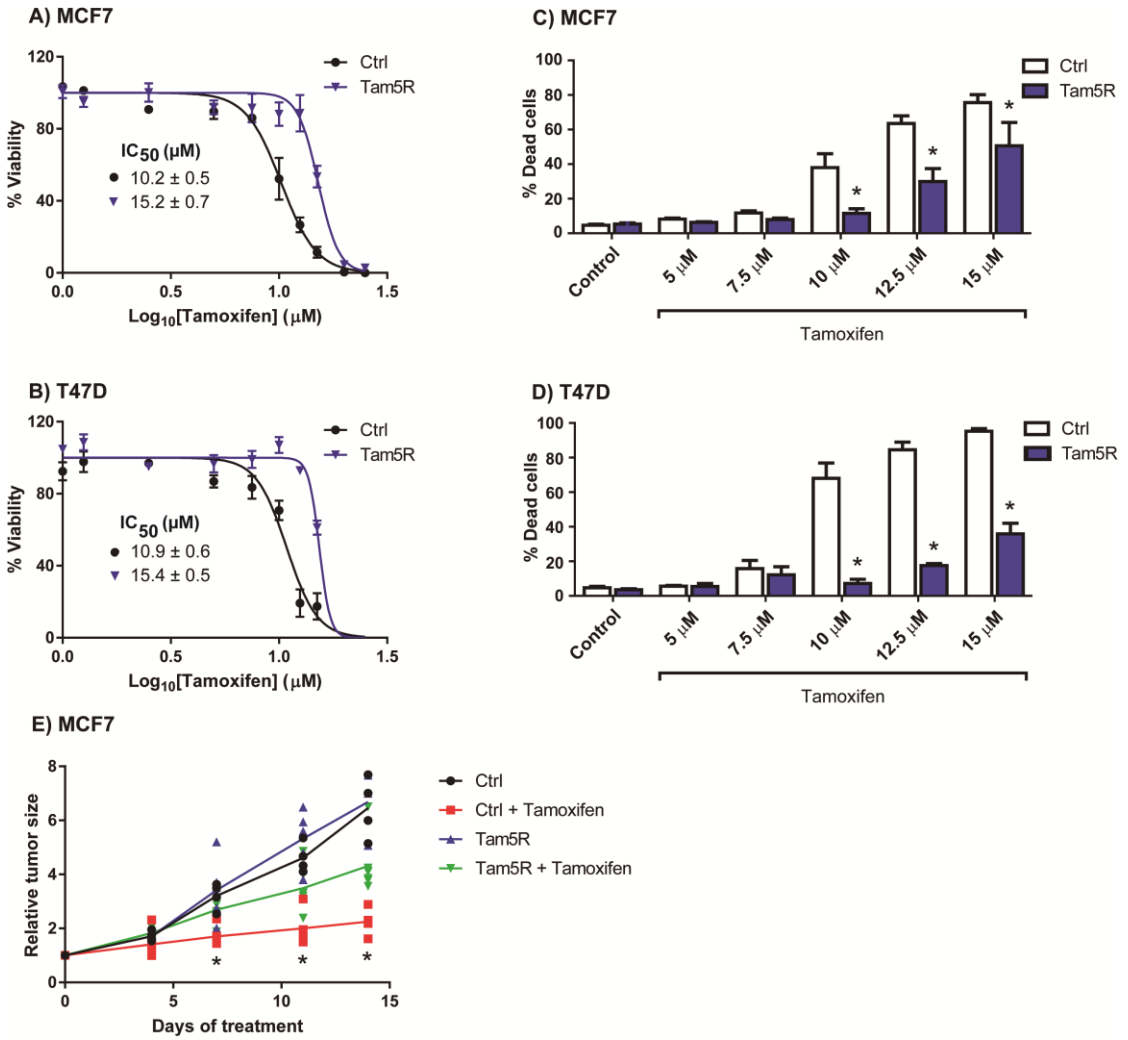

Figure 3. Evaluation of the established experimental model of Tam5R cells. Dose-response curves for the number of viable **(A)** MCF7 and **(B)** T47D Ctrl and Tam5R cells after incubation with increasing concentrations of tamoxifen (1-25 μM) for 48 hours measured by crystal violet staining. IC_{50} values for tamoxifen in each cell line are shown inside the graphs. Results are expressed as mean viability ± SEM of at least 3 independent experiments. Cytotoxic effect of tamoxifen on **(C)** MCF7 and **(D)** T47D Ctrl and Tam5R cells after 48 hours incubation, measured by AV/PI double staining. Results are expressed as mean % dead cells ± SD of at least 3 independent experiments. *$p \leq 0.05$ relative to Ctrl cells. **(E)** Tumor growth curves in mice injected with 2×10^6 of either MCF7 Ctrl or Tam5R cells. When tumors reached ~ 30 mm^3, mice were treated i.p.with tamoxifen (30 mg/kg weight) or vehicle 2 times per week for 14 days. The tumor sizes are expressed relative to day 0 (corresponding to the first day of treatment). Each group consisted of at least 5 animals. *$p \leq 0.05$ relative to Ctrl

I.2.2 Tam5R cells exhibit cancer stem-like cell properties

Cumulative evidence shows that tamoxifen resistant cells are enriched in BCSCs *in vitro* [55, 56, 58, 59]. Hence, we investigated if our model of Tam5R cells exhibits a similar phenotype. We tested the expression of several BCSCs markers (*ABCG2*, *CD44*, *CXCR4*, *SOX2*) as well as the EMT marker cadherin 2 (*CDH2;* coding for N-cadherin) by qPCR. Significant upregulation of *ABCG2* (10.1-fold), *CD44* (4.6-fold), *CXCR4* (2.6-fold), *CDH2* (14.8-fold) and *SOX2* (2.5-fold) was detected in MCF7 Tam5R cell line compared to parental MCF7 cells (Figure 4A). T47D Tam5R cells showed elevated mRNA level of *CXCR4* (2.6-fold) and *SOX2* (17.7-fold) but significant downregulation of *ABCG2* (-0.5-fold), *CD44* (-3.3-fold) and *CDH2* (-20-fold) (Figure 4B).

In addition, we assessed the protein level of the markers mentioned above by western blot (Figure 4C). Both Tam5R cells showed significantly increased level of SOX2, which corroborates the data from qPCR. Similarly, ABCG2 level was significantly higher in MCF7 Tam5R cells, and lower in T47D Tam5R cells compared to their normal counterparts. Moreover, T47D Tam5R cell line also showed decreased protein level of CD44 marker while this protein was not detectable in MCF7 cells. Protein level of CXCR4 and N-cadherin was not detected in any cell line, possibly due to their very low level, and therefore they are not shown in the figure.

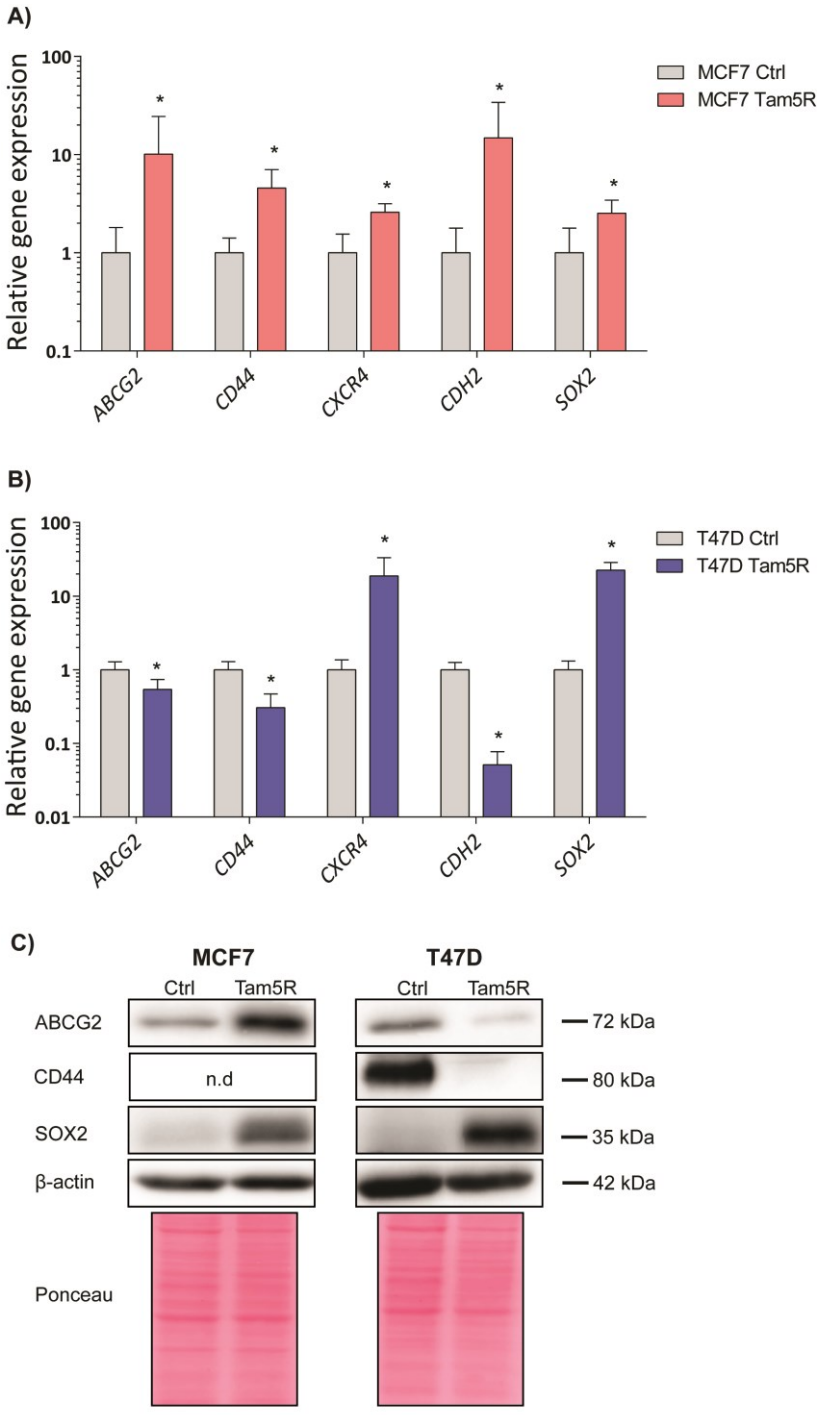

Figure 4. CSC and EMT markers in Tam5R cells. Relative gene expression of *ABCG2*, *CD44*, *CXCR4*, *CDH2* and *SOX2* (log scale) in **(A)** MCF7 and **(B)** T47D Ctrl and Tam5R cells measured by Fluidigm qPCR in MCF7 and standard qPCR in T47D cell line. Results are expressed as mean ± SD of at least 3 independent samples. *$p \leq 0.05$ relative to Ctrl cells. **(C)** Representative pictures of protein level of ABCG2, CD44 and SOX2 in MCF7 and T47D Ctrl and Tam5R cells assessed by western blot. Experiment was performed with 3 sets of independent samples with β-actin and Ponceau staining used as loading controls. n.d = not detected

I.3 Discussion

We successfully established the model of tamoxifen resistant cells that are able to grow long-term in the presence of 5 μM tamoxifen. Similar tamoxifen concentrations (or even higher) were used by other researchers as well [60-62]. Of note, even though average serum concentrations of tamoxifen lie around 0.2-0.5 μM [63], in some patients tamoxifen has been reported to reach concentrations of up to 8 μM [64]. Such interpatient variability in serum tamoxifen level was proposed to be linked with the polymorphisms in the *CYP2D6* gene encoding the key enzyme responsible for the bioconversion of tamoxifen into its active metabolite endoxifen [65-67].

Phenol red free medium supplemented with charcoal stripped serum is an alternative approach used for the cultivation of tamoxifen resistant cells. Phenol red acts a weak estrogen which potentiates ER signaling and thus interferes with the antiestrogen (tamoxifen) binding. Charcoal stripped serum is selectively deprived of hormones without losing other serum components. However, in our model we use medium containing phenol red supplemented with 10% FBS. We believe that this experimental setup represents more physiological conditions and better reflects the situation in patients who carry estrogens in their circulation. In addition, while some studies routinely use 4-OH tamoxifen, we cultivate Tam5R cells in the presence of tamoxifen as we did not see a more potent effect of 4-OH tamoxifen (data not shown).

We confirmed the tamoxifen resistance of our experimental model, as Tam5R cells show higher viability as well as decreased cell death compared to parental cells when exposed to tamoxifen. Moreover, the model was evaluated also *in vivo*, where tumors originated from Ctrl cells slowed their growth during tamoxifen treatment while tumors derived from Tam5R cells continued to grow, thus mimicking the resistant phenotype seen in human patients.

The next step was to determine whether our experimental model shows expression of CSC and EMT markers. We documented increased gene expression of several stem cell markers as well as EMT markers in MCF7 Ctrl and Tam5R cells by using Fluidigm qPCR [6]. Since T47D Tam5R cell line was generated later, the expression of stem cell and EMT markers was measured by standard qPCR as the sample size was too small to merit the use of a Fluidigm chip.

Interestingly, the only detected stem cell marker elevated in both Tam5R cell lines was SOX2, which was increased on mRNA as well as on protein level, in line with previous reports [55, 59]. Even though CD44 level has been shown to be increased

tamoxifen resistant cells [68], we did not confirm such observations in our Tam5R models. We believe that conflicting results might be explained by different experimental models and cultivation conditions used in the studies.

Elevated expression of ABCG2 has also been documented in tamoxifen resistant cells [56], which was confirmed in our MCF7 Tam5R cells, but not in T47D Tam5R cells. Different expression pattern between MCF7 Tam5R cells and T47D Tam5R cells may be explained by the study published by Liu et al., where they report the high inter-tumoral variation in the expression of breast cancer stem cell markers as well as the heterogeneous distribution of these markers in patient samples [69]. The same observations were shown for *in vitro* breast cancer cell lines, where the expression of each marker was rather unique for specific cell subpopulations [69]. Based on such observations it may be possible that even though our Tam5R cell lines do not show the same pattern of tested stem cell markers, they may be enriched with cell subpopulations expressing different markers. Of note, basal protein level of CD44 was increased in T47D cells compared to MCF7 cells, suggesting they might exhibit cancer stem-like phenotype even without tamoxifen treatment. Better characterization of CSC properties would thus require further experiments that would assess the ability of Tam5R cells to form spheres *in vitro* or to generate tumors *in vivo*.

The EMT program which is important for the maintenance of stem cell population has been linked to tamoxifen resistance in some reports [59, 70, 71]. Even though the expression of one of the key EMT markers *CDH2* was elevated in both Tam5R cells, no protein was detected by western blot, possibly either due to its low level or not properly functional antibody. The same applies for the detection of the CXCR4 marker (previously described to maintain stem-like cell phenotype of tamoxifen resistant cells [56]).

Although additonal CSC markers such as octamer-binding transcription factor 4 (Oct4) [59, 72], CD133 [59] and ALDH1 [38, 56, 72] have been shown to be upregulated in tamoxifen resistant cells and patients samples, they were not assessed in our experimental model as we do not have functional and validated antibodies.

II. Mitochondria and tamoxifen resistance

II. 1 Literature overview

II.1.1 Mitochondria

Mitochondria are double-membrane organelles whose main function is energy production through the process of oxidative phosphorylation (OXPHOS). Therefore, they are often referred to as 'powerhouses of the cell' [73]. Moreover, they govern multiple other vital cellular processes such as cellular redox status through the production of ROS and their detoxification, cellular signaling, apoptosis, and calcium homeostasis [74, 75]. Notably, mitochondria are crucial organelles for the synthesis of Fe-S clusters and heme, that represent necessary cofactors for many proteins [76].

Mitochondria contain their own DNA (mtDNA) which is packed into mtDNA-protein complexes called nucleoids. Human mtDNA is a double-stranded circular molecule with an approximate size of 16.5 kB, and encodes only 37 genes. 13 of them code for subunits of respiratory chain complexes, the remaining are 2 rRNAs and 22 tRNAs which help translate mitochondrially coded polypeptides [77, 78] (Figure 5). More than 1000 proteins that participate in processes within mitochondria are nuclearly coded, translated on cytosolic ribosomes and subsequently transported into mitochondria *via* import machineries [79]. Therefore, the crosstalk between nucleus and mitochondria is strictly regulated and responds to both intra and extracellular changes in order to maintain cellular homeostasis [80].

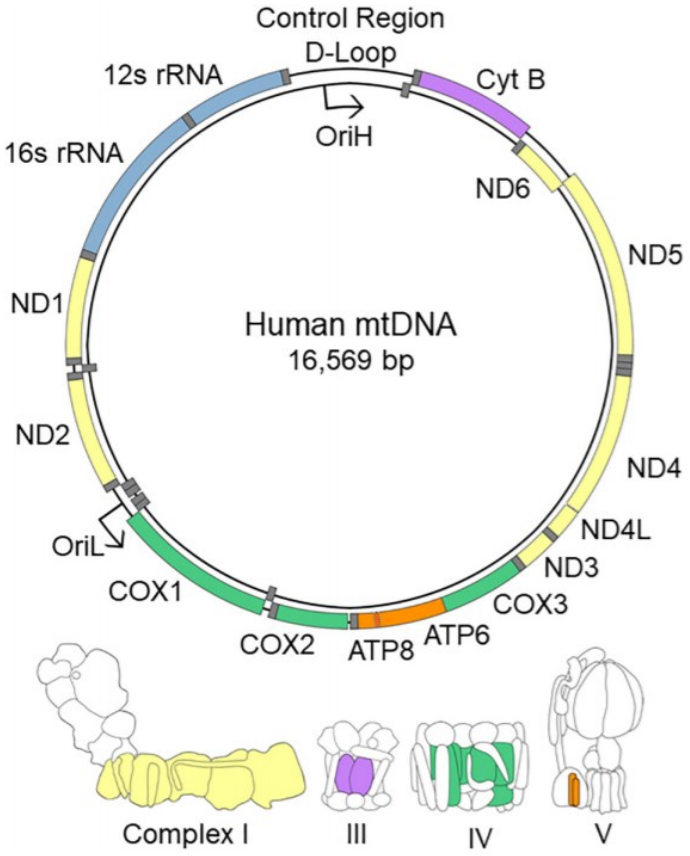

Figure 5. The structure of the human mtDNA (schematic). The human mtDNA is a double-stranded circular molecule consisting of heavy (H) and light (L) strands, with a total length of 16,569 bp. It encodes 13 proteins that form the subunits of the respiratory chain complexes, 2 rRNAs and 22 rRNAs. Human mtDNA also contains a non-coding region called displacement loop (D-loop), which regulates mtDNA replication (adapted from [81]).

II.1.2 Mitochondrial metabolism

As already mentioned above, mitochondria are central organelles in cellular metabolism and energy production. Mitochondria possess the necessary enzymatic tools to complete the oxidation of macronutrients such as sugars, lipids and proteins in order to produce ATP and generate metabolic substrates [74]. Sugars are metabolized in the process of glycolysis in the cytosol and enter the mitochondria in the form of pyruvate (under aerobic conditions) which is converted into acetyl coenzyme A (acetyl-CoA) by the pyruvate dehydrogenase protein complex. Metabolic degradation of fatty acids (or β-oxidation) occurs in the mitochondrial matrix and produces acetyl-CoA as its final product. The degradation of amino acids (AAs) is a more complex process assisted by multiple enzymes metabolizing AAs directly into pyruvate or acetyl-CoA [82]. Produced

acetyl-CoA enters the tricarboxylic acid (TCA) cycle in the mitochondrial matrix (also known as Krebs cycle or citric acid cycle). TCA cycle involves a series of reactions generating energy in form of ATP and GTP together with the reduced equivalents nicotinamide adenine dinucleotide (NADH) and flavin adenine dinucleotide ($FADH_2$) which then serve as electron donors for mitochondrial complexes (described in chapter II.1.3) [83].

II.1.3 Mitochondrial respiration

One of the main metabolic processes occurring within mitochondria is mitochondrial respiration. This process requires molecular oxygen as the final acceptor of the electrons from the reducing equivalents generated by the TCA cycle and is coupled with the production of energy in the form of ATP [74].

Multi-subunit protein structures known as mitochondrial respiratory complexes [complex I (CI), complex II (CII), complex III (CIII) and complex IV (CIV)] form the electron transport chain (ETC) and are embedded (CI, CIII and CIV) or closely associated (CII) with the inner mitochondrial membrane [84]. Importantly, individual complexes are often assembled into higher order structures called supercomplexes (SCs). The most described organization of SCs is $I_1III_2IV_{1\text{-}2}$, also called respirasome, which can perform all respiratory reactions [85-87]. The organization of respiratory complexes into SCs is tissue dependent and responds to cellular energy demands. It has been suggested that forming entities such as SCs increases the stability and activity of complexes [88].

NADH and $FADH_2$ generated in TCA cycle donate electrons to the ETC, where they undergo a series of redox reactions to reach their final acceptor – molecular oxygen (Figure 6) [89, 90]. This process is coupled with proton pumping from the matrix into the intermembrane space through CI, CIII and CIV, thus creating a proton gradient which subsequently drives ATP synthesis in the process of OXPHOS *via* the F1F0 ATP synthase (or complex V; CV) [74, 91].

Under physiological conditions, approximately 0.2-2% of electrons leak from the ETC and react directly with molecular oxygen, producing ROS - superoxide or hydrogen peroxide - which are harmful for the cell [92]. The main sites for ROS production are considered to be CI and CIII. The level of ROS in the mitochondria is guarded by highly efficient antioxidant mechanisms, such as superoxide dismutase 2 (SOD2), catalase and the glutathione (GSH) and thioredoxin systems [92-94]. Of note, assembly of respiratory complexes into SCs also helps to reduce ROS generation [88].

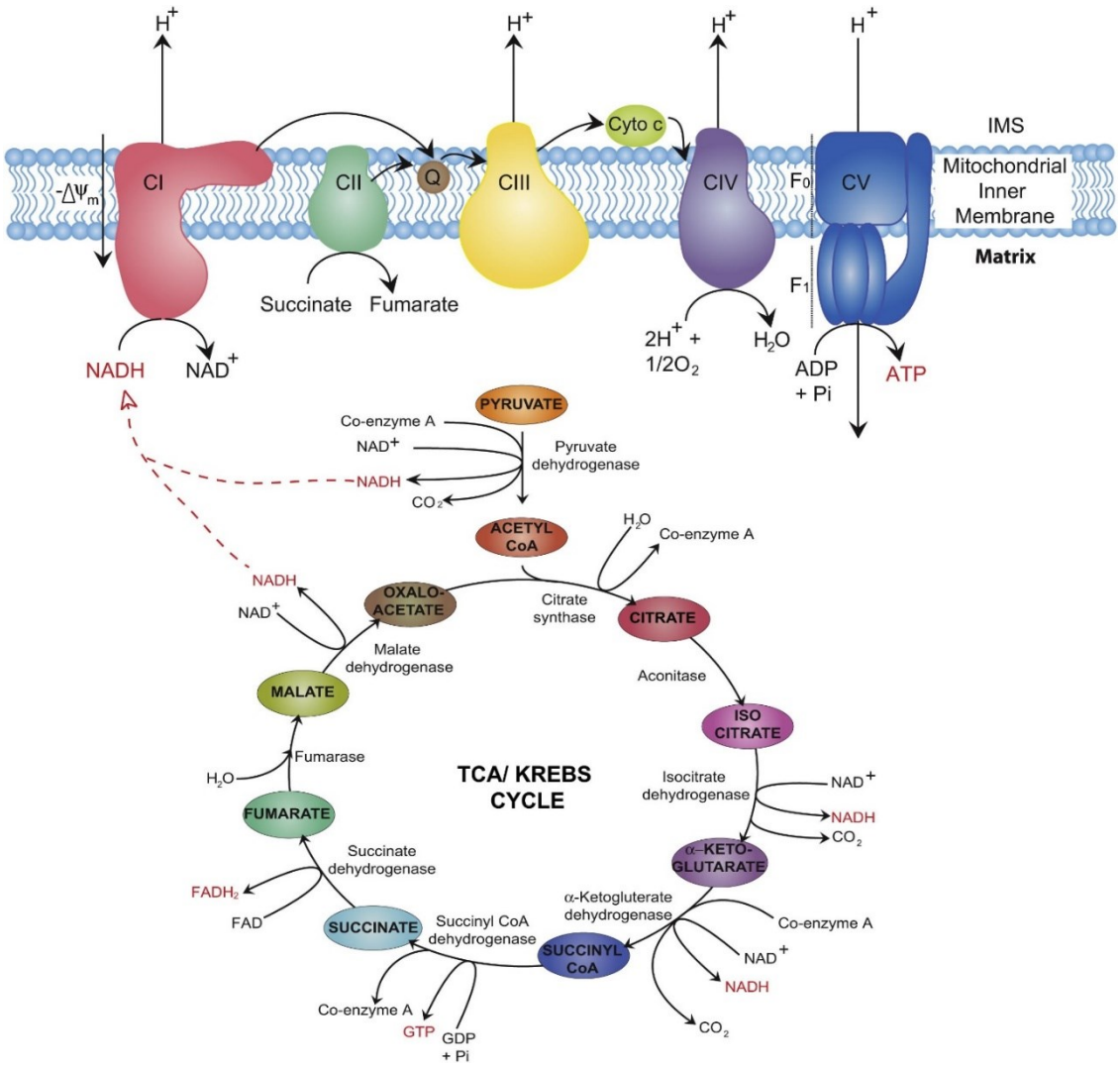

Figure 6. Overview of the TCA cycle, ETC and OXPHOS within mitochondria. Pyruvate generated by the metabolism of macronutrients enters the TCA cycle in the form of acetyl-CoA which in the subsequent enzymatic reactions is oxidized back to oxaloacetate, producing high-energy molecules GTP, NADH and $FADH_2$. NADH then passes the electrons to CI and is oxidized to NAD^+. CII gains electrons from $FADH_2$ which is then oxidized to FAD. Transfer of electrons through ETC coupled with the pumping of the protons into intermembrane space generates the membrane potential which is utilized in the process of OXPHOS *via* CV (adapted from [74]).

II.1.4 Mitochondrial dynamics

Mitochondria undergo coordinated cycles of fission and fusion (collectively referred to as 'mitochondrial dynamics') in order to maintain their shape, size as well as their cellular distribution [95].

Mitochondrial fission is the process of division of one mitochondrion into two, functionally distinct mitochondria. The daugher mitochondria with high membrane potential posess high probability of subsequent fusion while mitochondria with low membrane potential and low respiration are targeted for the elimination by the process termed mitophagy, therefore maintaining the quality of mitochondria [96]. Mitochondrial fission is mediated by the GTPase dynamin-related protein 1 (DRP1) which is recruited at the outer mitochondrial membrane forming a ring-like structure. The GTP hydrolysis powers the mitochondrial constriction at this site and wrapping of endoplasmic reticulum and dynamin 2 recruitment finalize this process [95].

Contrary to mitochondrial fission, mitochondrial fusion results in long tubular mitochondria and enables the exchange of the mitochondrial content in order to prevent the loss of essential mitochondrial components [97]. The fusion of outer mitochondrial membrane is facilitated by mitofusins (mitofusin 1 and mitofusin 2) while the optic atrophy 1 (OPA1) protein ensures the fusion of inner mitochondrial membrane [98].

These events are not only important in processes such as apoptosis or cell division, but also mediate cellular response and adaptation to external stimuli and shape cellular metabolism in order to maintain a healthy mitochondrial network [99]. In addition, dysregulated mitochondrial dynamics is a common feature in many types of cancer, which utilize the processes of fission/fusion for their enhanced proliferation, migration, maintenance of higher ROS level as well as other metabolic adaptations [100].

II.1.5 Mitochondria and cancer

A century ago, Oto Warburg observed that cancer cells not only uptake more glucose than normal cells, but also ferment the glucose molecule into lactate, instead of fully oxidizing it to CO_2, even in the presence of oxygen. This phenomenon is known as aerobic glycolysis or the 'Warburg effect' and has brought attention to the role of mitochondria in tumorigenesis [101]. Originally, the high rate of glycolysis in tumor cells was attributed to defects in mitochondrial function which is compensated by increased ATP production from glycolysis [101]. However, these claims were in contrast with findings by Weinhouse et al., who proved that neoplastic tissues have normal OXPHOS when supplemented with NAD^+ [102, 103]. After many years of research in this field, it is clear that although the Warburg effect can be the result of damaged mitochondria in

some cases, many cancers exhibiting Warburg effect have healthy mitochondria that are essential for their survival [104].

Metabolic rewiring towards alternative pathways for energy production seems to be important for cancer cells in order to support proliferation, differentiation and growth, and to adapt to changing environments such as nutrient depletion, hypoxia or cancer treatment [104]. The metabolic alterations may vary depending on the subtype of cancer or tissue of origin (some tumors prefer OXPHOS, other are more glycolytic) [105].

Furthermore, increased ROS level is a characteristic of many cancer cells and is usually a consequence of higher metabolic rates in mitochondria [106]. Elevated ROS are compensated by increased activity of antixodant defense systems under normal circumstances. ROS have critical functions in all stages of cancer: initiation, promotion and progression, and are known to activate several signaling pathways such as PI3K/Akt, MAPK or NF-κB, leading to cell survival, proliferation and enhanced invasivity and metastatic activity [106]. Importantly, increased ROS level in mammospheres [6], an *in vitro* model of CSCs, supports a possible connection between ROS and the CSC phenotype [107].

II.1.6 Mitochondria and cancer stem cells

Metabolic plasticity is recognized as one of the hallmarks of cancer cells [108]. Similarly, undifferentiated CSCs have the ability to switch between different metabolic pathways. Such adaptability seems to be crucial for their phenotype and maintenance [109]. Interestingly, CSCs derived from distinct types of tumor show differential preferences for metabolic pathways and energy production. It has been shown that glycolysis is the main metabolic pathway for CSCs derived from glioblastoma [110], colon cancer [111], ovarian cancer [112] or osteosarcoma [113]. Concomitantly, increased glucose uptake, elevated protein level of glycolytic enzymes as well as enhanced lactate production together with decreased function of mitochondria are features of glycolytic CSCs [114]. In contrast with the previously mentioned reports, some authors claim that CSCs prefer OXPHOS for ATP production. This has been documented for CSCs of glioblastoma [115], lung [116] and ovarian origin [117].

There is also controversial evidence regarding the preferential metabolic program of BCSCs. Several studies report significantly reduced BCSCs population upon glycolysis inhibition by 2-DG or 3-bromo-2-oxopropionate-1-propyl ester (3-BrOP)

suggesting their more glycolytic nature [118, 119]. On the contrary, some authors document increased dependence of BCSCs on OXPHOS [120-122]. Such contradition might be explained by culturing conditions where glucose-rich conditions favor glycolysis while glucose depletion forces the cells to utilize OXPHOS [123].

CSCs remain an obstacle in the successful treatment of many cancer types. Therefore, elucidating mechanisms regulating metabolic plasticity in CSCs could help to develop new targeting strategies directly aimed at their elimination or reprogramming.

II.1.7 Mitochondria and tamoxifen resistance

Tamoxifen is known to act throught the inhibition of ER signaling. Interestingly, several studies have documented that tamoxifen can also directly alter the function of mitochondria through the process of mtDNA synthesis and replication [124], respiration [124-126] or fatty acid oxidation [124]. Indeed, some of the complexes of the ETC have been reported as direct targets of tamoxifen [125, 126]. More specifically, Moreira et al. showed that the flavin mononucleotide site in the respiratory CI is a binding site for tamoxifen [125]. This fact was further confirmed by mitochondrial targeting of tamoxifen that enhances its potency, making it an effective treatment even in triple negative breast cancer cells, the underlying mechanism being CI inhibition and ROS production [127]. However, all mentioned reports were addressing only acute effects of tamoxifen and do not explore the metabolic changes after long-term tamoxifen exposure, which would mimic the situation in patients who receive tamoxifen for years. Although there have been some studies proposing a connection between metabolic reprogramming and tamoxifen resistance [128, 129], the reported data are contradictory and do not provide any deeper mechanistic insight. In our study, we present a more detailed overview of the role of mitochondria in the maintenance of a tamoxifen resistant phenotype [130]. We believe that exploring the bioenergetic changes in the model of tamoxifen resistant cells may shed light on the processes leading to tamoxifen resistance and bring some new perspectives and targets that might be utilized to effectively treat breast cancer.

II.2 Results

The results presented in this chapter were published in:

Tomková V, Sandoval-Acuña C, Torrealba N, Truksa J. (2019). Mitochondrial fragmentation, elevated mitochondrial superoxide and respiratory supercomplexes disassembly is connected with the tamoxifen-resistant phenotype of breast cancer cells. Free Radic Biol Med 143:510-521.

In order to find out whether mitochondria play a role in tamoxifen resistance, we employed the model of Tam5R cells described in the previous chapter and analyzed various aspects of their mitochondrial structure, function and metabolism.

II.2.1 Tam5R cells show decreased abundance, assembly and activity of mitochondrial SCs

In order to address the effect of long-term tamoxifen treatment on the abundance and composition of mitochondrial respiratory SCs in Tam5R cells, we performed BNE on isolated mitochondrial samples, which allows determination of multimeric complexes in their native state. Figures 7A and 7B (upper panels) demonstrate a tremendous decrease in the amount of assembled canonical SC (respirasome) in both Tam5R cells compared to parental cells. Tam5R cell lines have also decreased assembly of lower forms of SCs, such as $CIII_2$/CIV. While the T47D Tam5R cell line also shows a decrease in the level of fully assembled CII and CV, no significant changes in these complexes were observed in MCF7 Tam5R cells. In order to assess whether the activity of SCs and individual complexes is also diminished, we measured their enzymatic activity by hr-CNE (Figures 7A and 7B, lower panels). The presented results confirm the data observed by BNE, as the activity of all complexes in T47D Tam5R cells was impaired, while a diminished activity in MCF7 Tam5R cells was detected only in case of CI, CIII and CIV. Therefore, we conclude that Tam5R cell lines show a decrease in the amount, assembly and activity of mitochondrial SCs.

II.2.2 Tam5R cells show decreased oxygen consumption

The assembly of individual mitochondrial complexes into SCs is necessary for the proper functioning of the ETC [88]. Since previous results revealed that Tam5R cells have disassembled mitochondrial SCs with diminished enzymatic activity, we assessed mitochondrial respiration in Tam5R cells by using a Seahorse XFe96 Analyzer.

Basal OCR, which reflects the respiration of the cells under the conditions provided in the culture medium, dropped from 62 pmol/min/10^4 cells in MCF7 Ctrl to 43 pmol/min/10^4 cells in MCF7 Tam5R cells. A less profound, yet still significant, difference was measured in the T47D cell line, which showed a decrease in the basal OCR from 40 pmol/min/10^4 cells in Ctrl to 29 pmol/min/10^4 cells in Tam5R cells. Similarly, the maximum respiratory capacity (measured after uncoupling OXPHOS by CCCP treatment) was significantly decreased in both Tam5R cell lines (from 72 pmol/min/10^4 cells in MCF7 Ctrl cells to 36 pmol/min/10^4 cells in MCF7 Tam5R cells; from 37 pmol/min/10^4 cells in T47D Ctrl cells to 24 pmol/min/10^4 cells in T47D Tam5R cells; Figures 7C and 7D). No alterations in the respiration that is not linked to ATP production (after inhibiting complex V by oligomycin addition) were detected between Ctrl and Tam5R cell lines. In addition, no differences were observed in the non-mitochondrial respiration, measured after inhibiting the ETC by the addition of rotenone and antimycin A.

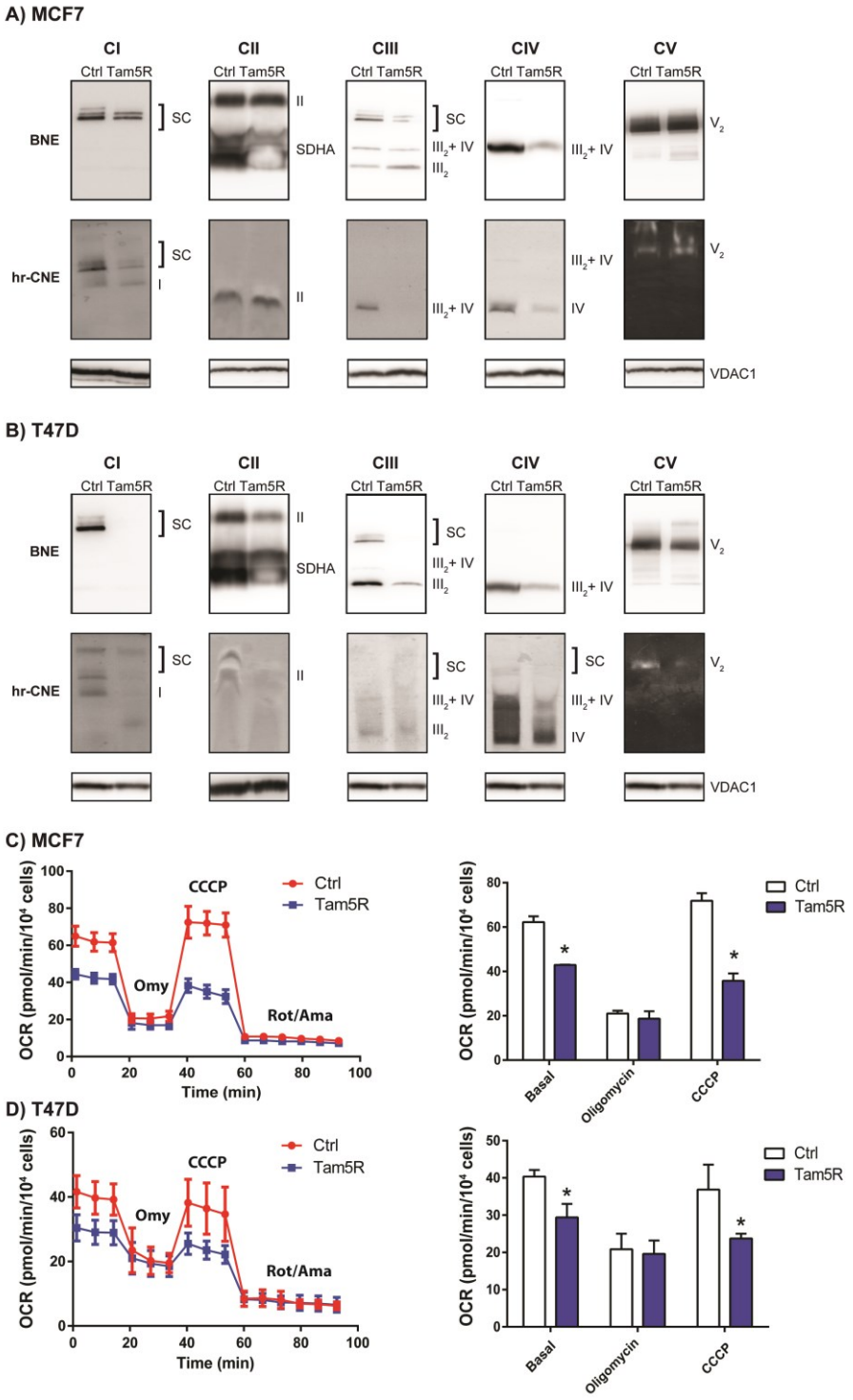

Figure 7. Tam5R cells show ETC dysfunction. Representative pictures from BNE (upper panels) and hr-CNE (lower panels) of **(A)** MCF7 and **(B)** T47D Ctrl and Tam5R cells showing the amount, assembly and activity of mitochondrial respiratory SCs. Experiments were performed from at least 3 independent sets of samples and VDAC1 was used as a loading control. Seahorse XFe96 flux analysis of OCR in **(C)** MCF7 and **(D)** T47D Ctrl and Tam5R cells. Average rates of basal, oligomycin inhibited and CCCP induced maximal respiration are shown as mean ± SD of at least 3 independent experiments. *$p \leq 0.05$ relative to Ctrl cells.

II.2.3 Tam5R cells have increased mitochondrial mass

Next, we tested the hypothesis that Tam5R cells compensate the decreased respiration by an increase in mitochondrial mass. Since mtDNA content reflects to some extent the amount of mitochondria, we compared the mtDNA/nuclear DNA ratio between parental and resistant cell lines (Figure 8A). MCF7 Tam5R cells exhibited an almost 1.8-fold higher ratio while no significant difference was detected in T47D Tam5R cells compared to parental cell cells.

To confirm those findings, we further assessed mitochondrial mass by immunostaining with the mitochondrial import receptor subunit TOM20 homolog (TOM20) with subsequent flow cytometry analysis (Figure 8B). Similarly to DNA ratio data, MCF7 Tam5R cells showed an almost 25% increase in fluorescence, while T47D Tam5R were not different from the parental ones. To investigate why T47D Tam5R cells do not increase their mitochondrial mass, we compared the basal level of mtDNA and TOM20 between parental cell lines. Results show that both parameters are higher in T47D cells compared to MCF7 cells (Figure 8B) and thus these cells contain significantly more mitochondria.

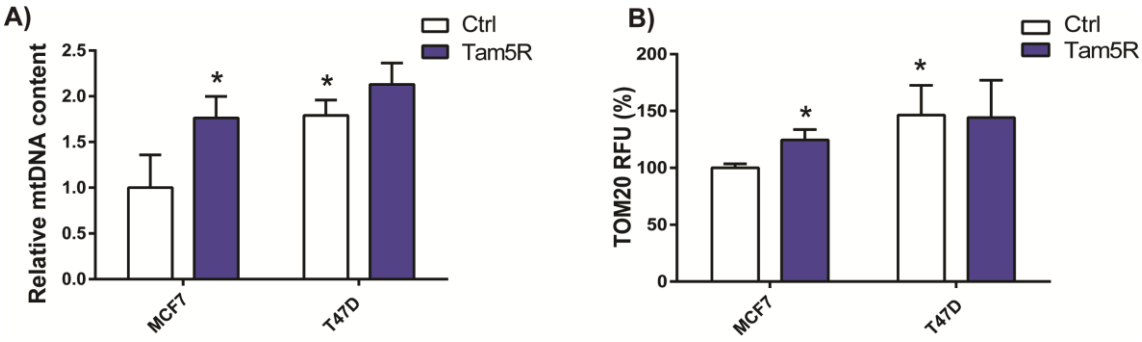

Figure 8. Assessment of mitochondrial mass. (A) Relative mtDNA content in MCF7 and T47D Ctrl and Tam5R cells measured by qPCR. **(B)** Mitochondrial mass in MCF7 and T47D Ctrl and Tam5R cells measured by TOM20 immunostaining followed by flow cytometry. Data are presented relative to MCF7 Ctrl cells and correspond to the mean ± SD of at least 3 independent experiments. *$p \leq 0.05$ relative to MCF7 Ctrl cells. RFU=relative fluorescence unit.

II.2.4 Tam5R cells have fragmented mitochondrial network

Mitochondrial dynamics strongly regulates mitochondrial function as well as cellular metabolism [99]. Hence, we compared the structure of the mitochondrial network between Ctrl and Tam5R lines by confocal microscopy.

The analysis of obtained images revealed that mitochondria of MCF7 Tam5R cells localized more to the cellular periphery, with a corresponding decrease in their perinuclear and medial localization (Figure 9A). Similarly, the localization of mitochondria in T47D Tam5R cells was rather medial and slightly radial while their perinuclear localization was significantly decreased (Figure 9B). Moreover, the number of individual mitochondria was markedly increased in both Tam5R cell lines (3.4- fold in MCF7 cells and 1.3- fold in T47D cells) compared to their parental counterparts. In addition, the average organelle size was smaller in Tam5R cells (2.2- fold in MCF7 cells and 1.8- fold in T47D cells; Figures 9C and 9D).

On the same line, we analyzed the level and phosphorylation status of the key regulator of mitochondrial fission DRP1. Results show that although the DRP1 protein level was not altered, the phosphorylation of DRP1 at Ser637 (activating) was significantly enhanced in both Tam5R cell lines while the phosphorylation at Ser616 (inhibiting) was hardly detectable (Figure 9E).

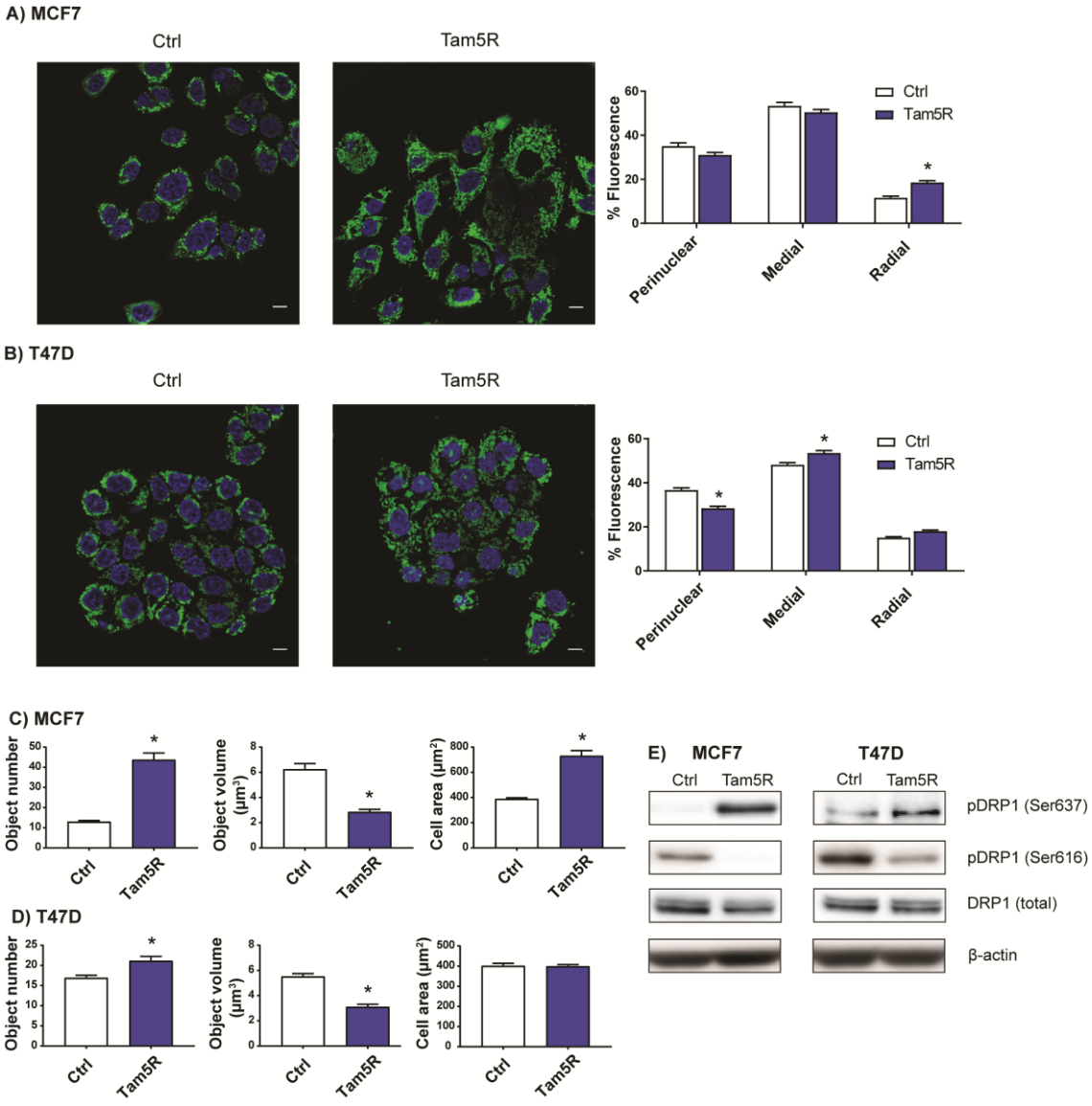

Figure 9. Tam5R cells have fragmented mitochondria. Representative confocal images of **(A)** MCF7 and **(B)** T47D Ctrl and Tam5R cells stained with MitoTracker Deep Red™ (green) and Hoechst (blue). Bar =10 µm. The quantification of total green fluorescence intensity in the perinuclear, medial and radial part of each cell is shown in graphs next. *$p \leq 0.05$ relative to Ctrl cells. Analysis of mitochondrial number and average size, and cell area of **(C)** MCF7 and **(D)** T47D Ctrl and Tam5R cells. *$p \leq 0.05$ relative to Ctrl cells. Analysis of images **(A-D)** was performed by the ImageJ software. Data are presented as mean values ± SD of at least 3 independent experiments, analyzing at least 50 cells from 5 images each. **(E)** Protein level and phosphorylation status of the DRP1 in MCF7 and T47D Ctrl and Tam5R cells evaluated by western blotting. The experiment was performed at least 3 times using independent samples. β-actin was used to assess proper loading.

II.2.5 Tam5R cells have elevated mitochondrial superoxide level accompanied by increased level of antioxidant enzymes

Due to the strong link between ETC activity, mitochondrial fragmentation and ROS production [131], we hypothesized that SCs disassembly and mitochondrial fragmentation might be accompanied by an increase in mitochondrial ROS level in Tam5R cells. Indeed, the mitochondrial superoxide level was significantly elevated in MCF7 Tam5R (1.9-fold increase) as well as in T47D Tam5R cells (2.5-fold increase) compared to Ctrl cells (Figure 10A). In line with these findings, both Tam5R cell lines showed an increase in ROS detoxifying enzymes SOD2 and glutathione peroxidase 1 (GPX1; Figure 10B). While MCF7 Tam5R cells also have increased level of the antioxidant enzyme catalase, this is not the case in T47D Tam5R cells (Figure 10B). Higher basal protein level of catalase in T47D cells compared to MCF7 cells together with noticeably higher basal level of mitochondrial superoxide and total cellular ROS may explain such difference (Figures 10A and 10C).

In addition, to see whether an increase in superoxide level is a persistent change following the continuous exposure to tamoxifen, we cultivated MCF7 Tam5R cells without tamoxifen for several weeks and measured mitochondrial superoxide level. Even in the absence of tamoxifen, Tam5R cells exhibited significantly elevated superoxide level (Figure 10D).

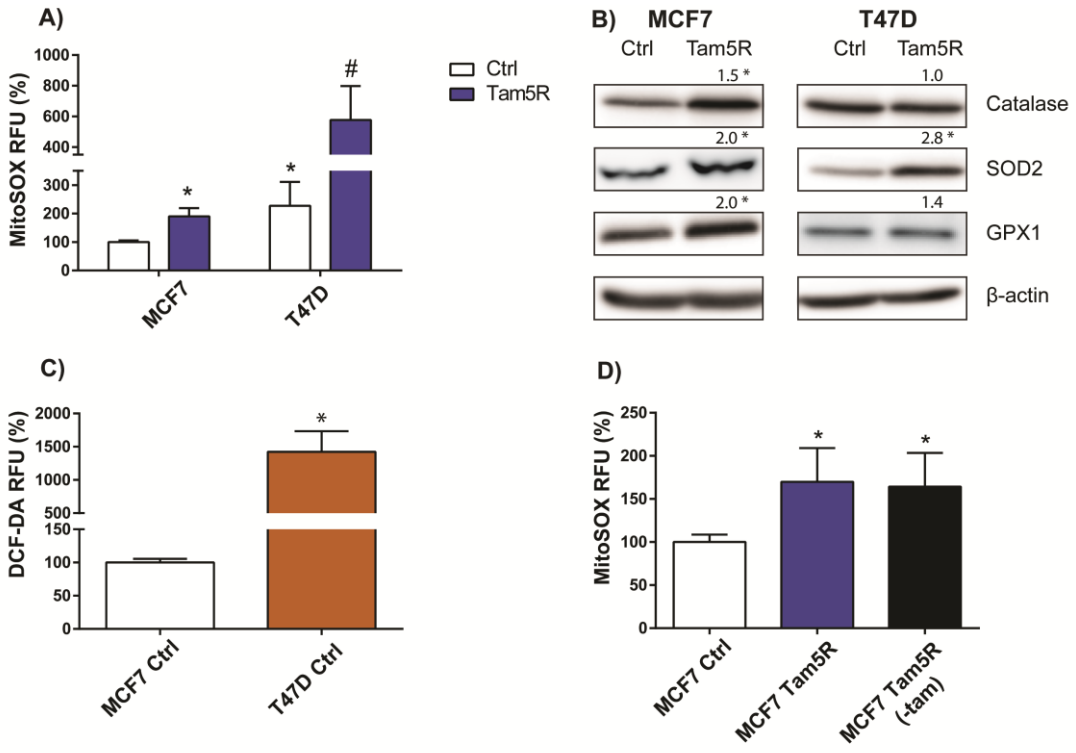

Figure 10. Tam5R cells exhibit elevated ROS and protein level of antioxidant enzymes. (A) Quantification of mitochondrial superoxide level in MCF7 and T47D Ctrl and Tam5R cells using the fluorescent probe MitoSOX™ by flow cytometry. Results are expressed as % of MitoSOX RFU normalized to MCF7 Ctrl cells and represent the mean ± SD of at least 3 independent experiments. *$p \leq 0.05$ relative to MCF7 Ctrl cells. # $p \leq 0.05$ relative to T47D Ctrl cells. **(B)** Protein level of antioxidant enzymes catalase, SOD2 and GPX1 in MCF7 and T47D Ctrl and Tam5R cells evaluated by western blot. Numbers above each band represent the mean value of band intensities quantified by ImageJ from at least 3 independent samples. *$p \leq 0.05$ relative to Ctrl cells. **(C)** Comparison of basal cellular ROS level in MCF7 and T47D Ctrl cells using the fluorescent probe DCF-DA by flow cytometry. **(D)** Quantification of mitochondrial superoxide level in MCF7 Ctrl, MCF7 Tam5R cells and MCF7 Tam5R cells cultivated without tamoxifen for 4 weeks, using the fluorescent probe MitoSOX™ by flow cytometry. Results are expressed as % of either (**C**) DCF-DA or (**D**) MitoSOX RFU normalized to MCF7 Ctrl cells and represent the mean ± SD of at least 3 independent experiments. *$p \leq 0.05$ relative to MCF7 Ctrl cells.

II.2.6 Tam5R cells have enhanced glycolysis, LDH-A_{low}/LDH-B_{high} phenotype and markedly activated mitochondrial aconitase

Our previous results documented a decrease in SCs together with lower respiration rates in Tam5R cells. Since cancer cells show metabolic plasticity and tend to switch from OXPHOS to glycolysis once mitochondrial function is compromised [104], we investigated the glycolytic status in Tam5R cells. Figure 11 demonstrates that both Tam5R cell lines have increased glucose uptake (1.47-fold in MCF7 and 1.26-fold in T47D

Tam5R cells; panel A) as well as extracellular lactate (1.32-fold in MCF7 and 1.19-fold in T47D Tam5R cells; panel B) compared to parental cells. To assess the proportion of ATP produced by glycolysis, the cells were treated with the uncleavable analogue of glucose, 2-DG (25 or 50 mM). We observed that the drop in ATP production was more profound in Tam5R cell lines (by 52% in MCF7 Tam5R vs. 35% in MCF7 Ctrl cells and by 59% in T47D Tam5R vs. 25% in T47D Ctrl cells; Figures 11C and 11D).

To further expand our findings, we measured the protein level of glucose transporter 1 (GLUT-1) together with several important enzymatic regulators of glycolysis such as hexokinase II (HKII), phosphofructokinase 2 (PFK2) or pyruvate dehydrogenase kinase 1 (PDK1; Figure 11E). Tam5R cells exhibit elevated protein level of all aforementioned proteins. Moreover, the lactate dehydrogenase A (LDH-A)/ lactate dehydrogenase B (LDH-B) ratio, that affects the direction of the pyruvate ↔ lactate reaction, was decreased in both Tam5R cell lines, suggesting higher tendency to convert lactate to pyruvate.

Similarly, in order to test the activity of the TCA cycle, we assessed the enzymatic activity and level of mitochondrial aconitase 2 (ACO2), which converts citrate to isocitrate. Increased activity and protein level (although not significant) of ACO2 was detected in MCF7 Tam5R and T47D Tam5R cells (Figure 11F). Despite the elevated activity of cytosolic aconitase 1 (ACO1) in MCF7 Tam5R cells compared to parental MCF7 cells, a decrease in ACO1 activity was observed in T47D Tam5R cells (Figure 11F).

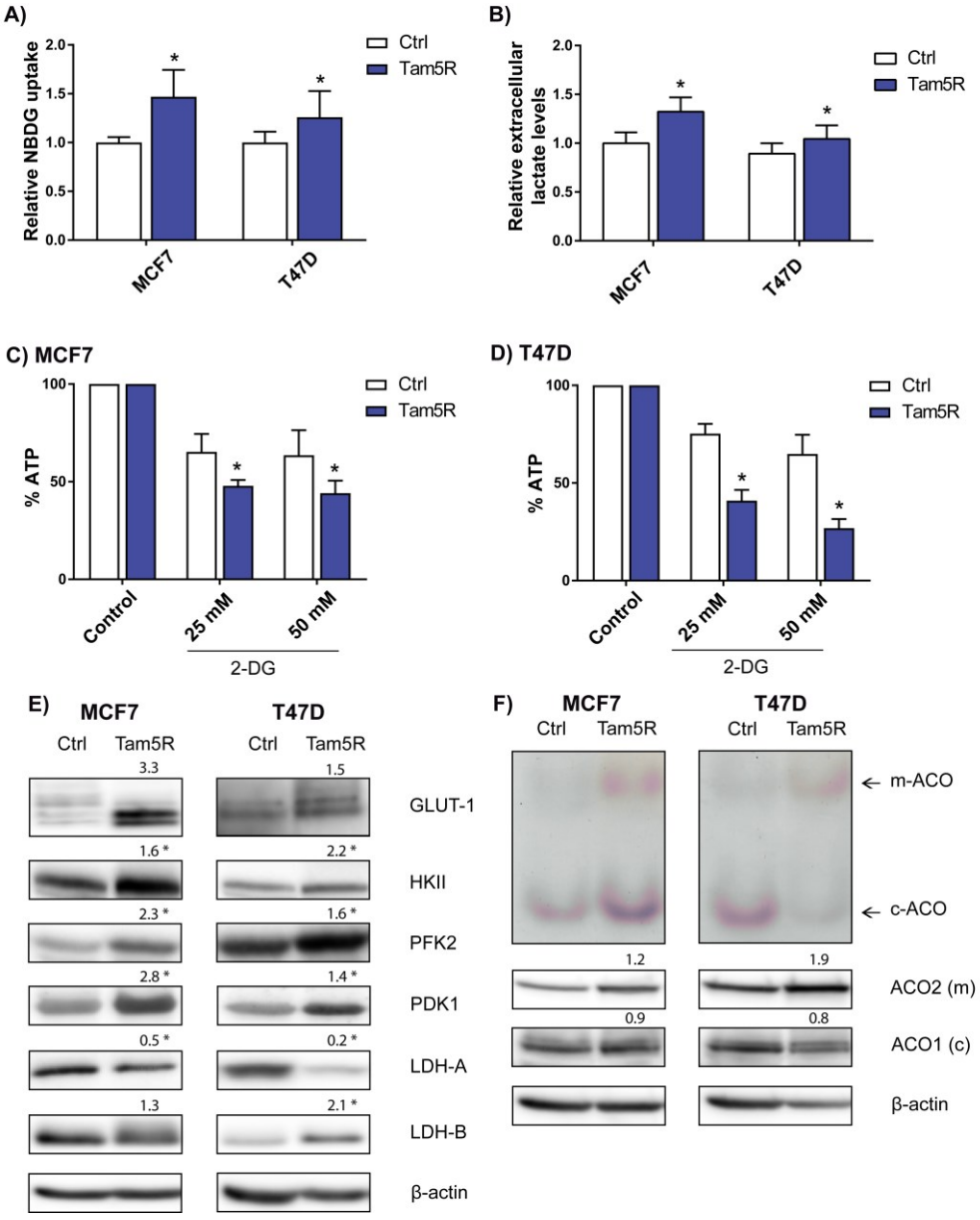

Figure 11. Tam5R cells show increased glycolytic dependence. (A) Glucose uptake of MCF7 and T47D Ctrl and Tam5R cells measured by NBDG probe and flow cytometry. **(B)** Extracellular lactate level of MCF7 and T47D Ctrl and Tam5R cells. **(A-B)** Data are shown as relative values compared to MCF7 Ctrl cells and represent the mean ± SD of at least 3 independent experiments. *$p \leq 0.05$ relative to corresponding Ctrl cells. ATP level in **(C)** MCF7 and **(D)** T47D Ctrl and Tam5R cells in the presence or absence of 2-DG (25 or 50 mM). Data are shown as % ATP level relative to each corresponding Ctrl condition and represent the mean ± SD of at least 3 independent experiments. *$p \leq 0.05$ relative to Ctrl cells with similar treatment. **(E)** Representative pictures of the protein level of the glucose transporter GLUT-1 and the glycolytic enzymes HKII, PFK2, PDK1, LDH-A and LDH-B in MCF7 and T47D Ctrl and Tam5R cell lines evaluated by western blot. **(F)** In-gel activity (upper panels) and protein level (lower panels) of mitochondrial and cytosolic aconitase. **(E-F)** Numbers above each band represent the mean value of band intensities quantified by ImageJ from at least 3 independent samples normalized to β-actin. *$p \leq 0.05$ relative to Ctrl cells.

II.2.7 Tam5R cells show increased phosphorylation of AMPK at Ser485/491 as well as increased level of SIRT3

In order to characterize the signaling pathways that could play a role in the metabolic rewiring in Tam5R cells, we first focused on the AMPK, since it is a fuel-sensing enzyme that has a major impact on cellular metabolism. Importantly, its activity is regulated by phosphorylation at different sites, resulting in either activation or inhibition [132]. When determining the phosphorylation status of AMPK we observed the phosphorylation at Ser485/491 to be significantly enhanced in both Tam5R cell lines (Figure 12A). In addition, the phosphorylation of Thr172 was decreased in T47D Tam5R and not changed in MCF7 Tam5R cells compared to parental cells (Figure 12A). Importantly, the phosphorylation pattern of downstream AMPK substrates was altered in both Tam5R cells, with an increase in phosphorylation of most substrates and a decrease in a few of them, suggesting overall activation of the kinase (Figure 12A).

Other important metabolic sensors are NAD(+)-dependent deacetylases – sirtuins. The major deacetylase regulating mitochondrial function is mitochondrially localized SIRT3 [133]. After assessing the protein level of SIRT3 in Ctrl and Tam5R cells, we detected increased expression in both Tam5R cells compared to parental cells (Figure 12B).

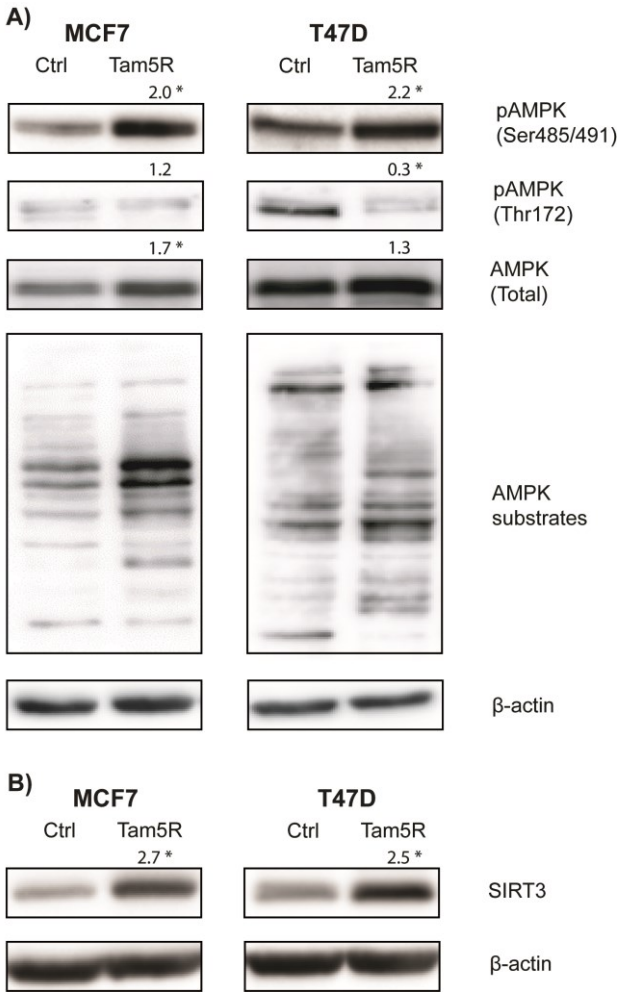

Figure 12. Tam5R cells exhibit AMPK activation and increased protein expression of SIRT3 **(A)** The phosphorylation of AMPK at Ser485/491 and Thr172, total AMPK level and phosphorylation pattern of AMPK substrates in MCF7 and T47D Ctrl and Tam5R cells evaluated by western blot. **(B)** Protein level of the mitochondrial SIRT3 in MCF7 and T47D Ctrl and Tam5R cells evaluated by western blot. Numbers above each band represent the mean value of band intensities quantified by ImageJ from at least 3 independent samples normalized to β-actin. *$p \leq 0.05$ relative to Ctrl cells.

II.2.8 MCF7 cells lacking mitochondrial DNA are resistant to tamoxifen

To further demonstrate the relationship between tamoxifen resistance and diminished mitochondrial function, we used ρ0 cells. ρ0 cells lack mtDNA, resulting in the absence of mitochondrial respiratory complexes I, III and IV, thus being respiratory deficient. Since we observed a major decrease in mitochondrial SCs in Tam5R cells, we hypothesized that ρ0 cells may resemble the phenotype of Tam5R cells and should be resistant to tamoxifen. We measured cell death in MCF7 ρ0 cells after the incubation with 10, 12.5 or 15 μM tamoxifen for 48 hours. Only 32% cell death was induced by 15 μM

tamoxifen in ρ0 cells in comparison with parental MCF7 cells which showed 75% cell death at the same concentration (Figure 13). Interestingly, MCF7 ρ0 cells were even more resistant to tamoxifen that MCF7 Tam5R cells (50% cell death in 15 μM tamoxifen), thus confirming our hypothesis.

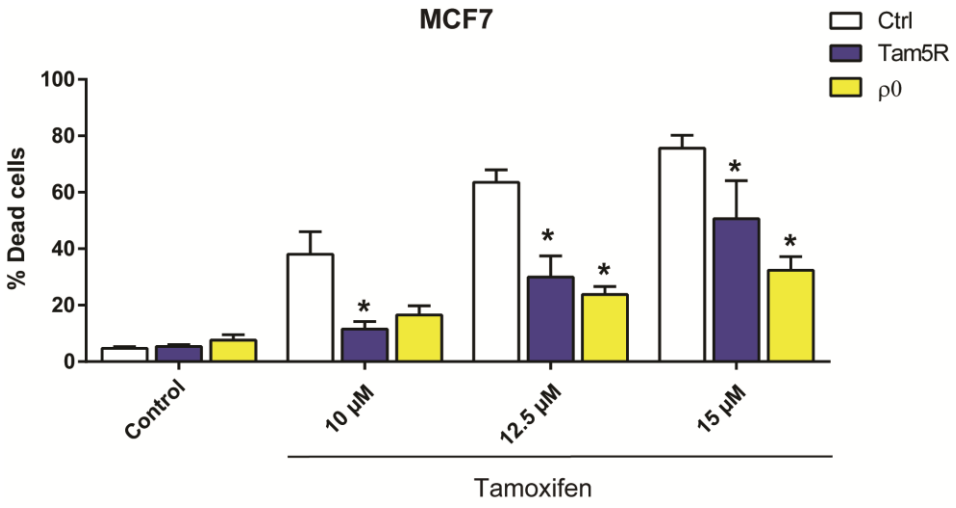

Figure 13. MCF7 ρ0 cells are resistant to tamoxifen. Assessment of cell death in MCF7 Ctrl, Tam5R and ρ0 cells after 48 hour incubation with tamoxifen, measured by AV/PI double staining. Results are expressed as mean % dead cells ± SD of at least 3 independent experiments. *$p \leq 0.05$ relative to Ctrl cells

II.3 Discussion

Tamoxifen represents one of the most used drugs in endocrine therapy for breast cancer [134]. Yet, the resistance to tamoxifen still remains a major clinical problem. Many patients are diagnosed either with *de novo* resistance and do not respond to the therapy from the beginning or acquire resistance to tamoxifen during the treatment and experience relapse [33].

Interestingly, besides the well described effect of tamoxifen on ER signaling, several reports document its effect on the mitochondrial function [124-126]. Although a possible link between tamoxifen resistance and mitochondria has already been proposed [128, 129], a deeper mechanistical insight into this topic is still missing. For this reason, the present work analyzed different aspects of mitochondrial function and metabolism in the *in vitro* model of tamoxifen resistant cells [130].

Since several reports linking tamoxifen and mitochondria point out that the complexes of the ETC are direct targets of the drug, we first analyzed the composition of SCs in Tam5R cells. Our results not only show the expected decrease in the activity of all the forms of SCs but also revealed their decreased abundance and altered composition in Tam5R cells. In line with these findings, such disassembly of SCs was coupled with a drop in basal and maximal respiration rates in resistant cells, although interestingly, to a much lesser extent than we expected. Such discordance could indicate the ability of Tam5R cells to respire through individual complexes. Of note, similar changes in maximal respiratory capacity were observed in 4-OH tamoxifen resistant LCC2 cells by Radde et al. [129]; however, basal respiration was not changed in their model. Furthermore, Fiorillo et al. [128] reported increase in both basal and maximal respiration in Tam5R cells, which is not in agreement with our data. Conflicting results might be explained by different experimental models as well as different cultivation conditions (phenol red free medium, charcoal stripped serum, 4-OH tamoxifen) as already discussed in detail in chapter I.3.

Since the decrease in the respiration in Tam5R cells was not as dramatic as we expected, we also speculated that Tam5R cells may compensate for deficient respiration through SCs by increasing their mitochondrial mass. Initially, we used the MitoTracker™ Deep Red FM probe to measure mitochondrial mass. Yet, we saw that in our setup, the labeling seemed to be dependent on mitochondrial membrane potential, which differed between Ctrl and Tam5R cells. Therefore, we decided to assess mitochondrial mass by measuring the amount of mtDNA and mitochondrial marker

TOM20 in Ctrl and Tam5R cells instead. Both experiments confirmed increased mitochondrial mass in MCF7 Tam5R cells, but no change in T47D Tam5R cells. A possible explanation is that since T47D parental cells have higher basal mitochondrial mass compared to MCF7 parental cells, they might have reached the achievable maximum and cannot further increase the amount of mitochondria. Therefore, we may speculate that MCF7 Tam5R cells partially compensate for their decreased respiration with increased mitochondrial mass while T47D Tam5R cells are not able to do so and probably still respire through individual CIV, as OCR measurement actually measures oxygen consumption by CIV.

The observed disassembly of respiratory SCs could be linked not only with impaired respiration, but also with increased ROS production [135, 136]. In agreement with such observations, Tam5R cells showed elevated level of mitochondrial superoxide. Importantly, high mitochondrial ROS may lead to mtDNA mutations, which have been shown to enhance metastatic potential and tumorigenicity [137]. Since withdrawal of tamoxifen from the cultivation medium in MCF7 Tam5R cells for 28 days did not change the mitochondrial superoxide level, we propose that mitochondrial ROS play an important role in the maintenance of the resistant phenotype.

Importantly, a connection between enhanced ROS production and mitochondrial fragmentation has also been reported [131, 138], being another characteristic of cancer stem-like cells and indicative of a more malignant phenotype [6, 139-142]. We documented a more fragmented mitochondrial network and decreased perinuclear mitochondrial localization in Tam5R cells, supported by an increase in the activating phosphorylation of DRP1, and a decrease in the inhibiting one. Even though such phosphorylation status is commonly connected with the inhibition of mitochondrial fission, some reports document increased fission under the same conditions [143, 144]. Mitochondrial fragmentation has also been reported to increase the migratory capacity of breast cancer cells, where mitochondrial accumulation at the edge of the cell provides energy utilized in the migration process [142, 145]. Although no experiments were performed in order to determine the migratory abilities of Tam5R cells, we can speculate that enhanced mitochondrial fission in Tam5R cells could be connected with an increased metastatic potential. Yet, this needs further experimental work.

Furthermore, mitochondrial fission can be triggered by the AMPK activation [141, 146] and has been shown to promote a metabolic switch of cancer cells from OXPHOS to glycolysis [147]. Cancer cells often switch to alternative pathways to

produce energy and the metabolic intermediates used for anabolic reactions when their mitochondrial function is impaired. Such change is also important for the migration, invasion and metastasis [148]. In line with this notion, mitochondrial dysfunction (reflected by SCs disassembly, lower respiration and significant mitochondrial fragmentation) in Tam5R cells was accompanied by AMPK activation and increased glycolytic dependence. Even though the AMPK phosphorylation pattern observed in Tam5R cells is considered to inhibit AMPK activity, increased phosphorylation of downstream AMPK targets rather documented an activation of the pathway in our conditions. Moreover, acute tamoxifen treatment can activate AMPK and enhance glucose uptake, as reported in [149], supporting the possible role of AMPK in the regulation of the metabolic switch in Tam5R cells.

Tam5R cells also showed a significantly lower LDH-A/LDH-B ratio, suggesting that the direction of the pyruvate↔lactate reaction is shifted to pyruvate. Thus, it seems that despite their increased lactate production, Tam5R cells do not convert all pyruvate to lactate and preferentially utilize pyruvate for other metabolic processes. Some of these processes might be anaplerotic reactions which can replenish metabolic pools of intermediates to fuel the TCA cycle [150]. For example, the conversion of pyruvate to oxaloacetate may increase mitochondrial biogenesis and prevent the damage induced by ROS [151]. The latter observation, together with the increased activity of mitochondrial aconitase in Tam5R cells, which converts citrate to isocitrate in the TCA cycle, could indicate that Tam5R cells employ a pyruvate/isocitrate cycle to produce nicotinamide adenine dinucleotide phosphate (NADPH) and α-ketoglutarate [152-154] which could serve as an additional antioxidant mechanism [155, 156].

Similarly to AMPK, sirtuins are also important regulators of cellular metabolism. Indeed, AMPK and sirtuins can activate each other through posttranslational modifications such as phosphorylation or deacetylation [157-159]. Several members of the sirtuin family participate in the regulation of mitochondrial biogenesis or glycolysis [133]. Mitochondrially localized SIRT3 has been shown to regulate cellular metabolism, stress response and antioxidant defense mechanisms [160-163]. In agreement with an already published study [164], protein level of SIRT3 was increased in both Tam5R cell lines. Since SIRT3 has been shown to upregulate SOD2 and catalase expression and is also involved in the process of assembly of the ETC components [163], its increased expression may be a response to SCs disassembly and high mitochondrial ROS level.

Noteworthy, by activating isocitrate dehydrogenase 2 (IDH2; catalyzes reaction isocitrate → α-ketoglutarate) [165] as well as acetyl-CoA synthetase 2 (ACS2; converts acetate into acetyl-CoA) [166], SIRT3 may play an important role in the metabolic rewiring of Tam5R cells [133]. In addition, higher protein level and activity of mitochondrial ACO2 in Tam5R cells produce isocitrate, which, after conversion to α – ketoglutarate by IDH2, is transported *via* the citrate/α-ketoglutarate shuttle into the cytosol and can serve as starting carbon skeleton for further anabolic reactions [167].

In summary, we believe that, in parallel with a mitochondrial dysfunction, there is an increased flux through the first reactions of the TCA cycle in Tam5R cells in order to support the production of metabolic intermediates that serve as precursors for biosynthetic pathways. However, there is still a clear need for more comprehensive metabolomic analysis in order to fully understand the metabolic rewiring of Tam5R cells.

Finally, a model of cells lacking mtDNA (ρ0 cells) was employed to answer the question whether the presence of dysfunctional mitochondria would affect the response to tamoxifen. MCF7 ρ0 cells do not contain functional mitochondrial respiratory complexes except intact CII, due to lack of the 13 protein subunits coded by mtDNA, and are thus respiration-deficient [10]. We hypothesized that they may exhibit a similar phenotype to our Tam5R cells. Interestingly, MCF7 ρ0 cells were actually even more resistant than MCF7 Tam5R cells, in line with the report that mtDNA depletion leads to tamoxifen resistance [168]. These data corroborate our hypothesis that low mitochondrial respiration and "dysfunction" of mitochondria support resistance to tamoxifen.

III. Iron metabolism and tamoxifen resistance

III. 1 Literature overview

III.1.1 The role of iron in biological systems

Iron is an essential micronutrient necessary for the vast majority of living organisms. The biologically active iron is incorporated into proteins in the form of heme or Fe-S clusters [169]. Iron bound within heme is crucial for oxygen transport in erythrocytes (hemoglobin) and muscle cells (myoglobin) and plays an important role in the mitochondrial ETC (cytochromes) and ROS detoxification (catalase). Iron in the form of Fe-S clusters is present in proteins participating in DNA synthesis (DNA primase, DNA polymerase), production of ribonucleotides (ribonucleotide reductase), energy metabolism (mitochondrial aconitase) and in mitochondrial respiratory complexes I-III [170, 171].

On the other hand, free iron in cells is potentially toxic as it participates in Haber-Weiss and Fenton reactions, generating the highly toxic hydroxyl radical along with other ROS, resulting in oxidative stress and subsequently damage of DNA, proteins or lipids [172]. High iron reactivity is attributed to its ability to easily donate and accept electrons and shuttle between reduced ferrous (Fe^{2+}) and oxidized ferric (Fe^{3+}) form [173].

Approximately 1-2 mg of nutritional iron is absorbed daily in the proximal duodenum by enterocytes. The absorbed iron that is not used or stored within these cells is transferred across the duodenal mucosa into the blood stream and transported *via* transferrin (Tf) to recipient tissues [174]. A substantial amout of iron is utilized in the bone marrow for erythropoesis (hemoglobin synthesis) and is recycled by reticuloendothelial macrophages. Iron which is not further used in the cellular processes is stored in the recycling macrophages in the spleen or in hepatocytes, both representing important iron storage sites of the human body [175]. Only 1-2 mg of iron is lost daily, primarily through desquamation of epithelial cells in the skin and gut, or blood loss in women during menstruation. However, these processes are not regulated and therefore the systemic iron level needs to be mainly maintained through absorption and recycling. Hepcidin, a 25 AA peptide regulates systemic iron metabolism by governing both iron transport from enterocytes into the circulation and its release from macrophages and hepatocytes. The molecular mechanism underlying its function involves a direct

interaction of hepcidin with the iron exporter ferroportin (FPN), inducing its internalization and thus inhibiting its function [176]. Decreased amount of hepcidin has been connected with mutations in the gene coding for hemochromatosis protein (*HFE*), resulting in the iron overload disease hereditary hemochromatosis [177].

III.1.2 Cellular iron trafficking

Since iron is a higly reactive element, maintaining its proper level and utilization within cells is crucial for maintaining cellular homeostasis. The representative scheme of cellular iron metabolism is shown in Figure 14.

III.1.2.1 Iron uptake

As already mentioned, transport of almost all non-heme iron through the bloodstream is mediated by the iron-binding protein Tf. The Tf-bound cellular iron uptake is facilitated by the transferrin receptor 1 (TfR1) localized in the plasma membrane of the recipient cells. A holo-Tf carrying two Fe^{3+} atoms binds to TfR1, which then undergoes clathrin-mediated endocytosis and is internalized within endosomes. An endosomal proton pump acidifies the endosomal environment, triggering the release of iron from Tf. Fe^{3+} is then reduced to Fe^{2+} form by ferrireductase six transmembrane epithelial antigen of the prostate 3 (STEAP3) and transported out of the endosome by divalent metal transporter 1 (DMT1) or the zinc transporter 14 (ZIP14). Finally, iron-free apo-Tf is delivered back to the cellular surface and secreted into the bloodstream to bind additional Fe^{3+} ions [175, 178].

Under iron overload conditions, iron can also circulate in the plasma as non-transferrin-bound iron (NTBI). In order to be taken up by cells, the NTBI is first reduced from Fe^{3+} to Fe^{2+} in the extracellular space by cytochrome b reductase 1 (CYBRD1; alternative name duodenal cytochrome B -DCYTB) and then transported into the cell *via* transporters ZIP14 [179] or DMT1 [180], representing an alternative pathway for iron uptake.

III.1.2.2 Iron storage and utilization

Acquired cellular iron initially enters the labile iron pool (LIP), which is characterized as a loosely bound, chelatable pool of redox active iron ions associated

with various types of ligands [181]. From LIP, iron is either utilized, stored or exported out of the cells.

Cytoplasmic chaperons poly(rC)-binding protein 1 and 2 (PCBP1 and PCBP2) help deliver iron to the iron-storage protein ferritin [182]. This protein is composed of 24 subunits of heavy (H) and light (L) chains forming a shell-resembling nanocage that allows the storage of around 4500 iron atoms mostly in the mineral form. H chains of ferritin possess ferroxidase activity, facilitating the conversion of Fe^{2+} to Fe^{3+}, while L chains promote nucleation and storage of Fe^{3+}. Iron stored as ferritin is bioavailable and can be easily transported out *via* pores in the nanocage [183].

Iron from LIP is directed to mitochondria, central organelles for iron utilization, *via* mitoferrin 1 or 2 (MFRN1 or MFRN2) [184]. MFRN1 physically interacts with the ABCB10 transporter and therefore facilitates mitochondrial iron import [185]. An alternative mechanism termed "kiss and run" has been postulated, suggesting that iron can be delivered to mitochondria *via* direct contact of endosomes and mitochondria [186]. Once taken up, mitochondrial iron can be either stored in the form of mitochondrial ferritin (FtMt) [187], or utilized for heme or Fe-S clusters synthesis [184].

Fe-S cluster biogenesis inside mitochondria is a multistep process orchestrated by the iron-sulfur cluster assembly enzyme (ISCU) together with the accessory proteins nitrogen fixation 1 (*S. Cerevisiae*, homolog) cysteine desulfurase (NFS1), LYR motif-containing protein 4 (LYRM4) and frataxin (FXN). Nascent Fe-S clusters are then released from the scaffold and either delivered to target mitochondrial apoproteins *via* chaperon systems with help of specialized transfer proteins such as glutaredoxin 5 (GLRX5) [184], or used for the synthesis of so far unknown sulfur-containing compounds and exported from mitochondria for cytosolic and nuclear Fe-S cluster assembly [188].

Heme biosynthesis is an 8-step biosynthetic pathway that occurs both in cytosol and in mitochondria. The first step is initiated in mitochondrial matrix and involves the synthesis of the heme precursor aminolevulinic acid (ALA) by ALA synthase. ALA is then transported to the cytosol where it undergoes a series of 4 reactions resulting in the formation of coproporphyrinogen III, which is translocated back into mitochondria. Coproporphyrinogen III is then oxidized to protoporphyrinogen IX and protoporphyrin IX. The terminal step includes the insertion of Fe^{2+}into the protoporphyrin IX ring to produce heme, catalyzed by the enzyme ferrochelatase [189, 190].

III.1.2.3 Iron export

Cells export Fe^{2+} iron *via* FPN. Subsequently, the ferroxidases hephaestin (HEPH) or serum ceruloplasmin convert Fe^{2+} to Fe^{3+}, which can further bind Tf [191]. FPN is the sole known iron mammalian exporter, coded by the solute carrier family 40 member 1 (*SLC40A1*) gene and its interaction with hepcidin regulates its abundance and iron transporter activity, thus playing a crucial role in systemic iron homeostasis [176].

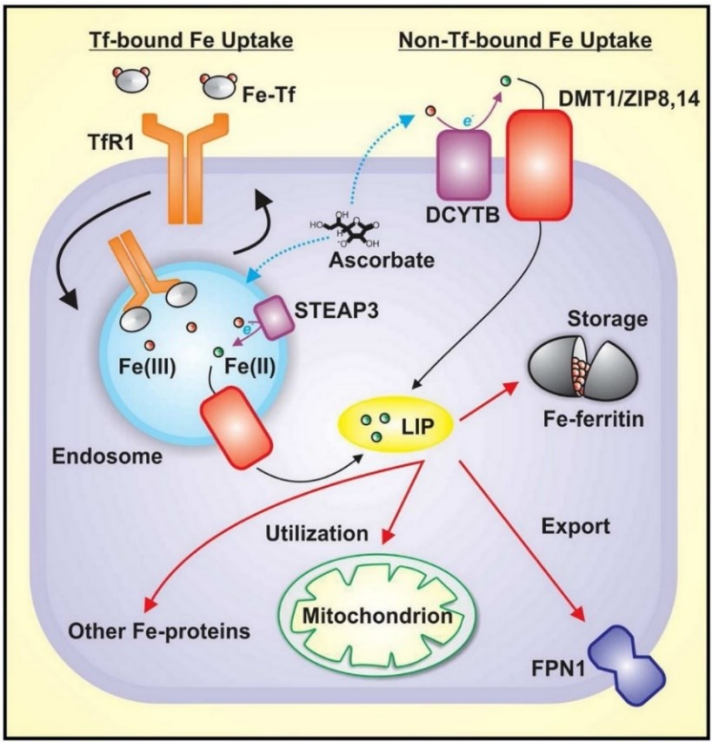

Figure 14. Cellular iron trafficking. Two major pathways of iron uptake are shown in the picture. Iron bound to Tf enters the cell through TfR1 on the cell surface *via* receptor-mediated endocytosis. NTBI is reduced to Fe^{2+} form by ferrireductases and transported *via* DMT1, ZIP8/ZIP14 inside the cell. Acquired iron then enters LIP and is further directed to mitochondria for Fe-S clusters and heme synthesis, or is incorporated in other iron-containing proteins necessary in processes such as DNA synthesis and repair or cell cycle regulation. Iron which is not utilized is either stored in the form of ferritin or exported out of the cell *via* FPN (adapted from [175]).

III.1.3 Regulation of intracellular iron metabolism

Maintaining balanced cellular iron level requires strict regulatory mechanisms. One of such mechanisms is the iron responsive protein/iron regulatory element (IRP/IRE) system. Iron responsive protein 1 (IRP1; encoded by *ACO1* gene) and iron responsive protein 2 (IRP2; encoded by *IREB2* gene) are cytosolic proteins which can sense intracellular iron level and regulate iron homeostasis. Under iron deficiency, IRP1 and IRP2 bind to IREs in the 5´ or 3´ untranslated regions (UTRs) of the mRNAs which encode for proteins involved in iron uptake, storage and export [192].

The localization of the IREs determines the final effect on the corresponding mRNA and protein level. IRPs bound to 5´UTR IREs prevent the translation of mRNAs by blocking the recruitment of ribosomes. On the contrary, binding of IRPs to 3´UTR IREs leads to mRNA stabilization by protecting it against degradation by endonucleases. These events ensure stimulation of iron uptake while decreasing iron storage and export.

In iron replete cells, IRP1 binds a 4Fe-4S cluster and gains enzymatic aconitase activity, while IRP2 is proteasomally degraded *via* F-Box And Leucine Rich Repeat Protein 5 (FBXL5) [193]. Therefore, when intracellular iron level is high, IRPs are removed from IREs resulting in enhanced translation of mRNAs containing 5´UTR IREs and increased degradation of mRNAs bearing 3´UTR IREs [194] (Figure 15). This scenario thus leads to a lower iron uptake and an increase in iron storage and export.

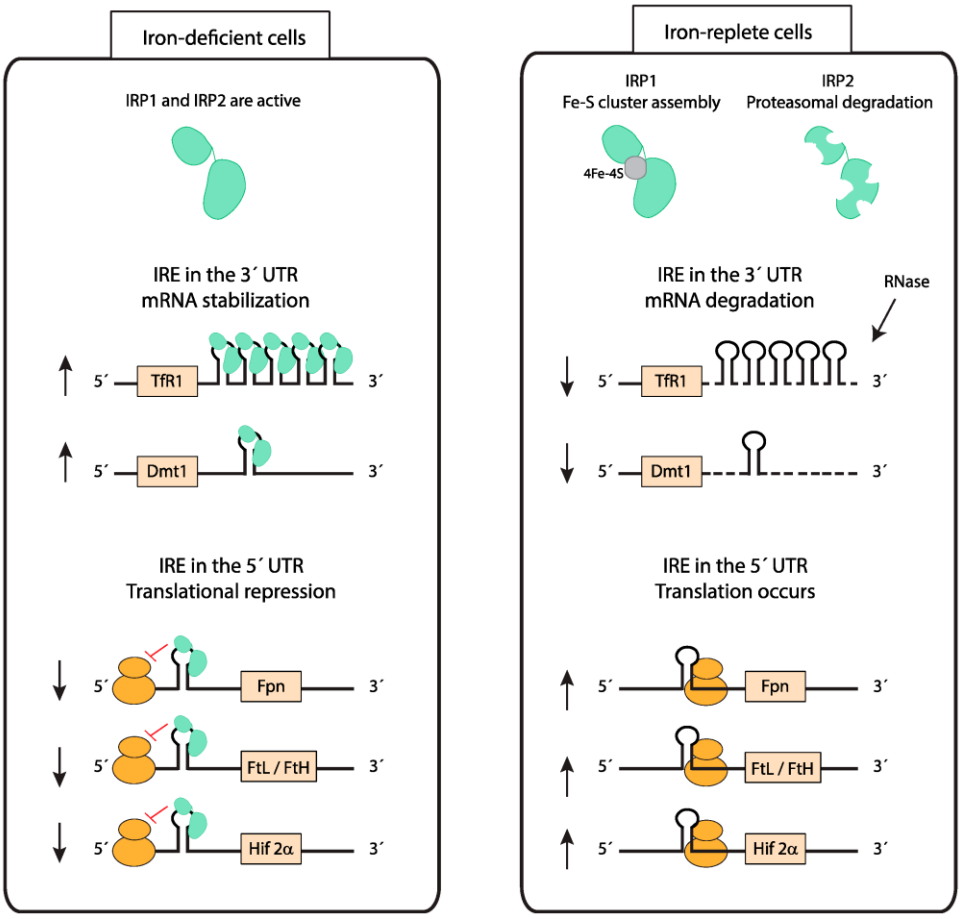

Figure 15. The control of cellular iron homeostasis by the IRP/IRE system. In iron-low conditions, IRP1 and IRP2 are active. Binding of IRPs to IREs localized in the 3′ UTR leads to mRNA stabilization while binding to IREs within 5′UTR of mRNA leads to translational repression. In such scenario, the cells increase iron uptake (↑ TfR1, ↑DMT1 expression) and decrease iron storage and export (↓FPN, ↓ferritin expression). Under high-iron conditions, IRPs do not bind to IREs. Instead, IRP2 is targeted for proteasomal degradation while IRP1 is converted to cytosolic aconitase by binding to a 4Fe-4S cluster. Subsequently, iron uptake is decreased and iron storage and export increased (adapted from [195]).

The regulation of iron metabolism and hypoxia are intertwined. Indeed, IRPs not only respond to intracellular iron level but are also responsive to hypoxia [196, 197], since *IRP1* contains hypoxia responsive elements (HREs) in its 5′UTR mRNA [198]. Furthermore, a hypoxic environment activates hypoxia-inducible factors (HIFs) which bind HREs in the promoters of their target genes, including some involved in iron metabolism such as Tf, TfR1 or ferritin [199]. In addition, HIF2α (also known as

endothelial PAS domain-containing protein 1 – EPAS1) is controlled by IRP1 *via* its 5'UTR IRE, and plays a key role in erythropoesis and iron absorption [200].

Noteworthy, iron is a required cofactor for prolyl hydroxylases that mark HIFs for degradation under normoxic conditions [201]. Thus, regardless of oxygen status, low iron level results in diminished hydroxylation and stabilization of HIFs. This process is termed as a 'pseudohypoxia' and has been connected with tumorigenesis [202].

One of the proteins regulated by HIFs is quiescin sulfhydryl oxidase 1 (QSOX1) which is responsible for disulfide bond formation during protein folding in the Golgi aparatus [203]. QSOX1 is a human ortholog of the yeast ERV protein, which has been shown crucial for Fe-S cluster biogenesis in yeasts [204]. QSOX1 can also be secreted into extracellular space where it helps to remodel extracellular matrix [203]. Moreover, high protein level of QSOX1 seems to be connected with the CSC phenotype [6] and the invasivity of the cells [205, 206].

III.1.4 Iron metabolism and cancer

Iron plays a dual role in cancer. As an essential growth factor, iron participates in regulating energy metabolism, proliferation, cell cycle and DNA replication. Therefore, the iron demand of cancer cells, which need to proliferate and replicate their DNA faster, is higher [207]. On the other hand, free iron promotes the formation of free radicals through Fenton reaction thus causing DNA mutations resulting either in cell death or malignant transformation [207].

Many studies document reprogrammed iron metabolism in various types of cancer, with a palette of differentially regulated proteins that participate in iron metabolism [208]. Increased iron uptake mediated by elevated protein level of TfR1 has been confirmed for many types of cancer including breast and colon cancer [208-210]. Besides increased iron uptake, some cancer cells have increased expression of ferritin. Iron sequestered by ferritin is not able to participate in ROS formation, thus protecting cancer cells from oxidative damage, and it also represents an iron reservoir for times where iron is limited [211]. In agreement with this, iron efflux facilitated by FPN, and controlled by the hormone hepcidin, is often diminished in cancer, leading also to accumulation of iron in cancer cells [211].

Furthermore, it has been shown that people with chronic iron overload diesases such as hereditary hemochromatosis have increased risk of liver or colon cancer due to

excessive iron accumulation, thus confirming the importance of iron for cancer initiation and promotion [212]. Importantly, various strategies for iron deprivation to treat cancer have been intensively studied over the past years. By using iron chelators, gallium-based compounds functioning as iron mimetics, or antibodies against TfR1 it is possible to either deprive cancer cells of iron or interfere with their iron metabolism, thereby inhibiting DNA synthesis, and inducing cell cycle arrest and apoptosis [208, 213].

Similarly to cancer cells, alterations in iron trafficking have been described in CSCs [214]. Level of TfR1 and its ligand Tf was reported to be increased in glioblastoma CSCs that uptake iron more effectively from extracellular environment [215]. Similar observations were published by Mai et al. in BCSCs [216]. In the study published by our laboratory, mammospheres showed activation of the IRP/IRE system resulting in increased iron uptake and decreased iron storage. Enzymatic activity of Fe-S cluster containing enzymes was diminished, together with reduced GSH level and increased ROS level. We also documented increased LIP, preferential mitochondrial iron accumulation and higher sensitivity to iron chelation, thus confirming the important role of redox balance and iron metabolism in the phenotype of BCSCs [6].

As already shown in the first part of this thesis, Tam5R cells exhibit stem-like cell properties making them reminiscent to BCSCs. To our knowledge, there is only one publication dealing with iron metabolism in tamoxifen resistant breast cancer cells [209]. However, it is focused only on TfR1, thus not bringing any detailed information about the iron metabolism in this resistant model. Given the importance of iron for cancer cells in general, we investigated the expression of genes that participate in iron uptake, trafficking, storage and utilization in our model of Tam5R cells. Taking into account the poor prognosis and more aggressive phenotype of Tam5R cells, understanding the principles and changes in their iron metabolism may lead to development of novel approaches resulting in a more effective and targeted cancer therapy.

III. 2 Results

Some results presented in this chapter were published as supplementary data in:

Rychtarcikova Z, Lettlova S, **Tomkova V**, Korenkova V, Langerova L, Simonova E, Zjablovskaja P, Alberich-Jorda M, Neuzil J, Truksa J. (2017) Tumor-initiating cells of breast and prostate origin show alterations in the expression of genes related to iron metabolism. Oncotarget 8(4): 6376–6398.

The main purpose of the paper was to analyze iron metabolism in different models of CSCs, including MCF7 Tam5R breast cancer cells. In order to provide a more detailed overview of iron trafficking in these cells, we performed further experiments and included also another Tam5R cell line derived from T47D breast cancer cells. These latter results are unpublished.

III.2.1 Tam5R cells show altered expression of iron metabolism-related genes and corresponding proteins

In the original manuscript the expression profile of the genes related to iron metabolism was assessed in CSCs derived from various cancer cell lines as well as in Tam5R MCF7 cells. Genes with changes in expression higher than 1.55-fold in at least 2/3 of the tested cell lines were selected for further analysis on protein level. The list of all tested genes is shown in the supplementary data of the original manuscript together with their protein level (Supplement, *Oncotarget* Supplementary Table 1, Supplementary Figure S5 and S6) [6]. To assess the alterations in the iron metabolism-related genes and proteins in Tam5R cells, we further expanded our analysis to T47D Tam5R cells. Thus, here we first show expression profile of genes related to iron metabolism in MCF7 Ctrl and Tam5R cells (Figures 16A and 17A) that were included in the *Oncotarget* manuscript and assessed by Fluidigm qPCR. The expression of identical genes was then evaluated in T47D Ctrl and Tam5R cells by standard qPCR (Figures 16B and 17B), with subsequent western blot analysis in both Ctrl and Tam5R cell lines (Figures 16C, 17C and 17D).

When assessing the changes in genes and proteins related to iron uptake, we observed significant upregulation of *TFRC* gene (coding for TfR1) in MCF7 Tam5R cells

compared to MCF7 Ctrl cells; however, this was not confirmed on the protein level where we detected decreased TfR1 expression in MCF7 Tam5R cells. On the contrary, T47D Tam5R cells exhibited elevated protein level of TfR1 in comparison with parental T47D cells, even though *TFRC* expression was not changed. Despite the fact that mRNA level of other genes participating in iron uptake were not changed in MCF7 Tam5R cells, an increased amount of protein was observed in case of CYBRD1 and DMT1 (encoded by solute carrier family 11 member 2 - *SLC11A2* gene), and a slight decrease in ZIP14 level (encoded by solute carrier family 39 member 14 -*SLC39A14* gene). *CYBRD1*, *SLC11A2* and *SLC39A14* genes were found overexpressed in T47D Tam5R cells compared to parental cells. Similarly, T47D Tam5R cells showed increased protein level of CYBRD1, DMT1 and decreased ZIP14 level. Finally, the mRNA level of *SLC25A37* (gene coding for MFRN1) was slightly increased in MCF7 Tam5R cells, although not significantly [6]. On the same line, increased MFRN1 protein level was detected in both Tam5R cell lines.

A significant upregulation of *ABCB10* and *GLRX5* coding for proteins participating in mitochondrial Fe-S cluster biogenesis was observed in MCF7 Tam5R cells, while their mRNA level was not changed in T47D Tam5R cells compared to Ctrl cells. Interestingly, opposite results were documented by western blot, where MCF7 Tam5R cells showed downregulation of ABCB10 and GLRX5. On the other hand, T47D Tam5R cells exhibited increased ABCB10 level, while protein expression of GLRX5 was not assessed in these cells (functional antibody missing).

Fluidigm qPCR data showed increased expression of the gene coding for ferritin light chain (*FTL*) in MCF7 Tam5R cells [6]. Similarly, the protein level of ferritin was upregulated in both Tam5R cell lines as documented by western blot analysis.

Further analysis of the expression of genes involved in the regulation of iron export (*HEPH*, *FPN*) revealed no differences between MCF7 Tam5R cells and Ctrl cells, corroborated by no change in the protein level of FPN. Unfortunately, HEPH level was not detectable in MCF7 Tam5R cells. Different observation was documented in T47D Tam5R cells, which showed a dramatic increase in *HEPH* expression confirmed also by western blot analysis. Even though significant downregulation of *FPN* was measured by qPCR, no significant change on the protein level was observed.

Next, assessment of the expression of hypoxia related genes *EPAS1* (coding for HIF2α protein) and *QSOX1* revealed their increased mRNA (although not significant in MCF7 Tam5R cells) and protein level in both Tam5R cell lines compared to their parental

counterparts. In addition, the analysis of the expression of genes involved in iron sensing and regulation (*ACO1*, *IREB2*) as well as in iron overload (*HFE*) revealed significant upregulation of *ACO1* and *HFE* in Tam5R cell lines, while no differences were observed in case of *IREB2* expression, even though its protein level was decreased in MCF7 Tam5R cells. Contrary to the qPCR data, protein expression of HFE was decreased in both Tam5R cells, while ACO1 was upregulated in MCF7 Tam5R cells and downregulated in T47D Tam5R cells.

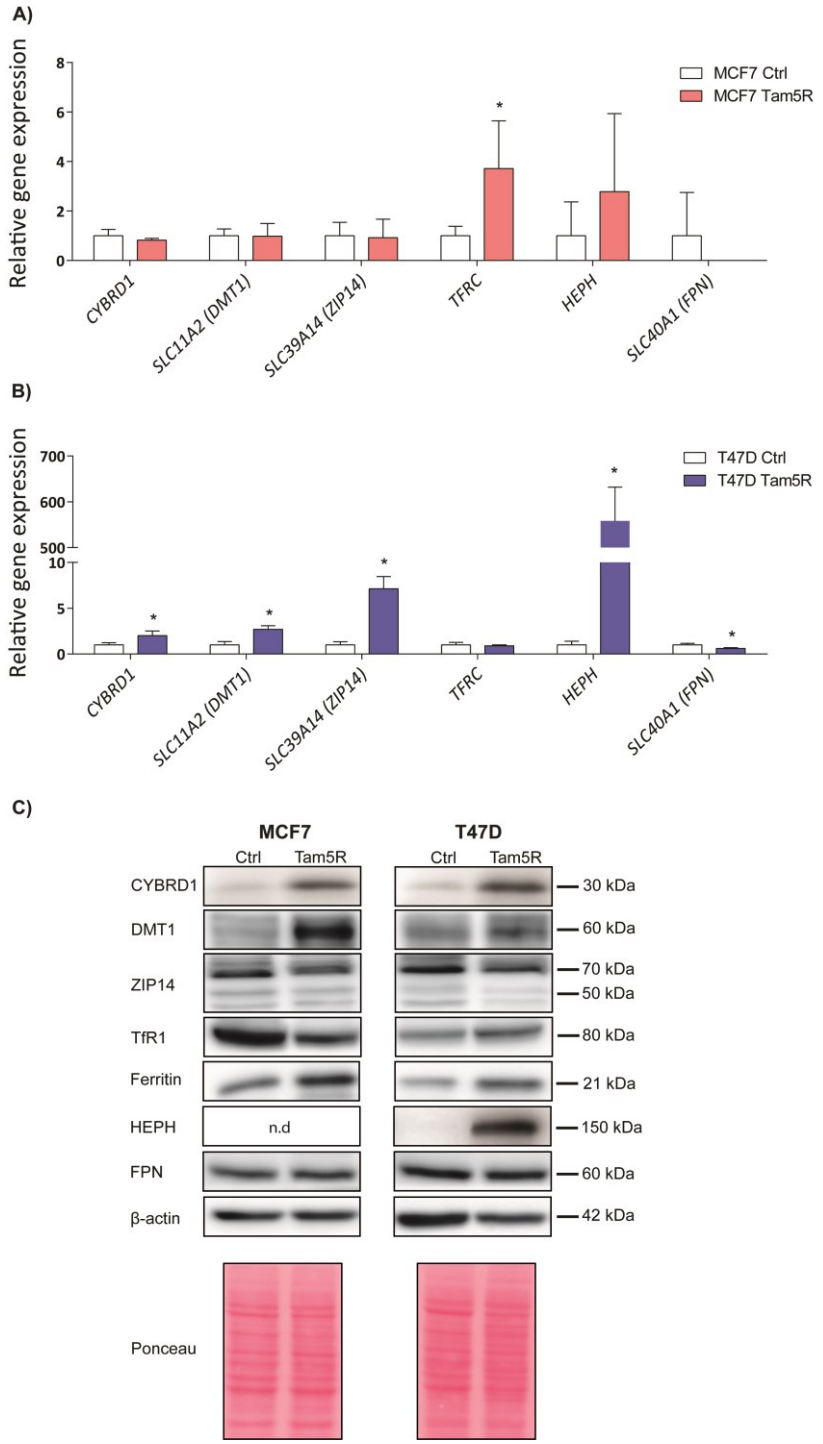

Figure 16. Tam5R cells have altered expression of genes and proteins connected with iron uptake, storage and export. Relative expression of *CYBRD1*, *SLC11A2*, *SLC39A14*, *TFRC*, *HEPH* and *FPN* in **(A)** MCF7 and **(B)** T47D Ctrl and Tam5R cell lines. The expression was determined by Fluidigm chip qPCR in MCF7 cells and by standard qPCR in T47D cells. Data were analyzed and statistical significance calculated by GenEx software and normalized to selected housekeeping genes. * $p < 0.05$ relative to Ctrl cells. **(C)** Representantive pictures of the protein level of CYBRD1, DMT1, ZIP14, TfR1, Ferritin, HEPH and FPN in MCF7 and T47D Ctrl and Tam5R cells evaluated by western blot of 3 independent sets of samples. β-actin and Ponceau were used as loading controls.

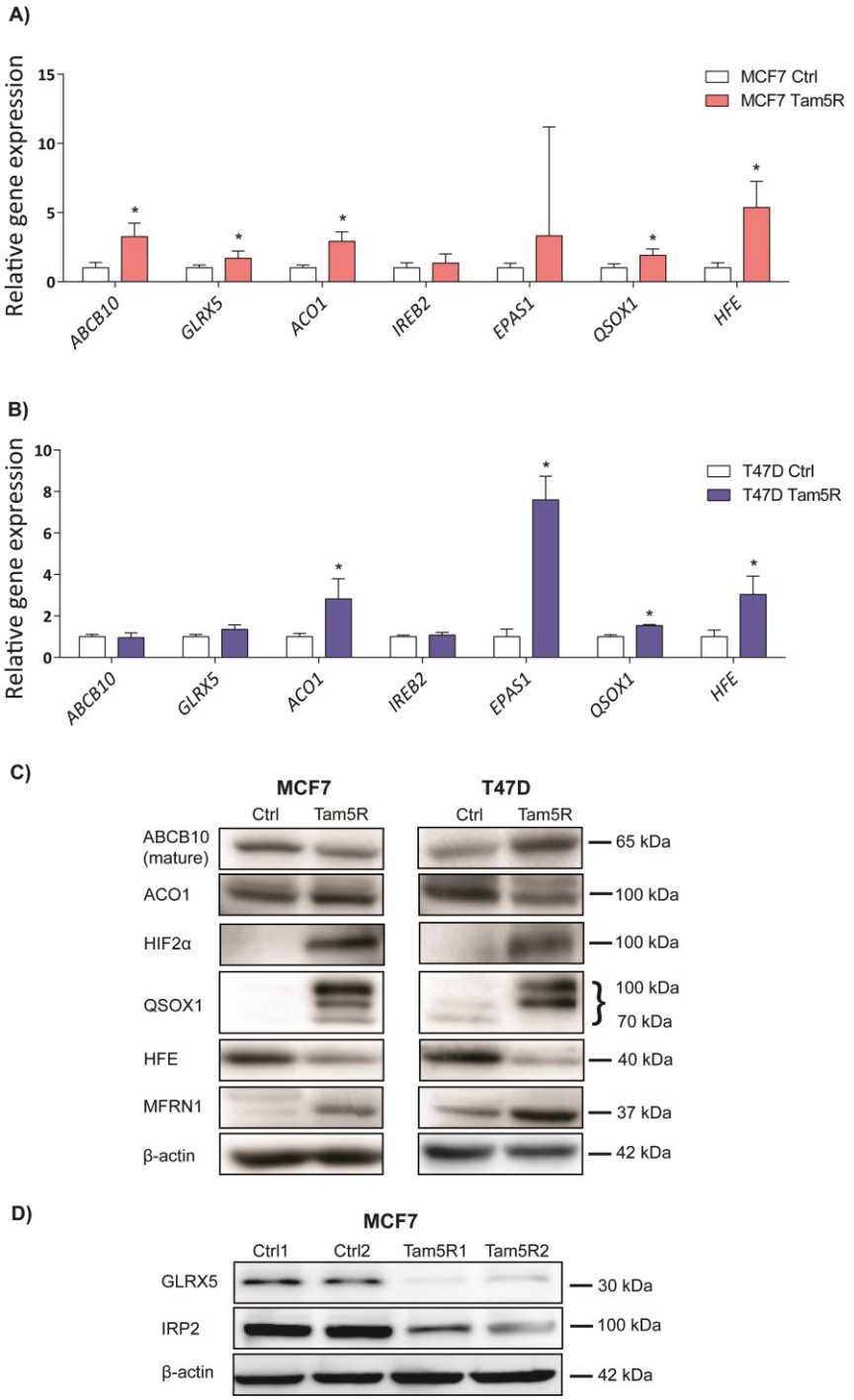

Figure 17. Tam5R cells have altered expression of genes and proteins connected with mitochondrial iron import and utilization, iron sensing, iron overload and hypoxia response. Relative expression of *ABCB10*, *GLRX5*, *ACO1*, *IREB2*, *EPAS1*, *OSOX1* and *HFE* in **(A)** MCF7 and **(B)** T47D Ctrl and Tam5R cell lines. The expression was determined by Fluidigm chip qPCR in MCF7 cells and by standard qPCR in T47D cells. Data were analyzed and statistical significance calculated by GenEx software and normalized to selected housekeeping genes. * $p < 0.05$ relative to Ctrl cells. **(C)** Protein level of mature ABCB10, ACO1, HIF2α, QSOX1, HFE and MFRN1 in MCF7 and T47D Ctrl and Tam5R cells evaluated by western blot of 3 independent sets of samples. β-actin was used as loading control. **(D)** Protein level of GLRX5 and IRP2 in MCF7 Ctrl and Tam5R cells from 2 sets of samples evaluated by western blot. β-actin was used as loading control (as published in [6]).

III.2.2 Tam5R cells show decreased incorporation of ^{55}Fe into proteins

In order to compare the iron incorporation into Fe-S cluster- or heme-containing proteins, we assessed their level in Ctrl and Tam5R cell lines. To do this, we incubated the cells with radioactive ^{55}Fe and subsequently harvested them either for subcellular fractionation or for the preparation of WCL. Isolated proteins were separated under native conditions and iron containing proteins were then visualized by ^{55}Fe autoradiography. Figure 18 shows a decrease in iron-containing proteins corresponding to SCs in the mitochondrial fraction of both Tam5R cell lines (Figures 18A and 18B). While MCF7 Tam5R cells show an increase in the band corresponding to ferritin in cytosol and WCL (Figure 18A), T47D Tam5R cells exhibit a very slight decrease in the ferritin in cytosol, no change in WCL and a slight increase in mitochondrial ferritin (Figure 18B).

When we measured the total amount of ^{55}Fe in WCL, and cytosolic and mitochondrial fractions, we observed an increase in ^{55}Fe level in WCL and cytosol and slightly lower mitochondrial ^{55}Fe content in MCF7 Tam5R cells compared to MCF7 Ctrl cells. However, the difference was not significant in both cases. In line with this observation, T47D Tam5R cells showed slightly decreased ^{55}Fe content in mitochondria and there was a trend towards higher ^{55}Fe content in cytosol (Figure 18C).

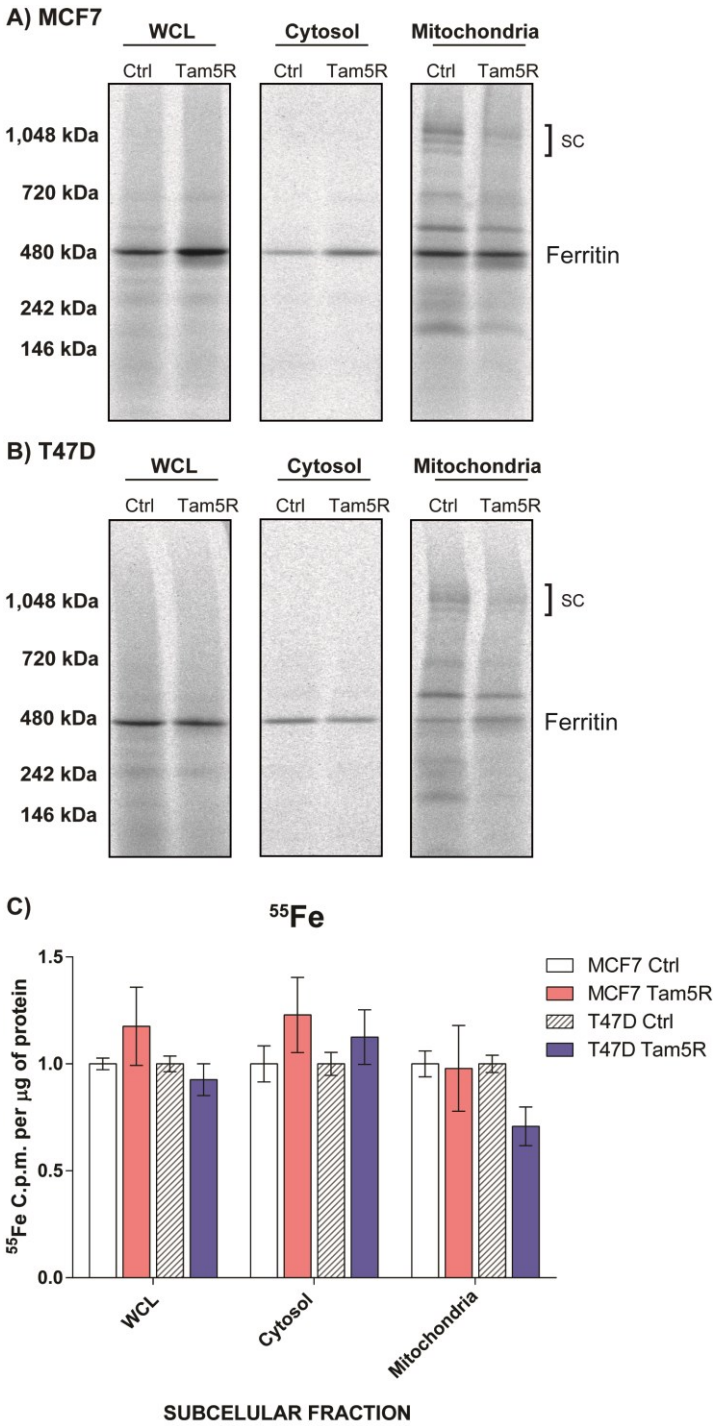

Figure 18. Incorporation of ^{55}Fe into proteins in WCL, cytosol and mitochondria. Representative pictures of autoradiography of proteins with incorporated ^{55}Fe in the WCL, cytosol and mitochondria of **(A)** MCF7 and **(B)** T47D Ctrl and Tam5R cells. The experiment was performed with 2 independent sets of samples and normalized to protein content. **(C)** ^{55}Fe content in WCL and subcellular fractions in MCF7 and T47D Ctrl and Tam5R cells, normalized per µg of protein.

III.3 Discussion

The relationship between breast cancer and iron metabolism has been well documented [217]. However, there is almost no data that would link alterations in iron metabolism and resistance to tamoxifen. The only report on this topic was published in 2010 by Habashy et.al [209], who showed an association between increased TfR1 level with tamoxifen resistance and poor therapeutic outcome. Since such study did not provide any deeper insight into changes in iron metabolism that could be connected with acquisition and maintenance of the tamoxifen resistant phenotype, we decided to examine the mRNA and protein level of selected proteins which are involved in the regulation of cellular iron homeostasis.

A significant difference in the expression of genes involved in iron uptake, iron sensing, iron export, iron overload, hypoxia and mitochondrial Fe-S cluster assembly was detected between parental and resistant cell lines, supporting an altered iron metabolism in Tam5R cells. Interestingly, the mRNA level of the tested genes showed a different pattern, with some genes being overexpressed only in MCF7 Tam5R or T47D Tam5R cell line. These differences are further discussed and suggest that Tam5R cells derived from a similar breast cancer subtype may utilize iron differently to reach the same goal. As mentioned before, although two different methods were used for the assessment of gene expression in MCF7 and T47D cells line, both measurements are valid and probably do not account for the observed difference in expression profiles. Importantly, the changes on the protein level between both Tam5R cells are quite constistent, suggesting that the regulation mostly occurs at the posttranscriptional level.

Increased iron uptake facilitated mainly through increased expression of TfR1 has been reported in breast tumors, particularly in the *in vitro* model of tamoxifen resistant cells [6, 209] as well as in BCSCs [216]. In line with such observations, we detected increased protein level of TfR1 in T47D Tam5R cells; however, we saw decreased level of the same protein in MCF7 Tam5R cells. Since cells can take up iron also from NTBI, we looked at protein level of DMT1 and ZIP14 that participate in this process. We found increased protein level of NTBI transporter DMT1 as well as ferroxidase CYBRD1 (or DCYTB) in both Tam5R cell lines. These data thus suggest that it is likely that Tam5R cells employ NTBI uptake to fulfill their iron needs, in addition to transferrin-bound iron. This nicely points to the fact that cells can enhance their iron uptake *via* several ways.

Increased iron uptake leads to increased intracellular LIP that can be stored inside ferritin. Its overexpression has been documented in various types of cancer, including breast cancer [218], being a signature of more aggressive and invasive phenotypes [219]. We observed elevated protein level of ferritin in both Tam5R cell lines, suggesting that Tam5R cells may store acquired iron in ferritin to supply processes such as proliferation or DNA damage repair mechanisms where iron plays an essential role as a cofactor. Furthermore, since increased ferritin has been linked to protection against ROS by sequestering free cellular iron [220], increased ferritin may protect Tam5R cells from ROS induced damage and provide them with a mechanism how to control their ROS level. Interestingly, it seems that MCF7 Tam5R cells incorporate more ^{55}Fe into cytosolic ferritin while T47D Tam5R cells seem to rather use the mitochondrial one. Both cell lines thus store iron in different compartments. Given the fact that ferritin has been linked to ROS protection, it is possible that such difference could be partially responsible for higher total ROS level in T47D cells.

We also observed a significant decrease in HFE in both Tam5R cell lines. The mutations in *HFE* gene result in excessive intestinal iron absorption and disease called hereditary hemochromatosis [221]. These mutations have been reported to increase the risk of cancer development, probably by inducing iron overload in the affected tissues [222-224]. However, the exact role of HFE in cancer has not been clearly described. It is also possible that the detected decrease in HFE protein does not affect iron handling but rather helps cancer cells to evade immune response as HFE belongs to MHC Class I-like proteins [225].

Iron efflux plays an important role in tumor growth and metastasis. Decreased expression of FPN has been implicated in supporting the growth of breast cancer since it should result in iron accumulation within cells [226, 227]. Our data from Ctrl and Tam5R cell lines do not show any changes in FPN level, suggesting no changes in iron export. Yet, the iron export is dependent on the activity of the FPN channel and our measurement shows solely FPN protein level. Therefore, measurement of the actual rate of iron export from cells loaded with ^{55}Fe would be required to fully address the question.

The ferroxidase HEPH acts in concert with FPN in iron efflux and its decreased expression has been shown to stimulate breast tumor growth *in vitro* and *in vivo* probably due to intracellular iron accumulation, and has been linked with poor prognosis [228]. Similarly, there are reports documenting lower HEPH level in colorectal cancer [210].

In our model, we originally detected significant downregulation of HEPH in MCF7 Tam5R cells (using the bs-15458R antibody from Bioss), corresponding with increased ferritin level and enhanced iron storage in these cells. Under such scenario, accumulated iron may serve as a reservoir to supply processes supporting the growth and survival of MCF7 Tam5R cell line. Yet, when employing a different and apparently more specific antibody (sc-365365 from Santa Cruz Biotechnology), we detected a dramatic increase in HEPH level in T47D Tam5R cells and we did not detect any HEPH in the MCF7 cell line. Since there is scarce evidence on the function of HEPH in cancer, it is possible that HEPH may play different roles in carcinogenesis that might not be directly connected to iron handling. Therefore, the actual role of HEPH in our model needs further clarification.

As described in the introduction, cellular iron homeostasis is controlled by IRP/IRE system [192]. Increased protein level and enzymatic activity of ACO1/IRP1 and decreased protein level of IRP2 in MCF7 Tam5R suggest a decreased activity of IRP/IRE in these cells. This is also documented by increased ferritin level and reduced TfR1 level, both of which are regulated by IRP/IRE. It is further supported by an increase in ^{55}Fe incorporation into ferritin in WCL and cytosolic fraction in MCF7 Tam5R cells. Moreover, a slight, although not significant increase in ^{55}Fe accumulation in WCL and cytosol could support our hypothesis and reflect the presence of ^{55}Fe-loaded ferritin. Importantly, it has been shown that IRP2 depletion in mouse embryonic fibroblasts increased protein level of HIFs resulting in increased glycolysis and decreased expression of Fe-S cluster biogenesis- and ETC-related genes, thereby weakening mitochondrial respiration [229]. This report is in agreement with our data in Tam5R cells, which show metabolic switch from OXPHOS to glycolysis, accompanied by reduced respiration and increased expression of HIF2α and glycolytic enzymes.

Interestingly, the opposite was shown for T47D Tam5R cells, where the IRP/IRE system seems to be active as the enzymatic activity of ACO1/IRP1 was diminished and TfR1 level was increased. Under such scenario, iron storage should be decreased; however, increased protein level of ferritin in T47D Tam5R cells indicates that these cells rather store iron. Yet, the protein level might not entirely reflect the actual ability of ferritin to store iron and it is also possible that ferritin is not regulated only by the IRP/IRE system in these cells [230]. The capacity to store iron was determined by ^{55}Fe labeling and we detected slightly decreased ^{55}Fe incorporation into cytosolic ferritin while mitochondrial ferritin ^{55}Fe content was slightly increased, resulting in a net

balance of no change in WCL. Furthermore, the observation of an active IRP/IRE system in T47D cells could also be explained by the fact that T47D cell line has highly increased basal intracellular level of ROS compared to MCF7 cell line. Since Fe-S cluster containing enzymes, and ACO1 in particular, are sensitive to ROS which cause destabilization of its Fe-S clusters, it is possible that increased activity of the IRP/IRE system in T47D cells could be also connected with oxidative damage. Unfortunately, IRP2 could not be determined in T47D cells as the antibody that we originally used did not work.

The biosynthetic pathways that incorporate iron into Fe-S clusters and heme represent another important aspect of intracellular utilization of iron [184]. Interestingly, many important enzymes that participate in these pathways reside within mitochondria. On that line, increased MFRN1 level in both Tam5R cell lines suggests an enhanced iron import into mitochondria in order to turn on compensatory mechanisms for the SCs disassembly that utilize Fe-S clusters and heme for their enzymatic activity. Interestingly, although no significant alterations in the mitochondrial ^{55}Fe level were detected, there was a strong decrease in ^{55}Fe incorporation in mitochondrial Fe-S- and heme-containing proteins in both Tam5R cell lines. Such results may suggest that even though Tam5R cells may import more iron into mitochondria, its utilization is compromised. This is supported in MCF7 Tam5R cells by downregulation of ABCB10, an important player in heme biosynthesis, together with GLRX5, participating in Fe-S cluster transfer inside mitochondria, similarly to changes seen in mammospheres [6]. Unexpectedly, T47D Tam5R cells showed ABCB10 upregulation and the data on GLRX5 protein level is missing due to the problems with the antibody. Since ABCB10 was shown to protect cells against oxidative stress [231-233], it is probably an adaptive mechanism elicited in T47D Tam5R cells to cope with their higher ROS. As the role of ABCB10 in cancer is not well defined and there is a scarce evidence showing that it is involved in the resistance to cisplatin, it is possible that ABCB10 may be involved not only in heme synthesis but may play an additional unrelated role in Tam5R cells. Further investigation would be necessary in order to describe the function of ABCB10 in our experimental model.

Importantly, the decreased incorporation of ^{55}Fe into mitochondrial proteins, possibly corresponding to SCs, strongly agrees with our data on disassembled SCs with diminished enzymatic activity in Tam5R cells, together with lower oxygen consumption in these cells. It is also important to note that measurements of ^{55}Fe incorporation into proteins are likely more reliable than the simple estimation of ^{55}Fe content within cytosol

and mitochondria, since mitochondria could be damaged during the isolation procedure and release loosely bound iron into cytosol, while membrane proteins of the mitochondrial respiratory complexes will remain there.

Iron metabolism and hypoxia are interconnected. Indeed, the proteins that target HIFs for degradation require iron, and HIF2α (EPAS1) contains an IRE sequence in its 5´ UTR [234]. HIF2α has been shown to induce the stem cell phenotype and drug resistance in breast cancer cell lines through activation of the Wnt and Notch signaling [235]. Similarly, several reports show the connection between increased tumorigenicity and enhanced HIF2α expression in renal cell carcinoma [236] and pancreatic cancer [237]. However, its role in tamoxifen resistance has not been explored yet. Therefore, we investigated the activation of HIF2α in Tam5R cells, and observed an increase in the protein level in both Tam5R cell lines, which is in agreement with the proposed enhanced iron uptake in these cells documented by increased DMT1 and CYBRD1 level, that are regulated by HIF2α [201, 238]. Therefore, HIF2α might be a very important player in the phenotype of Tam5R cells and requires further studies.

Additionally, HIFs regulate many proteins connected with the hypoxic response and hypoxic adaptation, one of them being QSOX1 [239]. This protein was found upregulated in both Tam5R cell lines and represents another interesting marker connected with tamoxifen resistance. There is emerging evidence on the role of QSOX1 in tumorigenesis [203] as its overexpression has been reported in breast cancer and has been suggested as a specific marker for the luminal B breast cancer subtype [205, 206, 240]. Upregulation of QSOX1 has also been linked with more aggressive phenotype and enhanced invasivity in breast cancer cell lines as well as in patients [205, 206]. Taken together, our results raise the possibility that HIF2α stimulates the expression of QSOX1 in Tam5R cells, thus contributing to extracellular matrix remodeling. We can speculate that such scenario may be important for CSC phenotype in Tam5R cells as well as for regulating their invasion and migration.

IV. ABC transporters and tamoxifen resistance

IV.1 Literature overview

IV.1.1 ABC transporters

ABC transporters are the largest known family of transmembrane proteins. Their ability to transport various compounds such as sugars, lipids, peptides or ions across biological membranes makes ABC transporters essential for maintaining normal cellular physiology [241].

ABC transporters are present in almost all life entities ranging from prokaryotes to complex eukaryotic organisms. While in prokaryotes they work both as importers and exporters, in eukaryotes they act mostly as exporters. Thanks to their ability to export cytotoxic molecules, they may confer resistance to antibiotics or anticancer drugs, thus being the reason for therapy failure, causing the multidrug resistance (MDR) phenomenon [242], where tumor cells are resistant to a broad range of unrelated chemotherapeutics.

IV.1.2 The structure and mechanism of action of ABC transporters

ABC transporters are composed of four core domains: two nucleotide binding domains (NBD1 and NBD2) and two transmembrane domains (TMD1 and TMD2). The different domains of prokaryotic ABC transporters are coded for as individual polypeptides that are assembled at the plasma membrane. In eukaryotes, these domains are translated as a single polypeptide chain or as two polypeptides, each consisting of one NDB and one TMD [243].

NBDs share high structural homology and are defined by several structurally conserved motifs such as Walker A and Walker B motifs, or ABC signature motif ´LSGGQ´. On the contrary, TMDs show almost no sequence conservation due to the diverse nature of the transported substrates. TMDs are formed by multiple membrane-spanning α-helices which form an internal cavity allowing the substrate to pass through the membrane [244].

The mechanism of action of ABC transporters can be described in several steps (Figure 19). The process is initiated by the binding of the substrate to high-affinity sites on the TMDs, triggering dimerization of NBDs and thus a conformational change from

opened to closed state. This increases the affinity for binding of 2 ATP molecules to NBDs. The closed structure then induces conformational changes in the TMDs, causing opening of the transporter and release of the substrate on the opposite site of the membrane. ATP bound to NBDs is hydrolyzed to ADP and Pi, generating the energy necessary to translocate the substrate across the membrane. The hydrolysis resets the entire transporter for the next transport cycle [245].

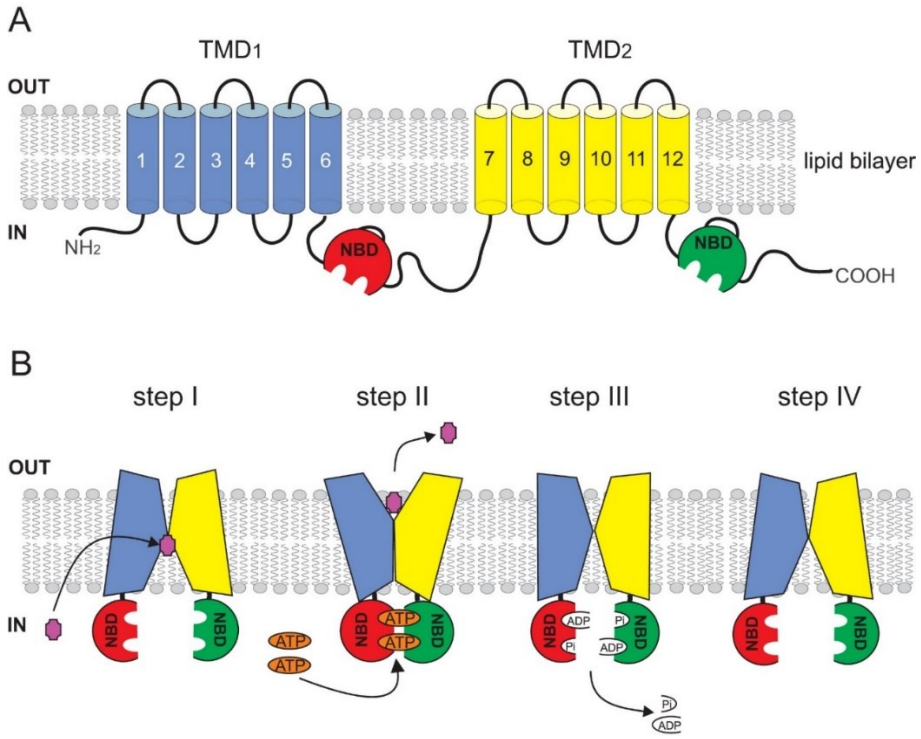

Figure 19. The structure and efflux mechanism of ABC transporters. (A) Full ABC transporter consisting of 2 transmembrane domains (TMD1 and TMD2) and two nucleotide binding domains (NBD1 and NBD2). **(B)** The ATP-switch model for the ABC transporter efflux mechanism. Binding of the substrate (purple) to the TMD (step I) leads to conformational change in NBD, facilitating ATP binding and closed dimer structure formation. TMDs then open towards the outside and translocate the substrate (step II). The closed NBD dimer structure is disrupted by ATP hydrolysis resulting in a conformational change in TMDs (step III). Finally, the release of Pi and ADP restores initial ABC transporter conformation (step IV; adapted from [246]).

IV.1.3 The classification and physiological function of ABC transporters

In humans, there are 49 ABC transporters divided into seven subfamilies (designated A-G), depending on amino-acid sequence, structure, and the character of

the transported substrates. The A family of ABC transporters has 12 members, some having more than 2,100 AAs in length. They are mostly involved in lipid transport and trafficking between cellular compartments in various organs [247]. Some members of this family (ABCA1, ABCA2, ABCA3 or ABCA6) have been suggested to play a role in drug resistance [247]. In particular, ABCA1 has been found to be involved in the resistance of lung carcinoma cells to α-tocopheryl succinate [248], as well as in the resistance to porphyrins in photodynamic therapy [249].

ABC transporters belonging to B family include 11 known members. There are both half and full transporters in this family, with different localization pattern (plasma membrane, endoplasmic reticulum, Golgi apparatus or mitochondria) and function [247]. The most studied and characterized protein from this family is the ABCB1 (also known as P-glycoprotein), which is normally expressed in the liver and hematoencefalic barrier and guards the cells from the deleterious effects of toxins and drugs. However, its overexpression has been detected in many types of cancer and is associated with the MDR phenotype [250]. A very interesting group of B family ABC transporters are the mitochondrial members, localized in the inner (ABCB7, ABCB8 and ABCB10) and outer (ABCB6) mitochondrial membrane. They participate mainly in Fe-S cluster biogenesis and heme biosynthesis [251], altough their precise role in such processes is still under debate. Interestingly, increased expression of ABCB6 has been linked with the resistance to chemotherapeutics such as 5-fluorouracil, SN-38 and vincristine in KAS cells [252] or to the combination of paclitaxel/FEC (5-fluorouracil, epirubicin, cyclophosphamide) in breast cancer [253]. Moreover, elevated level of ABCB7 has been proposed to mediate the resistance to carmustine [254], elevated ABCB8 has been shown to confer resistance to doxorubicin in melanoma cells [255] and ABCB10 overexpression has been linked to cisplatin resistance in epidermoid carcinoma cells [256].

There are 13 ABC transporters belonging to the C family. 9 members are known as multidrug resistance proteins (MRP1-MRP9) and are able to export various xenobiotics, drugs and toxins out of the cell. This group of ABC transporters is thus mostly related to the MDR phenotype and cancer therapy failure [257]. The rest of the transporters have not been connected with MDR phenotype. Although they do not seem to play an important role in the cancer resistance, some of these proteins have been linked with human diseases. For example, ABCC7, the cystic fibrosis transmembrane conductance regulator (CFTR), is a chloride ion channel and, as indicated in the name, its mutation has been documented as a cause of cystic fibrosis [258]. The transport

function and substrates of sulfonylurea receptors SUR1 (ABCC8) and SUR2A/B (ABCC9) have not been described yet; however, they are important regulators of cellular homeostasis due to their association with K_{ATP} channels and their participation in the release of insulin from pancreatic β-cells [259]. The last member, ABCC13, is considered to be a pseudogene [260].

The members of D family are localized predominantly into peroxisomes. They help transport long chain fatty acids and branched chain fatty acids together with acyl-CoA esters into peroxisomes [261]. ABCD4, which was previously identified as a peroxisomal protein but is in fact localized in lysosomes, helps with the export of cobalamin into the cytosol [262].

Transporters belonging to E and F families have an ATP-binding domain; however, the lack of TMD in their structure makes it very unlikely that they would act as transporters. ABCE1, the single member of its family and also known as RNase L inhibitor, possesses strong antiviral activity and regulates ribosomal recycling [263]. F family has three known members (ABCF1, ABCF2 and ABCF3) which participate in inflammatory processes [247].

Subfamily G comprises 5 members involved in regulating lipid homeostasis. One member, ABCG2 (BCRP) is also able to export chemotherapeutics out of the cells and is considered to contribute to MDR [264].

The most prominent ABC transporters participating in cancer resistance are further discussed in the next chapter.

IV.1.4 ABC transporters in multidrug resistance

ABC transporters are widely expressed in excretory organs and physiological barriers, where they ensure the efflux of xenobiotics or metabolites, thus having protective and physiological functions in normal cells [265, 266]. However, some members can mediate the efflux of chemotherapeutics, and their increased expression has been detected in many types of cancer, contributing to the MDR phenotype and therapy failure. The exogenous substrates of several ABC transporters are shown in the Table 1.

Name	Exogenous cytotoxic substrate
ABCB1	doxorubucin, daunorubicin, etoposide, teniposide, methotrexate , mitomycin C, mitoxantrone,paclitaxel, docetaxel, vincristine, vinblastine, colchicine
ABCC1/MRP1	doxorubicin, daunorubicin, etoposide, heavy metals, vincristine, vinblastine, paclitaxel
ABCC2/MRP2	cisplatin, irinotecan, doxorubicin, etoposide, methotrexate, vincristine, vinblastine
ABCC3/MRP3	cisplatin, doxorubicin, etoposide, methotrexate, teniopside, vincristine
ABCC4/MRP4	methotrexate, nucleotide analogs, PMEA, topotecan
ABCC5/MRP5	doxorubicin, methotrexate, nucleotide analogs, topotecan
ABCC11/MRP8	5'-Fluorouracil, 5'-fluoro-2'-deoxyuridine, 5'-fluoro-5'-deoxyuridine, PMEA
ABCG2/BCRP	Anthracyclines, bisantrene, camptothecin, epirubicin, flavopiridol, mitoxantrone, topotecan, methotrexate

Table 1. Exogenous substrates of ABC transporters. PMEA- 9'-(2'-phosphonylmethoxynyl) adenine. Adapted and modified from [7, 267].

The most extensively characterized MDR proteins are ABCB1, ABCC1 and ABCG2 [268] and will be discussed in detail further.

ABCB1 exports a wide range of substrates including chemotherapeutic agents such as taxanes, anthracyclines or vinca alcaloids (Table 1). Therefore, enhanced expression of ABCB1 highly contributes to MDR phenotype in many cancers, including breast tumors [269].

ABCC1 was initially characterized in a doxorubicin-selected human lung cancer cell line [270]. Although, the character of effluxed drugs partially overlaps with ABCB1 (Table 1), ABCC1 also exports GSH, glutathione disulfide (GSSG) and glucuronide conjugates, as well as leukotrienes and prostaglandins [271]. Overexpression of ABCC1 strongly correlates with poor clinical outcome in lung [272] and breast cancer [273], and neuroblastoma [274].

The contribution of ABCG2 to MDR phenomenon was first described in a MCF7 breast cancer cell line resistant to doxorubicin [275]. Since then, many other substrates of ABCG2 have been identified such as camptothecins, methotrexate, 5-fluorouracil, the tyrosine kinase inhibitors imatinib and gefitinib, photodynamic therapy agents and many more (Table 1) [276]. The overexpression of ABCG2 has been reported in acute myeloid leukemia, breast and lung cancer [277]. Interestingly, ABCG2 has been found highly expressed in side populations which are characterized by the ability to efflux the fluorescent dye Hoechst 33342 and show stem-like properties [278] (reviewed in [279]). This strongly indicates the enrichment of side populations with CSCs [280-283].

While the participation of ABC transporters in the MDR phenotype is generally accepted, an emerging concept is the additional role of ABC transporters contributing to tumorigenicity independently of drug efflux [284]. It appears that in addition to the ability of ABC transporters to efflux chemotherapeutics, they are also involved in the transport of other metabolites and signaling molecules such as prostaglandins, leukotrienes, sphingosine-1-phosphate (S1P), platelet activating factor (PAF), cholesterol metabolites and cyclic nucleotides, leading to the activation of pro-survival pathways, increased angiogenesis, invasiveness and metastatic potential, and enhanced proliferation [284].

As already mentioned, ABC transporters linked with MDR show enhanced expression in CSCs compared to cancer and non-malignant cells. This is the case for BCSCs and ABCG2 or ovarian CSCs and ABCB1 [285]. In addition, distinct subpopulations in human melanoma have been documented to coexpress ABCB1, ABCB5 and ABCC2 in addition to stem cell markers [286]. Furthermore, active EMT program, which is necessary for the maintentance of CSCs, has been reported to cause overexpression of ABC transporters and promote drug resistance [287, 288]. Of note, another important condition causing upregulation of ABC transporters in tumor cells is hypoxia, thereby influencing efflux of the chemotherapeutics [288].

Some ABC transporters such as ABCB1, ABCC1 or ABCC2 have been reported to export tamoxifen and its metabolites [289-291] and are further discussed in section IV.3. However, the role of other ABC transporters in tamoxifen resistance has not been well documented.

IV.2 Results

The results shown in this section have not been published.

IV.2.1 Tam5R cells show altered expression of ABC transporters

Since ABC transporters were implicated in many cases of drug resistance, linked to the CSC phenotype and some have even been reported to transport tamoxifen metabolites, we assessed the expression profile of all human ABC transporters in our model of Tam5R cells by standard qPCR. In addition, the protein level of the most differentially expressed genes was measured by western blot. However, due to initial lack of correlation between mRNA and protein level, we further decided to also test additional ABC transporters on the western blot, even though their expression was not changed at the mRNA level. The summary table (Table 2) of the qPCR data with all tested ABC transporters, showing fold change and P-values is shown below.

Regarding the A family, *ABCA2*, *ABCA5*, *ABCA7* and *ABCA10* transporters, involved mainly in lipid trafficking, were significantly overexpressed in MCF7 Tam5R cells compared to parental cells, while the expression of *ABCA1* and *ABCA12* was decreased. Fewer significant alterations were observed in T47D Tam5R cells, where the expression of *ABCA1* and *ABCA12* was upregulated and *ABCA3* showed downregulation compared to Ctrl cells. Moreover, T47D Tam5R cells exhibited also increased mRNA level of *ABCA13*, while in MCF7 Tam5R cells the expression of this gene was not detected. None of the alterations of gene expression was confirmed on the protein level.

When analyzing the gene expression of transporters belonging to the B family, we detected significant overexpression of mitochondrial *ABCB10* in MCF7 Tam5R cells, while T47D Tam5R cells exhibited upregulation of the MDR gene *ABCB1* as well as 2 other members, *ABCB3* and *ABCB9*. Interestingly, mitochondrial transporters ABCB10 as well as ABCB7 were decreased on the protein level in MCF7 Tam5R cells and increased in T47D Tam5R cells compared to parental cell lines (Figure 20).

		(MCF7 Tam5R) vs (MCF7 ctrl)		(T47D Tam5R) vs (T47D ctrl)	
		Fold change	P value	Fold change	P value
A family	*ABCA1*	**-1.90**	0.006104267	**1.71**	0.023623371
	ABCA2	**1.72**	8.13E-05	-1.20	0.143452828
	ABCA3	1.31	0.107053803	**-2.03**	1.65E-06
	ABCA4	1.79	0.242919391	-1.23	0.352271954
	ABCA5	**3.28**	0.000151966	-1.26	0.38350325
	ABCA7	**1.94**	0.000650572	1.01	0.971573065
	ABCA10	**2.72**	7.25E-07	1.33	0.443191813
	ABCA12	**-4.70**	3.68E-06	**1.93**	0.016177429
	ABCA13	excluded		**72.39**	1.10E-07
B family	*ABCB1*	-1.22	0.508615236	**3.12**	0.012385253
	ABCB3	1.29	0.280590831	**1.72**	0.004796193
	ABCB6	1.16	0.496808664	1.03	0.87998876
	ABCB7	1.25	0.092527985	-1.07	0.573843352
	ABCB8	-1.16	0.201024213	1.19	0.345905278
	ABCB9	-1.36	0.108094983	**2.59**	1.54E-05
	ABCB10	**2.53**	3.82E-06	-1.04	0.757955857
C family	*ABCC1*	**1.60**	0.005136399	1.10	0.558282858
	ABCC2	-1.58	0.050378087	**80.23**	1.00E-08
	ABCC3	**1.82**	0.049298472	1.13	0.590204162
	ABCC4	**13.63**	2.69E-05	excluded	
	ABCC5	**4.09**	5.72E-06	**2.83**	0.000482732
	ABCC6	**1.70**	0.014758872	1.26	0.135343414
	ABCC8	**6.72**	3.30E-08	**1.60**	0.006742227
	ABCC9	**2.04**	0.001411914	1.50	0.150533331
	ABCC10	**2.09**	0.001227899	1.33	0.085603274
	ABCC11	-1.27	0.245855568	-1.35	0.415089801
	ABCC12	excluded		1.41	0.249912839
D family	*ABCD1*	**-1.56**	0.00074815	1.34	0.212086015
	ABCD3	**-1.70**	1.22E-05	1.11	0.49901666
	ABCD4	**2.01**	4.94E-05	-1.29	0.19212474
E family	*ABCE1*	**1.35**	0.025089989	1.16	0.541607919
F family	*ABCF1*	1.27	0.196875003	**1.76**	0.02096591
	ABCF2	**-1.49**	0.000259135	1.23	0.075209497
	ABCF3	**2.02**	9.52E-05	1.12	0.326486766
G family	*ABCG1*	**-4.98**	4.21E-05	**-4.85**	0.000108265
	ABCG2	**2.54**	0.037012878	**-1.85**	0.005160629
	ABCG4	**-2.27**	0.028314472	-1.20	0.449968291

Table 2. The gene expression of human ABC transporters (previous page). The expression profiling was performed by standard qPCR. The results are shown as fold change with negative values corresponding to significant downregulation (blue color) and positive values corresponding to significant upregulation (red color) in Tam5R cells compared to Ctrl cells. Data were analyzed and statistical significance calculated by GenEx software and normalized to selected housekeeping genes. $p < 0.05$ (green color), n=6. The following genes were excluded from the analysis either due to low efficacy of the assay or very low expression: *ABCA6*, *ABCA8*, *ABCA9*, *ABCA13* (MCF7), *ABCB2*, *ABCB4*, *ABCB5*, *ABCB11*, *ABCC4* (T47D), *ABCC7*, *ABCC12* (MCF7), *ABCC13*, *ABCD2*, *ABCG5* and *ABCG8*.

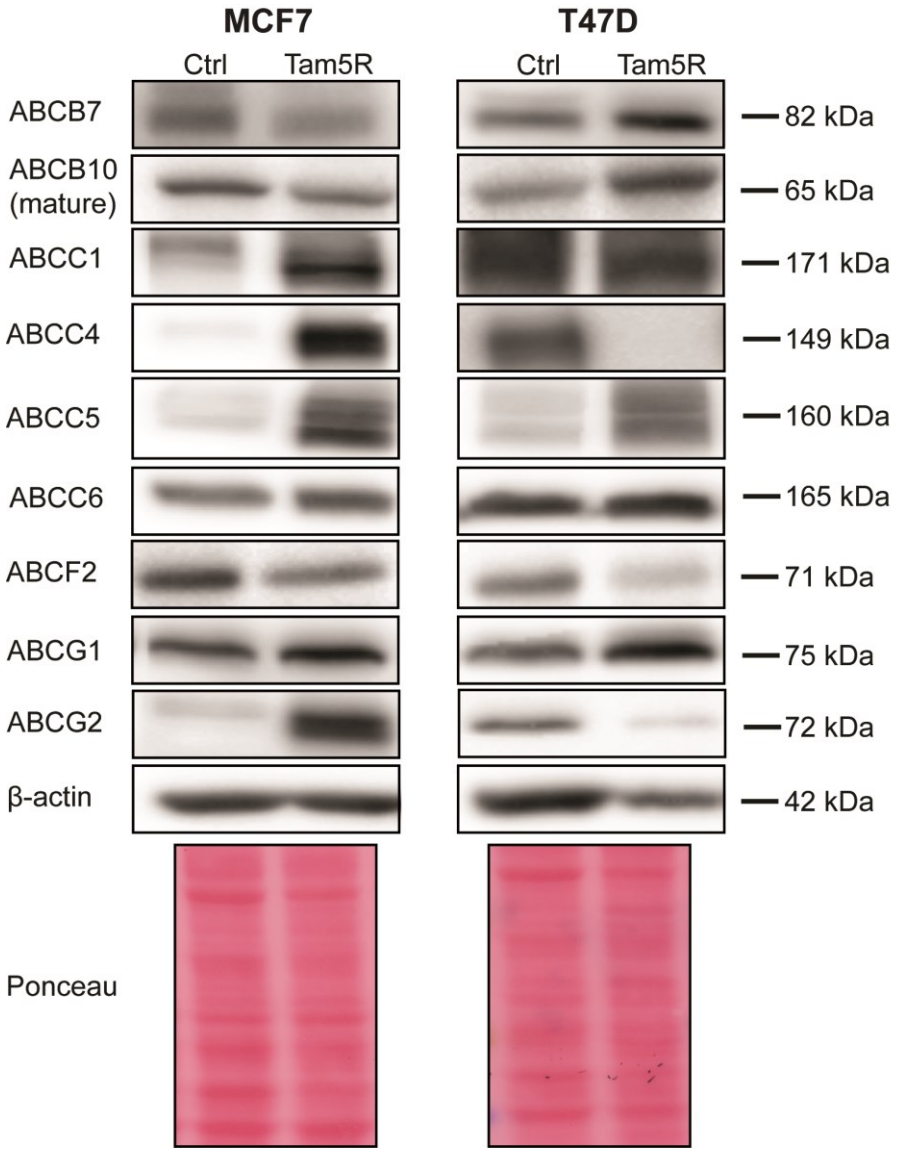

Figure 20. The protein level of selected ABC transporters. Representative western blot pictures of ABCB7, ABCB10, ABCC1, ABCC4, ABCC5, ABCC6, ABCF2, ABCG1 and ABCG2 in MCF7 and T47D Ctrl and Tam5R cell lines from 3 independent sets of samples. β-actin and Ponceau were used to assess proper loading.

Analysis of C family members revealed their increased expression in both Tam5R cell lines, with *ABCC1*, *ABCC3*, *ABCC4*, *ABCC5*, *ABCC6*, *ABCC8*, *ABCC9* and *ABCC10* being overexpressed in MCF7 Tam5R cells, while T47D Tam5R cells showed elevated mRNA level of *ABCC5*, *ABCC8,* and also *ABCC2*. When we assessed the protein level, we observed increased amount of ABCC1, ABCC4 , ABCC5 and ABCC6 transporters in MCF7 Tam5R cells compared to Ctrl cells (Figure 20). T47D Tam5R exhibited increased protein level of ABCC5, similarly to MCF7 Tam5R cells, however the level of ABCC4 was dramatically decreased and ABCC1 showed no change (Figure 20).

Members of the D family of ABC transporters, participating in the transport of long chain fatty acids, were significantly altered on mRNA level only in MCF7 cell line, with overexpression of *ABCD4* and lower expression of *ABCD1* and *ABCD3* in Tam5R cells compared to Ctrl cells. Protein level was not assessed.

E and F families lacking TMD were also assessed by qPCR. MCF7 Tam5R cells showed overexpression of *ABCE1* and *ABCF3*, while *ABCF2* mRNA level was downregulated compared to parental cells. On the other hand, we detected a significant upregulation of *ABCF1* in T47D Tam5R cells, while the rest of genes was not altered. Protein level of ABCF2 was significantly lower in both Tam5R cell lines compared to parental cell lines (Figure 20).

Regarding the G family, *ABCG1* was significantly downregulated in both Tam5R cell lines on mRNA; however, the protein level was increased in both Tam5R cells (Figure 20). *ABCG2* was differentially expressed in Tam5R cell lines (overexpressed in MCF7 Tam5R cells and downregulated in T47D Tam5R cells compared to parental cells). The same observations were documented on western blot. Finally, *ABCG4* mRNA level was significantly lower in MCF7 Tam5R cells and not changed in T47D Tam5R cells.

IV.3 Discussion

ABC transporters represent the broadest family of transmembrane efflux pumps, playing an essential role in the maintenance of cellular homeostasis by transporting various types of substrates across biological membranes [241]. Their increased expression has been linked with the MDR phenomenon in cancer cells due to their ablity to efflux structurally diverse anticancer agents [292]. Since ABC transporters normally participate in healthy tissue defense, targeting their function specifically in cancer cells is very problematic. Despite ongoing attempts to design and test new inhibitors, very few have been translated into clinics due to severe side effects and toxicity, and none has been officially approved by the authorities [292].

To address the contribution of ABC transporters to tamoxifen resistance, we performed expression profiling of all human ABC transporters followed by western blot in MCF7 and T47D Ctrl and Tam5R cell lines. Unexpectedly, there was almost no overlap in the expression of ABC transporters between both Tam5R cell lines with only *ABCC5*, *ABCC8* and *ABCG1* being similarly altered on mRNA level. When we checked the protein level of these three transporters, we observed a change only in ABCC5. Yet, importantly, we detected a similar pattern of protein level change in case of ABCC5, ABCG1 and ABCF2 in both Tam5R cells, suggesting that the expression of ABC transporters is regulated not only at transcriptional, but also at translational and post-translational level [293-296].

ABCC5 was characterized 20 years ago as an efflux pump for cyclic nucleotides [297] and nucleotide analogues [298]. Its elevated level was documented to confer resistance to paclitaxel in nasopharyngeal carcinoma cells [299], and to antifolates [300] or 5-fluorouracil in breast and colon tumors by exporting its monophosphorylated metabolites [301]. In addition, a role for ABCC5 in promoting the metastatic process into bones in breast cancer has been proposed [302]. Although there is no report on a link between ABCC5 expression and tamoxifen resistance so far, the ability of ABCC5 to efflux cytosolic nucleotides which act as second messengers could activate pro-survival pathways in Tam5R cells and therefore indirectly confer resistance. Furthermore, ABCC5 has been documented to transport heme in many experimental models [303]. Since Tam5R cells show a clear alteration in iron metabolism, a connection between ABCC5 overexpression, iron metabolism and tamoxifen resistance can not be excluded and warrants further research.

Another transporter whose increased protein level was observed in both Tam5R cell lines is ABCG1. A recent report has demonstrated that ABCG1 can localize to intracellular endosomes and transport sterols away from the endoplasmic reticulum [304]. ABCG1 has been found highly expressed in very aggresive metastatic colon cancer cells and its depletion markedly reduced tumorigenesis and metastatic potential [305]. Moreover, a role of ABCG1 in CSC maintenance in gliomas has been documented as well [306, 307]. All these reports indicate that increased ABCG1 level in Tam5R cells could alter lipid trafficking resulting in activation of oncogenic signaling [308] and the maintenance of their cancer stem-like phenotype [309].

The last ABC transporter that was similarly altered in both Tam5R cells was ABCF2. Amplification of *ABCF2* was identified in various cell lines resistant to cisplatin [310], possibly indicating its role in the resistance to this drug. ABCF2 was shown to be regulated by nuclear factor erythroid 2-related factor 2 (NRF2) and contribute to the cisplatin resistance in ovarian cancer cells [311]. Different observations were reported in breast cancer, where ABCF2 positive tumors had better prognosis than ABCF2 negative tumors and a negative correlation between ABCF2 expression and metastasis together with the response to endocrine therapy was proposed [312]. Downregulation of ABCF2 in Tam5R cell lines is in line with such observations and therefore ABCF2 loss may play a role in tamoxifen resistance.

Another interesting observation was in ABCC4. This transporter is able to efflux various molecules participating in cellular signaling, including cycling nucleotides, leukotrienes or prostaglandins [313]. Export of prostaglandin E2 by ABCC4 has been reported to contribute to metastatic process in breast cancer cells [314]. The protein level of ABCC4 was dramatically increased in MCF7 Tam5R cells and dramatically decreased in T47D Tam5R cells. Although we have not assessed the invasivity and migration in Tam5R cells, we can speculate that ABCC4 in MCF7 Tam5R cells modulates cellular signaling contributing to more aggressive and cancer stem-like phenotype. Since T47D Tam5R cells have higher basal level of ABCC4 and already behave like CSCs, they probably do not need to increase ABCC4 level and may transport different substrates to promote pro-survival pathways.

A noteworthy group of ABC transporters are the mitochondrial members. ABCB7 is important for cytosolic and mitochondrial Fe-S clusters assembly [315, 316] and its upregulation has been shown to lead to an aggressive phenotype in human glioblastoma cells by influencing iron metabolism [317]. On the other hand, its deletion

leads to mitochondrial iron accumulation, oxidative damage and defective Fe-S cluster assembly [315, 318]. As previously discussed, the function of ABCB10 in cancer as well as endogenous substrates of ABCB10 have not been described, with only one report suggesting its involvement in cisplatin resistance [256]. In Tam5R cells, protein level of ABCB7 and ABCB10 dramatically differs between MCF7 and T47D cells. Since ABCB7 and ABCB10 transporters are involved in the regulation of iron homeostasis, we can speculate that both Tam5R cells utilize these transporters for their iron metabolism and Fe-S clusters differently in order to maintain their resistant phenotype. For example, the increase in protein level of ABCB7 and ABCB10 in T47D Tam5R cells could be a result of diminished cytosolic aconitase activity, in line with their higher basal ROS level. Therefore, they might represent a compensatory mechanism to transport more Fe-S cluster intermediates into cytosol, documented also by dramatic disassembly of mitochondrial SCs which need Fe-S clusters for their proper functioning. Contrary, MCF7 Tam5R cells do not exhibit such a dramatic SCs disassembly as T47D Tam5R cells and they have increased cytosolic aconitase 1 activity and therefore possibly do not need to support cytosolic Fe-S cluster assembly to such extent.

ABCB1, ABCC1 and ABCC2 transporters are able to export tamoxifen and its metabolites *in vitro* [289-291]. Even though overexpression of ABCC2 has been already documented in tamoxifen resistant cells [319], we were not able to detect its protein level in our models probably because the level is below the detection limit of the used antibody. Upregulation of ABCC1 has been linked with poor prognosis in patients treated with tamoxifen [320], which is in line with our observations of increased ABCC1 in MCF7 Tam5R cells. Since we were not able to detect ABCB1 protein by western blot, it probably does not play a key role in the acquisition of the resistant phenotype in our model.

To sum up, significant alterations in the expression of ABC transporters were observed in Tam5R cells compared to parental cells. However, the overlap in the expression of ABC transporters between two Tam5R cell lines was only in a few members. Noteworthy, the expression of ABC transporters can be regulated by various factors including EMT proteins or multiple oncogenic pathways resulting in their different expression depending on the cellular context [287, 288]. Our results may also be explained by different basal ABC protein level in MCF7 and T47D cell line. Therefore, it seems that a different combination of ABC transporters in different cell types may be important in the acquisition of the Tam5R phenotype, rather than a single transporter.

Summary of the main findings

1) We successfully established breast cancer cell lines resistant to 5 μM tamoxifen (MCF7 Tam5R and T47D Tam5R) and confirmed their resistant phenotype. Further, we documented increased expression of several CSC markers in Tam5R cells, suggesting their partial CSC phenotype

2) We compared the mitochondrial function between Ctrl and Tam5R cells and showed:

- Decreased amount, dramatic disassembly and diminished enzymatic activity of mitochondrial SCs accompanied by decreased respiration in both Tam5R cells
- Increased level of mtDNA and mitochondrial mass in MCF7 Tam5R cells
- Fragmentation of mitochondrial network along with an activating phosphorylation status of DRP1 in Tam5R cells. Moreover, resistant cells show diminished localization of mitochondria in the perinuclear region of the cell
- Increased mitochondrial ROS level together with increased expression of antioxidant enzymes catalase, SOD2 and GPX1 in Tam5R cells
- Increased dependence of Tam5R cells on glycolysis documented by enhanced glucose uptake and GLUT-1 level, increased extracellular lactate production, higher sensitivity to 2-DG treatment, accompanied by increased expression of key glycolytic enzymes HKII, PFK2 and PDK1
- Activation of the AMPK metabolic sensor, and increased activity of mitochondrial aconitase and protein level of SIRT3
- Higher resistance of MCF7 ρ0 cells to tamoxifen

3) Evaluation of iron metabolism in Tam5R cells showed:

- Higher gene expression and level of proteins regulating iron uptake (TfR1, CYBRD1, DMT1 and MFRN1) and storage (ferritin) in Tam5R cells
- Increased level of HIF2α and QSOX1 in Tam5R cells
- Less incorporation of ^{55}Fe into Fe-S cluster- and heme-containing proteins in mitochondrial fractions of Tam5R cells
- Increased ^{55}Fe-loaded cytosolic ferritin in MCF7 Tam5R cells and ^{55}Fe-loaded mitochondrial ferritin in T47D Tam5R cells

4) Gene and protein expression profiling of ABC transporters in Tam5R cells showed:

- Poor correlation between mRNA and protein level in most ABC transporters
- Increased level of ABCC5 and ABCG1, and decreased ABCF2 level in both Tam5R cell lines

Conclusions

This work investigated different mechanisms of tamoxifen resistance in the newly established model of two Tam5R breast cancer cell lines. We show that dysfunctional and fragmented mitochondria in Tam5R cells lead to a metabolic rewiring towards glycolysis and possible utilization of alternative sources of energy. Increased level of mitochondrial ROS results in the activation of canonical antioxidant pathways in resistant cells. Similarly, indirect antioxidant pathways that involve regeneration of NADPH through the partial utilization of the TCA cycle were evidenced in Tam5R cells. Furthermore, an increase in proteins regulating iron uptake and storage suggests a higher iron dependence of Tam5R cells. However, a decrease of the incorporation of iron into Fe-S cluster- or heme-containing mitochondrial proteins points to perturbations in iron utilization.

Different expression pattern of ABC transporters between both Tam5R cell lines have been documented in this work, proposing that alternative combinations of ABC transporters, rather than a single transporter, may be important for tamoxifen resistance. The transporters found to be similarly altered in both Tam5R cell lines might play a role in tamoxifen resistance and require further research.

Based on the previous reports as well as from our work it seems that the crosstalk of several mechanisms and signaling pathways underlies the acquisition of the tamoxifen resistant phenotype. Indeed, cell lines derived from the same breast cancer subtype exhibit different adaptations in order to become resistant. Therefore, fully understanding the phenomenon of tamoxifen resistance represents a challenge and warrants further investigation.

References

[1] Bray F, Ferlay J, Soerjomataram I, Siegel RL, Torre LA, Jemal A. Global cancer statistics 2018: GLOBOCAN estimates of incidence and mortality worldwide for 36 cancers in 185 countries. CA Cancer J Clin. 2018;68:394-424.
[2] Housman G, Byler S, Heerboth S, Lapinska K, Longacre M, Snyder N, et al. Drug resistance in cancer: an overview. Cancers (Basel). 2014;6:1769-92.
[3] Visvader JE, Lindeman GJ. Cancer stem cells in solid tumours: accumulating evidence and unresolved questions. Nat Rev Cancer. 2008;8:755-68.
[4] Batlle E, Clevers H. Cancer stem cells revisited. Nat Med. 2017;23:1124-34.
[5] Recalcati S, Gammella E, Cairo G. Dysregulation of iron metabolism in cancer stem cells. Free Radic Biol Med. 2019;133:216-20.
[6] Rychtarcikova Z, Lettlova S, Tomkova V, Korenkova V, Langerova L, Simonova E, et al. Tumor-initiating cells of breast and prostate origin show alterations in the expression of genes related to iron metabolism. Oncotarget. 2017;8:6376-98.
[7] Begicevic RR, Falasca M. ABC Transporters in Cancer Stem Cells: Beyond Chemoresistance. Int J Mol Sci. 2017;18.
[8] Peiris-Pages M, Martinez-Outschoorn UE, Pestell RG, Sotgia F, Lisanti MP. Cancer stem cell metabolism. Breast Cancer Res. 2016;18:55.
[9] Snyder V, Reed-Newman TC, Arnold L, Thomas SM, Anant S. Cancer Stem Cell Metabolism and Potential Therapeutic Targets. Front Oncol. 2018;8:203.
[10] Chandel NS, Schumacker PT. Cells depleted of mitochondrial DNA (rho0) yield insight into physiological mechanisms. FEBS Lett. 1999;454:173-6.
[11] Vondrusova M, Bezawork-Geleta A, Sachaphibulkij K, Truksa J, Neuzil J. The effect of mitochondrially targeted anticancer agents on mitochondrial (super)complexes. Methods Mol Biol. 2015;1265:195-208.
[12] Tong WH, Rouault TA. Functions of mitochondrial ISCU and cytosolic ISCU in mammalian iron-sulfur cluster biogenesis and iron homeostasis. Cell Metab. 2006;3:199-210.
[13] Bravo-Sagua R, Lopez-Crisosto C, Parra V, Rodriguez-Pena M, Rothermel BA, Quest AF, et al. mTORC1 inhibitor rapamycin and ER stressor tunicamycin induce differential patterns of ER-mitochondria coupling. Sci Rep. 2016;6:36394.
[14] Schmitt S, Saathoff F, Meissner L, Schropp EM, Lichtmannegger J, Schulz S, et al. A semi-automated method for isolating functionally intact mitochondria from cultured cells and tissue biopsies. Anal Biochem. 2013;443:66-74.
[15] Zaha DC. Significance of immunohistochemistry in breast cancer. World J Clin Oncol. 2014;5:382-92.
[16] Perou CM, Sorlie T, Eisen MB, van de Rijn M, Jeffrey SS, Rees CA, et al. Molecular portraits of human breast tumours. Nature. 2000;406:747-52.
[17] Sorlie T, Perou CM, Tibshirani R, Aas T, Geisler S, Johnsen H, et al. Gene expression patterns of breast carcinomas distinguish tumor subclasses with clinical implications. Proc Natl Acad Sci U S A. 2001;98:10869-74.
[18] Dai X, Li T, Bai Z, Yang Y, Liu X, Zhan J, et al. Breast cancer intrinsic subtype classification, clinical use and future trends. Am J Cancer Res. 2015;5:2929-43.
[19] Miller E, Lee HJ, Lulla A, Hernandez L, Gokare P, Lim B. Current treatment of early breast cancer: adjuvant and neoadjuvant therapy. F1000Res. 2014;3:198.
[20] Davies C, Pan H, Godwin J, Gray R, Arriagada R, Raina V, et al. Long-term effects of continuing adjuvant tamoxifen to 10 years versus stopping at 5 years after diagnosis of oestrogen receptor-positive breast cancer: ATLAS, a randomised trial. Lancet. 2013;381:805-16.
[21] Early Breast Cancer Trialists' Collaborative G. Effects of chemotherapy and hormonal therapy for early breast cancer on recurrence and 15-year survival: an overview of the randomised trials. Lancet. 2005;365:1687-717.
[22] Cronin-Fenton DP, Damkier P, Lash TL. Metabolism and transport of tamoxifen in relation to its effectiveness: new perspectives on an ongoing controversy. Future Oncol. 2014;10:107-22.

[23] Lee HR, Kim TH, Choi KC. Functions and physiological roles of two types of estrogen receptors, ERalpha and ERbeta, identified by estrogen receptor knockout mouse. Lab Anim Res. 2012;28:71-6.
[24] Kumar R, Zakharov MN, Khan SH, Miki R, Jang H, Toraldo G, et al. The dynamic structure of the estrogen receptor. J Amino Acids. 2011;2011:812540.
[25] Renoir JM, Marsaud V, Lazennec G. Estrogen receptor signaling as a target for novel breast cancer therapeutics. Biochem Pharmacol. 2013;85:449-65.
[26] Hall JM, Couse JF, Korach KS. The multifaceted mechanisms of estradiol and estrogen receptor signaling. J Biol Chem. 2001;276:36869-72.
[27] Bennesch MA, Picard D. Minireview: Tipping the balance: ligand-independent activation of steroid receptors. Mol Endocrinol. 2015;29:349-63.
[28] Filardo EJ, Quinn JA, Bland KI, Frackelton AR, Jr. Estrogen-induced activation of Erk-1 and Erk-2 requires the G protein-coupled receptor homolog, GPR30, and occurs via trans-activation of the epidermal growth factor receptor through release of HB-EGF. Mol Endocrinol. 2000;14:1649-60.
[29] Bjornstrom L, Sjoberg M. Mechanisms of estrogen receptor signaling: convergence of genomic and nongenomic actions on target genes. Mol Endocrinol. 2005;19:833-42.
[30] Fuentes N, Silveyra P. Estrogen receptor signaling mechanisms. Adv Protein Chem Struct Biol. 2019;116:135-70.
[31] Michalides R, Griekspoor A, Balkenende A, Verwoerd D, Janssen L, Jalink K, et al. Tamoxifen resistance by a conformational arrest of the estrogen receptor alpha after PKA activation in breast cancer. Cancer Cell. 2004;5:597-605.
[32] Dutertre M, Smith CL. Molecular mechanisms of selective estrogen receptor modulator (SERM) action. J Pharmacol Exp Ther. 2000;295:431-7.
[33] Garcia-Becerra R, Santos N, Diaz L, Camacho J. Mechanisms of resistance to endocrine therapy in breast cancer: focus on signaling pathways, miRNAs and genetically based resistance. Int J Mol Sci. 2012;14:108-45.
[34] Chang M. Tamoxifen resistance in breast cancer. Biomol Ther (Seoul). 2012;20:256-67.
[35] Ottaviano YL, Issa JP, Parl FF, Smith HS, Baylin SB, Davidson NE. Methylation of the estrogen receptor gene CpG island marks loss of estrogen receptor expression in human breast cancer cells. Cancer Res. 1994;54:2552-5.
[36] Zhou Q, Atadja P, Davidson NE. Histone deacetylase inhibitor LBH589 reactivates silenced estrogen receptor alpha (ER) gene expression without loss of DNA hypermethylation. Cancer Biol Ther. 2007;6:64-9.
[37] Sharma D, Blum J, Yang X, Beaulieu N, Macleod AR, Davidson NE. Release of methyl CpG binding proteins and histone deacetylase 1 from the Estrogen receptor alpha (ER) promoter upon reactivation in ER-negative human breast cancer cells. Mol Endocrinol. 2005;19:1740-51.
[38] Wang Q, Jiang J, Ying G, Xie XQ, Zhang X, Xu W, et al. Tamoxifen enhances stemness and promotes metastasis of ERalpha36(+) breast cancer by upregulating ALDH1A1 in cancer cells. Cell Res. 2018;28:336-58.
[39] Li G, Zhang J, Jin K, He K, Zheng Y, Xu X, et al. Estrogen receptor-alpha36 is involved in development of acquired tamoxifen resistance via regulating the growth status switch in breast cancer cells. Mol Oncol. 2013;7:611-24.
[40] Ye P, Fang C, Zeng H, Shi Y, Pan Z, An N, et al. Differential microRNA expression profiles in tamoxifen-resistant human breast cancer cell lines induced by two methods. Oncol Lett. 2018;15:3532-9.
[41] Howard EW, Yang X. microRNA Regulation in Estrogen Receptor-Positive Breast Cancer and Endocrine Therapy. Biol Proced Online. 2018;20:17.
[42] Lettlova S, Brynychova V, Blecha J, Vrana D, Vondrusova M, Soucek P, et al. MiR-301a-3p Suppresses Estrogen Signaling by Directly Inhibiting ESR1 in ERalpha Positive Breast Cancer. Cell Physiol Biochem. 2018;46:2601-15.
[43] Miller TE, Ghoshal K, Ramaswamy B, Roy S, Datta J, Shapiro CL, et al. MicroRNA-221/222 confers tamoxifen resistance in breast cancer by targeting p27Kip1. J Biol Chem. 2008;283:29897-903.
[44] Murdter TE, Schroth W, Bacchus-Gerybadze L, Winter S, Heinkele G, Simon W, et al. Activity levels of tamoxifen metabolites at the estrogen receptor and the impact of genetic polymorphisms

of phase I and II enzymes on their concentration levels in plasma. Clin Pharmacol Ther. 2011;89:708-17.
[45] Stearns V, Rae JM. Pharmacogenetics and breast cancer endocrine therapy: CYP2D6 as a predictive factor for tamoxifen metabolism and drug response? Expert Rev Mol Med. 2008;10:e34.
[46] Droog M, Beelen K, Linn S, Zwart W. Tamoxifen resistance: from bench to bedside. Eur J Pharmacol. 2013;717:47-57.
[47] Shou J, Massarweh S, Osborne CK, Wakeling AE, Ali S, Weiss H, et al. Mechanisms of tamoxifen resistance: increased estrogen receptor-HER2/neu cross-talk in ER/HER2-positive breast cancer. J Natl Cancer Inst. 2004;96:926-35.
[48] Massarweh S, Osborne CK, Creighton CJ, Qin L, Tsimelzon A, Huang S, et al. Tamoxifen resistance in breast tumors is driven by growth factor receptor signaling with repression of classic estrogen receptor genomic function. Cancer Res. 2008;68:826-33.
[49] Sin WC, Lim CL. Breast cancer stem cells-from origins to targeted therapy. Stem Cell Investig. 2017;4:96.
[50] Prasetyanti PR, Medema JP. Intra-tumor heterogeneity from a cancer stem cell perspective. Mol Cancer. 2017;16:41.
[51] Loh CY, Chai JY, Tang TF, Wong WF, Sethi G, Shanmugam MK, et al. The E-Cadherin and N-Cadherin Switch in Epithelial-to-Mesenchymal Transition: Signaling, Therapeutic Implications, and Challenges. Cells. 2019;8.
[52] Liu S, Cong Y, Wang D, Sun Y, Deng L, Liu Y, et al. Breast cancer stem cells transition between epithelial and mesenchymal states reflective of their normal counterparts. Stem Cell Reports. 2014;2:78-91.
[53] Mani SA, Guo W, Liao MJ, Eaton EN, Ayyanan A, Zhou AY, et al. The epithelial-mesenchymal transition generates cells with properties of stem cells. Cell. 2008;133:704-15.
[54] Saeg F, Anbalagan M. Breast cancer stem cells and the challenges of eradication: a review of novel therapies. Stem Cell Investig. 2018;5:39.
[55] Piva M, Domenici G, Iriondo O, Rabano M, Simoes BM, Comaills V, et al. Sox2 promotes tamoxifen resistance in breast cancer cells. EMBO Mol Med. 2014;6:66-79.
[56] Dubrovska A, Hartung A, Bouchez LC, Walker JR, Reddy VA, Cho CY, et al. CXCR4 activation maintains a stem cell population in tamoxifen-resistant breast cancer cells through AhR signalling. Br J Cancer. 2012;107:43-52.
[57] Raffo D, Berardi DE, Pontiggia O, Todaro L, de Kier Joffe EB, Simian M. Tamoxifen selects for breast cancer cells with mammosphere forming capacity and increased growth rate. Breast Cancer Res Treat. 2013;142:537-48.
[58] Wang X, Wang G, Zhao Y, Liu X, Ding Q, Shi J, et al. STAT3 mediates resistance of CD44(+)CD24(-/low) breast cancer stem cells to tamoxifen in vitro. J Biomed Res. 2012;26:325-35.
[59] Liu H, Zhang HW, Sun XF, Guo XH, He YN, Cui SD, et al. Tamoxifen-resistant breast cancer cells possess cancer stem-like cell properties. Chin Med J (Engl). 2013;126:3030-4.
[60] Shaw LE, Sadler AJ, Pugazhendhi D, Darbre PD. Changes in oestrogen receptor-alpha and -beta during progression to acquired resistance to tamoxifen and fulvestrant (Faslodex, ICI 182,780) in MCF7 human breast cancer cells. J Steroid Biochem Mol Biol. 2006;99:19-32.
[61] Loh YN, Hedditch EL, Baker LA, Jary E, Ward RL, Ford CE. The Wnt signalling pathway is upregulated in an in vitro model of acquired tamoxifen resistant breast cancer. BMC Cancer. 2013;13:174.
[62] Xue X, Yang YA, Zhang A, Fong KW, Kim J, Song B, et al. LncRNA HOTAIR enhances ER signaling and confers tamoxifen resistance in breast cancer. Oncogene. 2016;35:2746-55.
[63] Kisanga ER, Gjerde J, Guerrieri-Gonzaga A, Pigatto F, Pesci-Feltri A, Robertson C, et al. Tamoxifen and metabolite concentrations in serum and breast cancer tissue during three dose regimens in a randomized preoperative trial. Clin Cancer Res. 2004;10:2336-43.
[64] Perez EA, Gandara DR, Edelman MJ, O'Donnell R, Lauder IJ, DeGregorio M. Phase I trial of high-dose tamoxifen in combination with cisplatin in patients with lung cancer and other advanced malignancies. Cancer Invest. 2003;21:1-6.
[65] Hertz DL, McLeod HL, Irvin WJ, Jr. Tamoxifen and CYP2D6: a contradiction of data. Oncologist. 2012;17:620-30.

[66] Regan MM, Leyland-Jones B, Bouzyk M, Pagani O, Tang W, Kammler R, et al. CYP2D6 genotype and tamoxifen response in postmenopausal women with endocrine-responsive breast cancer: the breast international group 1-98 trial. J Natl Cancer Inst. 2012;104:441-51.
[67] Goetz MP, Rae JM, Suman VJ, Safgren SL, Ames MM, Visscher DW, et al. Pharmacogenetics of tamoxifen biotransformation is associated with clinical outcomes of efficacy and hot flashes. J Clin Oncol. 2005;23:9312-8.
[68] Hiscox S, Baruha B, Smith C, Bellerby R, Goddard L, Jordan N, et al. Overexpression of CD44 accompanies acquired tamoxifen resistance in MCF7 cells and augments their sensitivity to the stromal factors, heregulin and hyaluronan. BMC Cancer. 2012;12:458.
[69] Liu Y, Nenutil R, Appleyard MV, Murray K, Boylan M, Thompson AM, et al. Lack of correlation of stem cell markers in breast cancer stem cells. Br J Cancer. 2014;110:2063-71.
[70] Hiscox S, Jiang WG, Obermeier K, Taylor K, Morgan L, Burmi R, et al. Tamoxifen resistance in MCF7 cells promotes EMT-like behaviour and involves modulation of beta-catenin phosphorylation. Int J Cancer. 2006;118:290-301.
[71] Wang Q, Gun M, Hong XY. Induced Tamoxifen Resistance is Mediated by Increased Methylation of E-Cadherin in Estrogen Receptor-Expressing Breast Cancer Cells. Sci Rep. 2019;9:14140.
[72] Gwak JM, Kim M, Kim HJ, Jang MH, Park SY. Expression of embryonal stem cell transcription factors in breast cancer: Oct4 as an indicator for poor clinical outcome and tamoxifen resistance. Oncotarget. 2017;8:36305-18.
[73] Scheibye-Knudsen M, Fang EF, Croteau DL, Wilson DM, 3rd, Bohr VA. Protecting the mitochondrial powerhouse. Trends Cell Biol. 2015;25:158-70.
[74] Osellame LD, Blacker TS, Duchen MR. Cellular and molecular mechanisms of mitochondrial function. Best Pract Res Clin Endocrinol Metab. 2012;26:711-23.
[75] Friedman JR, Nunnari J. Mitochondrial form and function. Nature. 2014;505:335-43.
[76] Stehling O, Lill R. The role of mitochondria in cellular iron-sulfur protein biogenesis: mechanisms, connected processes, and diseases. Cold Spring Harb Perspect Biol. 2013;5:a011312.
[77] Schon EA, DiMauro S, Hirano M. Human mitochondrial DNA: roles of inherited and somatic mutations. Nat Rev Genet. 2012;13:878-90.
[78] Lee SR, Han J. Mitochondrial Nucleoid: Shield and Switch of the Mitochondrial Genome. Oxid Med Cell Longev. 2017;2017:8060949.
[79] Wiedemann N, Pfanner N. Mitochondrial Machineries for Protein Import and Assembly. Annu Rev Biochem. 2017;86:685-714.
[80] Cagin U, Enriquez JA. The complex crosstalk between mitochondria and the nucleus: What goes in between? Int J Biochem Cell Biol. 2015;63:10-5.
[81] Chocron ES, Munkacsy E, Pickering AM. Cause or casualty: The role of mitochondrial DNA in aging and age-associated disease. Biochim Biophys Acta Mol Basis Dis. 2019;1865:285-97.
[82] Zhou Z, Austin GL, Young LEA, Johnson LA, Sun R. Mitochondrial Metabolism in Major Neurological Diseases. Cells. 2018;7.
[83] Akram M. Citric acid cycle and role of its intermediates in metabolism. Cell Biochem Biophys. 2014;68:475-8.
[84] Guo R, Gu J, Zong S, Wu M, Yang M. Structure and mechanism of mitochondrial electron transport chain. Biomed J. 2018;41:9-20.
[85] Wu M, Gu J, Guo R, Huang Y, Yang M. Structure of Mammalian Respiratory Supercomplex I1III2IV1. Cell. 2016;167:1598-609 e10.
[86] Gu J, Wu M, Guo R, Yan K, Lei J, Gao N, et al. The architecture of the mammalian respirasome. Nature. 2016;537:639-43.
[87] Letts JA, Fiedorczuk K, Sazanov LA. The architecture of respiratory supercomplexes. Nature. 2016;537:644-8.
[88] Acin-Perez R, Enriquez JA. The function of the respiratory supercomplexes: the plasticity model. Biochim Biophys Acta. 2014;1837:444-50.
[89] Anand P, Kunnumakkara AB, Sundaram C, Harikumar KB, Tharakan ST, Lai OS, et al. Cancer is a preventable disease that requires major lifestyle changes. Pharm Res. 2008;25:2097-116.
[90] Fernie AR, Carrari F, Sweetlove LJ. Respiratory metabolism: glycolysis, the TCA cycle and mitochondrial electron transport. Curr Opin Plant Biol. 2004;7:254-61.

[91] Zhao RZ, Jiang S, Zhang L, Yu ZB. Mitochondrial electron transport chain, ROS generation and uncoupling (Review). Int J Mol Med. 2019;44:3-15.
[92] Slimen IB, Najar T, Ghram A, Dabbebi H, Ben Mrad M, Abdrabbah M. Reactive oxygen species, heat stress and oxidative-induced mitochondrial damage. A review. Int J Hyperthermia. 2014;30:513-23.
[93] Kumari S, Badana AK, G MM, G S, Malla R. Reactive Oxygen Species: A Key Constituent in Cancer Survival. Biomark Insights. 2018;13:1177271918755391.
[94] Mailloux RJ. Mitochondrial Antioxidants and the Maintenance of Cellular Hydrogen Peroxide Levels. Oxid Med Cell Longev. 2018;2018:7857251.
[95] Tilokani L, Nagashima S, Paupe V, Prudent J. Mitochondrial dynamics: overview of molecular mechanisms. Essays Biochem. 2018;62:341-60.
[96] Otera H, Ishihara N, Mihara K. New insights into the function and regulation of mitochondrial fission. Biochim Biophys Acta. 2013;1833:1256-68.
[97] Chen H, Chan DC. Physiological functions of mitochondrial fusion. Ann N Y Acad Sci. 2010;1201:21-5.
[98] Westermann B. Mitochondrial fusion and fission in cell life and death. Nat Rev Mol Cell Biol. 2010;11:872-84.
[99] Youle RJ, van der Bliek AM. Mitochondrial fission, fusion, and stress. Science. 2012;337:1062-5.
[100] Simula L, Nazio F, Campello S. The mitochondrial dynamics in cancer and immune-surveillance. Semin Cancer Biol. 2017;47:29-42.
[101] Warburg O. On the origin of cancer cells. Science. 1956;123:309-14.
[102] Wenner CE, Weinhouse S. Metabolism of neoplastic tissue. III. Diphosphopyridine nucleotide requirements for oxidations by mitochondria of neoplastic and non-neoplastic tissues. Cancer Res. 1953;13:21-6.
[103] Weinhouse S. On respiratory impairment in cancer cells. Science. 1956;124:267-9.
[104] Wallace DC. Mitochondria and cancer. Nat Rev Cancer. 2012;12:685-98.
[105] Vyas S, Zaganjor E, Haigis MC. Mitochondria and Cancer. Cell. 2016;166:555-66.
[106] Liou GY, Storz P. Reactive oxygen species in cancer. Free Radic Res. 2010;44:479-96.
[107] Luo M, Shang L, Brooks MD, Jiagge E, Zhu Y, Buschhaus JM, et al. Targeting Breast Cancer Stem Cell State Equilibrium through Modulation of Redox Signaling. Cell Metab. 2018;28:69-86 e6.
[108] Hanahan D, Weinberg RA. Hallmarks of cancer: the next generation. Cell. 2011;144:646-74.
[109] Chae YC, Kim JH. Cancer stem cell metabolism: target for cancer therapy. BMB Rep. 2018;51:319-26.
[110] Zhou Y, Zhou Y, Shingu T, Feng L, Chen Z, Ogasawara M, et al. Metabolic alterations in highly tumorigenic glioblastoma cells: preference for hypoxia and high dependency on glycolysis. J Biol Chem. 2011;286:32843-53.
[111] Emmink BL, Verheem A, Van Houdt WJ, Steller EJ, Govaert KM, Pham TV, et al. The secretome of colon cancer stem cells contains drug-metabolizing enzymes. J Proteomics. 2013;91:84-96.
[112] Liao J, Qian F, Tchabo N, Mhawech-Fauceglia P, Beck A, Qian Z, et al. Ovarian cancer spheroid cells with stem cell-like properties contribute to tumor generation, metastasis and chemotherapy resistance through hypoxia-resistant metabolism. PLoS One. 2014;9:e84941.
[113] Palorini R, Votta G, Balestrieri C, Monestiroli A, Olivieri S, Vento R, et al. Energy metabolism characterization of a novel cancer stem cell-like line 3AB-OS. J Cell Biochem. 2014;115:368-79.
[114] Loureiro R, Mesquita KA, Magalhaes-Novais S, Oliveira PJ, Vega-Naredo I. Mitochondrial biology in cancer stem cells. Semin Cancer Biol. 2017;47:18-28.
[115] Janiszewska M, Suva ML, Riggi N, Houtkooper RH, Auwerx J, Clement-Schatlo V, et al. Imp2 controls oxidative phosphorylation and is crucial for preserving glioblastoma cancer stem cells. Genes Dev. 2012;26:1926-44.
[116] Ye XQ, Li Q, Wang GH, Sun FF, Huang GJ, Bian XW, et al. Mitochondrial and energy metabolism-related properties as novel indicators of lung cancer stem cells. Int J Cancer. 2011;129:820-31.

[117] Pasto A, Bellio C, Pilotto G, Ciminale V, Silic-Benussi M, Guzzo G, et al. Cancer stem cells from epithelial ovarian cancer patients privilege oxidative phosphorylation, and resist glucose deprivation. Oncotarget. 2014;5:4305-19.
[118] O'Neill S, Porter RK, McNamee N, Martinez VG, O'Driscoll L. 2-Deoxy-D-Glucose inhibits aggressive triple-negative breast cancer cells by targeting glycolysis and the cancer stem cell phenotype. Sci Rep. 2019;9:3788.
[119] Liu PP, Liao J, Tang ZJ, Wu WJ, Yang J, Zeng ZL, et al. Metabolic regulation of cancer cell side population by glucose through activation of the Akt pathway. Cell Death Differ. 2014;21:124-35.
[120] Vlashi E, Lagadec C, Vergnes L, Reue K, Frohnen P, Chan M, et al. Metabolic differences in breast cancer stem cells and differentiated progeny. Breast Cancer Res Treat. 2014;146:525-34.
[121] Banerjee A, Arvinrad P, Darley M, Laversin SA, Parker R, Rose-Zerilli MJJ, et al. The effects of restricted glycolysis on stem-cell like characteristics of breast cancer cells. Oncotarget. 2018;9:23274-88.
[122] JAIN S, Wolf DA. Abstract LB-397: SMIP004-7: A novel oxidative phosphorylation inhibitor selectively kills Breast Cancer Stem-Like Cells with metabolic vulnerabilities. Cancer Research. 2018;78:LB-397-LB-.
[123] Walsh HR, Cruickshank BM, Brown JM, Marcato P. The Flick of a Switch: Conferring Survival Advantage to Breast Cancer Stem Cells Through Metabolic Plasticity. Front Oncol. 2019;9:753.
[124] Larosche I, Letteron P, Fromenty B, Vadrot N, Abbey-Toby A, Feldmann G, et al. Tamoxifen inhibits topoisomerases, depletes mitochondrial DNA, and triggers steatosis in mouse liver. J Pharmacol Exp Ther. 2007;321:526-35.
[125] Moreira PI, Custodio J, Moreno A, Oliveira CR, Santos MS. Tamoxifen and estradiol interact with the flavin mononucleotide site of complex I leading to mitochondrial failure. J Biol Chem. 2006;281:10143-52.
[126] Tuquet C, Dupont J, Mesneau A, Roussaux J. Effects of tamoxifen on the electron transport chain of isolated rat liver mitochondria. Cell Biol Toxicol. 2000;16:207-19.
[127] Rohlenova K, Sachaphibulkij K, Stursa J, Bezawork-Geleta A, Blecha J, Endaya B, et al. Selective Disruption of Respiratory Supercomplexes as a New Strategy to Suppress Her2(high) Breast Cancer. Antioxid Redox Signal. 2017;26:84-103.
[128] Fiorillo M, Sotgia F, Sisci D, Cappello AR, Lisanti MP. Mitochondrial "power" drives tamoxifen resistance: NQO1 and GCLC are new therapeutic targets in breast cancer. Oncotarget. 2017;8:20309-27.
[129] Radde BN, Ivanova MM, Mai HX, Alizadeh-Rad N, Piell K, Van Hoose P, et al. Nuclear respiratory factor-1 and bioenergetics in tamoxifen-resistant breast cancer cells. Exp Cell Res. 2016;347:222-31.
[130] Tomkova V, Sandoval-Acuna C, Torrealba N, Truksa J. Mitochondrial fragmentation, elevated mitochondrial superoxide and respiratory supercomplexes disassembly is connected with the tamoxifen-resistant phenotype of breast cancer cells. Free Radic Biol Med. 2019;143:510-21.
[131] Yu T, Robotham JL, Yoon Y. Increased production of reactive oxygen species in hyperglycemic conditions requires dynamic change of mitochondrial morphology. Proc Natl Acad Sci U S A. 2006;103:2653-8.
[132] Kim J, Yang G, Kim Y, Kim J, Ha J. AMPK activators: mechanisms of action and physiological activities. Exp Mol Med. 2016;48:e224.
[133] Martinez-Pastor B, Mostoslavsky R. Sirtuins, metabolism, and cancer. Front Pharmacol. 2012;3:22.
[134] Shagufta, Ahmad I. Tamoxifen a pioneering drug: An update on the therapeutic potential of tamoxifen derivatives. Eur J Med Chem. 2018;143:515-31.
[135] Lopez-Fabuel I, Le Douce J, Logan A, James AM, Bonvento G, Murphy MP, et al. Complex I assembly into supercomplexes determines differential mitochondrial ROS production in neurons and astrocytes. Proc Natl Acad Sci U S A. 2016;113:13063-8.
[136] Maranzana E, Barbero G, Falasca AI, Lenaz G, Genova ML. Mitochondrial respiratory supercomplex association limits production of reactive oxygen species from complex I. Antioxid Redox Signal. 2013;19:1469-80.

[137] Ishikawa K, Takenaga K, Akimoto M, Koshikawa N, Yamaguchi A, Imanishi H, et al. ROS-generating mitochondrial DNA mutations can regulate tumor cell metastasis. Science. 2008;320:661-4.
[138] Lin HY, Weng SW, Chang YH, Su YJ, Chang CM, Tsai CJ, et al. The Causal Role of Mitochondrial Dynamics in Regulating Insulin Resistance in Diabetes: Link through Mitochondrial Reactive Oxygen Species. Oxid Med Cell Longev. 2018;2018:7514383.
[139] Porporato PE, Payen VL, Perez-Escuredo J, De Saedeleer CJ, Danhier P, Copetti T, et al. A mitochondrial switch promotes tumor metastasis. Cell Rep. 2014;8:754-66.
[140] Peiris-Pages M, Bonuccelli G, Sotgia F, Lisanti MP. Mitochondrial fission as a driver of stemness in tumor cells: mDIVI1 inhibits mitochondrial function, cell migration and cancer stem cell (CSC) signalling. Oncotarget. 2018;9:13254-75.
[141] Han SY, Jeong YJ, Choi Y, Hwang SK, Bae YS, Chang YC. Mitochondrial dysfunction induces the invasive phenotype, and cell migration and invasion, through the induction of AKT and AMPK pathways in lung cancer cells. Int J Mol Med. 2018;42:1644-52.
[142] Zhao J, Zhang J, Yu M, Xie Y, Huang Y, Wolff DW, et al. Mitochondrial dynamics regulates migration and invasion of breast cancer cells. Oncogene. 2013;32:4814-24.
[143] Arena G, Cisse MY, Pyrdziak S, Chatre L, Riscal R, Fuentes M, et al. Mitochondrial MDM2 Regulates Respiratory Complex I Activity Independently of p53. Mol Cell. 2018;69:594-609 e8.
[144] Wang WJ, Wang Y, Long JY, Wang JR, Haudek SB, Overbeek P, et al. Mitochondrial Fission Triggered by Hyperglycemia Is Mediated by ROCK1 Activation in Podocytes and Endothelial Cells. Cell Metabolism. 2012;15:186-200.
[145] Han XJ, Yang ZJ, Jiang LP, Wei YF, Liao MF, Qian Y, et al. Mitochondrial dynamics regulates hypoxia-induced migration and antineoplastic activity of cisplatin in breast cancer cells. Int J Oncol. 2015;46:691-700.
[146] Toyama EQ, Herzig S, Courchet J, Lewis TL, Jr., Loson OC, Hellberg K, et al. Metabolism. AMP-activated protein kinase mediates mitochondrial fission in response to energy stress. Science. 2016;351:275-81.
[147] Hagenbuchner J, Kuznetsov AV, Obexer P, Ausserlechner MJ. BIRC5/Survivin enhances aerobic glycolysis and drug resistance by altered regulation of the mitochondrial fusion/fission machinery. Oncogene. 2013;32:4748-57.
[148] Frezza C. Metabolism and cancer: the future is now. Br J Cancer. 2020;122:133-5.
[149] Daurio NA, Tuttle SW, Worth AJ, Song EY, Davis JM, Snyder NW, et al. AMPK Activation and Metabolic Reprogramming by Tamoxifen through Estrogen Receptor-Independent Mechanisms Suggests New Uses for This Therapeutic Modality in Cancer Treatment. Cancer Res. 2016;76:3295-306.
[150] Owen OE, Kalhan SC, Hanson RW. The key role of anaplerosis and cataplerosis for citric acid cycle function. J Biol Chem. 2002;277:30409-12.
[151] Wilkins HM, Harris JL, Carl SM, E L, Lu J, Eva Selfridge J, et al. Oxaloacetate activates brain mitochondrial biogenesis, enhances the insulin pathway, reduces inflammation and stimulates neurogenesis. Hum Mol Genet. 2014;23:6528-41.
[152] Bain JR, Stevens RD, Wenner BR, Ilkayeva O, Muoio DM, Newgard CB. Metabolomics applied to diabetes research: moving from information to knowledge. Diabetes. 2009;58:2429-43.
[153] Ronnebaum SM, Ilkayeva O, Burgess SC, Joseph JW, Lu D, Stevens RD, et al. A pyruvate cycling pathway involving cytosolic NADP-dependent isocitrate dehydrogenase regulates glucose-stimulated insulin secretion. J Biol Chem. 2006;281:30593-602.
[154] Altman BJ, Stine ZE, Dang CV. From Krebs to clinic: glutamine metabolism to cancer therapy. Nat Rev Cancer. 2016;16:773.
[155] Chin RM, Fu X, Pai MY, Vergnes L, Hwang H, Deng G, et al. The metabolite alpha-ketoglutarate extends lifespan by inhibiting ATP synthase and TOR. Nature. 2014;510:397-401.
[156] Liu S, He L, Yao K. The Antioxidative Function of Alpha-Ketoglutarate and Its Applications. Biomed Res Int. 2018;2018:3408467.
[157] Ruderman NB, Xu XJ, Nelson L, Cacicedo JM, Saha AK, Lan F, et al. AMPK and SIRT1: a long-standing partnership? Am J Physiol Endocrinol Metab. 2010;298:E751-60.
[158] Huh JE, Shin JH, Jang ES, Park SJ, Park DR, Ko R, et al. Sirtuin 3 (SIRT3) maintains bone homeostasis by regulating AMPK-PGC-1beta axis in mice. Sci Rep. 2016;6:22511.

[159] Kincaid B, Bossy-Wetzel E. Forever young: SIRT3 a shield against mitochondrial meltdown, aging, and neurodegeneration. Front Aging Neurosci. 2013;5:48.
[160] Weir HJ, Lane JD, Balthasar N. SIRT3: A Central Regulator of Mitochondrial Adaptation in Health and Disease. Genes Cancer. 2013;4:118-24.
[161] Verdin E, Hirschey MD, Finley LW, Haigis MC. Sirtuin regulation of mitochondria: energy production, apoptosis, and signaling. Trends Biochem Sci. 2010;35:669-75.
[162] Osborne B, Bentley NL, Montgomery MK, Turner N. The role of mitochondrial sirtuins in health and disease. Free Radic Biol Med. 2016;100:164-74.
[163] Bause AS, Haigis MC. SIRT3 regulation of mitochondrial oxidative stress. Exp Gerontol. 2013;48:634-9.
[164] Zhang L, Ren X, Cheng Y, Huber-Keener K, Liu X, Zhang Y, et al. Identification of Sirtuin 3, a mitochondrial protein deacetylase, as a new contributor to tamoxifen resistance in breast cancer cells. Biochem Pharmacol. 2013;86:726-33.
[165] Someya S, Yu W, Hallows WC, Xu J, Vann JM, Leeuwenburgh C, et al. Sirt3 mediates reduction of oxidative damage and prevention of age-related hearing loss under caloric restriction. Cell. 2010;143:802-12.
[166] Hallows WC, Lee S, Denu JM. Sirtuins deacetylate and activate mammalian acetyl-CoA synthetases. Proc Natl Acad Sci U S A. 2006;103:10230-5.
[167] Blacker TS, Duchen MR. Investigating mitochondrial redox state using NADH and NADPH autofluorescence. Free Radic Biol Med. 2016;100:53-65.
[168] Naito A, Carcel-Trullols J, Xie CH, Evans TT, Mizumachi T, Higuchi M. Induction of acquired resistance to antiestrogen by reversible mitochondrial DNA depletion in breast cancer cell line. Int J Cancer. 2008;122:1506-11.
[169] Kaplan J, Ward DM. The essential nature of iron usage and regulation. Curr Biol. 2013;23:R642-6.
[170] Dev S, Babitt JL. Overview of iron metabolism in health and disease. Hemodial Int. 2017;21 Suppl 1:S6-S20.
[171] Winter WE, Bazydlo LA, Harris NS. The molecular biology of human iron metabolism. Lab Med. 2014;45:92-102.
[172] Winterbourn CC. Toxicity of iron and hydrogen peroxide: the Fenton reaction. Toxicol Lett. 1995;82-83:969-74.
[173] Goswami T, Rolfs A, Hediger MA. Iron transport: emerging roles in health and disease. Biochem Cell Biol. 2002;80:679-89.
[174] Abbaspour N, Hurrell R, Kelishadi R. Review on iron and its importance for human health. J Res Med Sci. 2014;19:164-74.
[175] Lane DJ, Merlot AM, Huang ML, Bae DH, Jansson PJ, Sahni S, et al. Cellular iron uptake, trafficking and metabolism: Key molecules and mechanisms and their roles in disease. Biochim Biophys Acta. 2015;1853:1130-44.
[176] Ganz T. Systemic iron homeostasis. Physiol Rev. 2013;93:1721-41.
[177] Papanikolaou G, Tzilianos M, Christakis JI, Bogdanos D, Tsimirika K, MacFarlane J, et al. Hepcidin in iron overload disorders. Blood. 2005;105:4103-5.
[178] Wang J, Pantopoulos K. Regulation of cellular iron metabolism. Biochem J. 2011;434:365-81.
[179] Liuzzi JP, Aydemir F, Nam H, Knutson MD, Cousins RJ. Zip14 (Slc39a14) mediates non-transferrin-bound iron uptake into cells. Proc Natl Acad Sci U S A. 2006;103:13612-7.
[180] Mackenzie B, Ujwal ML, Chang MH, Romero MF, Hediger MA. Divalent metal-ion transporter DMT1 mediates both H+ -coupled Fe2+ transport and uncoupled fluxes. Pflugers Arch. 2006;451:544-58.
[181] Kruszewski M. Labile iron pool: the main determinant of cellular response to oxidative stress. Mutat Res. 2003;531:81-92.
[182] Philpott CC, Ryu MS, Frey A, Patel S. Cytosolic iron chaperones: Proteins delivering iron cofactors in the cytosol of mammalian cells. J Biol Chem. 2017;292:12764-71.
[183] Carmona F, Poli M, Bertuzzi M, Gianoncelli A, Gangemi F, Arosio P. Study of ferritin self-assembly and heteropolymer formation by the use of Fluorescence Resonance Energy Transfer (FRET) technology. Biochim Biophys Acta Gen Subj. 2017;1861:522-32.
[184] Paul BT, Manz DH, Torti FM, Torti SV. Mitochondria and Iron: current questions. Expert Rev Hematol. 2017;10:65-79.

[185] Chen W, Paradkar PN, Li L, Pierce EL, Langer NB, Takahashi-Makise N, et al. Abcb10 physically interacts with mitoferrin-1 (Slc25a37) to enhance its stability and function in the erythroid mitochondria. Proc Natl Acad Sci U S A. 2009;106:16263-8.
[186] Sheftel AD, Zhang AS, Brown C, Shirihai OS, Ponka P. Direct interorganellar transfer of iron from endosome to mitochondrion. Blood. 2007;110:125-32.
[187] Levi S, Corsi B, Bosisio M, Invernizzi R, Volz A, Sanford D, et al. A human mitochondrial ferritin encoded by an intronless gene. J Biol Chem. 2001;276:24437-40.
[188] Braymer JJ, Lill R. Iron-sulfur cluster biogenesis and trafficking in mitochondria. J Biol Chem. 2017;292:12754-63.
[189] Hamza I, Dailey HA. One ring to rule them all: trafficking of heme and heme synthesis intermediates in the metazoans. Biochim Biophys Acta. 2012;1823:1617-32.
[190] Chiabrando D, Vinchi F, Fiorito V, Mercurio S, Tolosano E. Heme in pathophysiology: a matter of scavenging, metabolism and trafficking across cell membranes. Front Pharmacol. 2014;5:61.
[191] Muckenthaler MU, Rivella S, Hentze MW, Galy B. A Red Carpet for Iron Metabolism. Cell. 2017;168:344-61.
[192] Bogdan AR, Miyazawa M, Hashimoto K, Tsuji Y. Regulators of Iron Homeostasis: New Players in Metabolism, Cell Death, and Disease. Trends Biochem Sci. 2016;41:274-86.
[193] Wilkinson N, Pantopoulos K. The IRP/IRE system in vivo: insights from mouse models. Front Pharmacol. 2014;5:176.
[194] Anderson CP, Shen M, Eisenstein RS, Leibold EA. Mammalian iron metabolism and its control by iron regulatory proteins. Biochim Biophys Acta. 2012;1823:1468-83.
[195] Neves J, Haider T, Gassmann M, Muckenthaler MU. Iron Homeostasis in the Lungs-A Balance between Health and Disease. Pharmaceuticals (Basel). 2019;12.
[196] Schneider BD, Leibold EA. Effects of iron regulatory protein regulation on iron homeostasis during hypoxia. Blood. 2003;102:3404-11.
[197] Hanson ES, Foot LM, Leibold EA. Hypoxia post-translationally activates iron-regulatory protein 2. J Biol Chem. 1999;274:5047-52.
[198] Luo QQ, Wang D, Yu MY, Zhu L. Effect of hypoxia on the expression of iron regulatory proteins 1 and the mechanisms involved. IUBMB Life. 2011;63:120-8.
[199] Chepelev NL, Willmore WG. Regulation of iron pathways in response to hypoxia. Free Radic Biol Med. 2011;50:645-66.
[200] Anderson SA, Nizzi CP, Chang YI, Deck KM, Schmidt PJ, Galy B, et al. The IRP1-HIF-2alpha axis coordinates iron and oxygen sensing with erythropoiesis and iron absorption. Cell Metab. 2013;17:282-90.
[201] Renassia C, Peyssonnaux C. New insights into the links between hypoxia and iron homeostasis. Curr Opin Hematol. 2019;26:125-30.
[202] Kluckova K, Tennant DA. Metabolic implications of hypoxia and pseudohypoxia in pheochromocytoma and paraganglioma. Cell Tissue Res. 2018;372:367-78.
[203] Lake DF, Faigel DO. The emerging role of QSOX1 in cancer. Antioxid Redox Signal. 2014;21:485-96.
[204] Coppock DL, Cina-Poppe D, Gilleran S. The quiescin Q6 gene (QSCN6) is a fusion of two ancient gene families: thioredoxin and ERV1. Genomics. 1998;54:460-8.
[205] Katchman BA, Ocal IT, Cunliffe HE, Chang YH, Hostetter G, Watanabe A, et al. Expression of quiescin sulfhydryl oxidase 1 is associated with a highly invasive phenotype and correlates with a poor prognosis in Luminal B breast cancer. Breast Cancer Res. 2013;15:R28.
[206] Knutsvik G, Collett K, Arnes J, Akslen LA, Stefansson IM. QSOX1 expression is associated with aggressive tumor features and reduced survival in breast carcinomas. Mod Pathol. 2016;29:1485-91.
[207] Torti SV, Torti FM. Iron and cancer: more ore to be mined. Nat Rev Cancer. 2013;13:342-55.
[208] Jung M, Mertens C, Tomat E, Brune B. Iron as a Central Player and Promising Target in Cancer Progression. Int J Mol Sci. 2019;20.
[209] Habashy HO, Powe DG, Staka CM, Rakha EA, Ball G, Green AR, et al. Transferrin receptor (CD71) is a marker of poor prognosis in breast cancer and can predict response to tamoxifen. Breast Cancer Res Treat. 2010;119:283-93.

[210] Brookes MJ, Hughes S, Turner FE, Reynolds G, Sharma N, Ismail T, et al. Modulation of iron transport proteins in human colorectal carcinogenesis. Gut. 2006;55:1449-60.
[211] Manz DH, Blanchette NL, Paul BT, Torti FM, Torti SV. Iron and cancer: recent insights. Ann N Y Acad Sci. 2016;1368:149-61.
[212] Huang X. Iron overload and its association with cancer risk in humans: evidence for iron as a carcinogenic metal. Mutat Res. 2003;533:153-71.
[213] Chitambar CR. Gallium and its competing roles with iron in biological systems. Biochim Biophys Acta. 2016;1863:2044-53.
[214] El Hout M, Dos Santos L, Hamai A, Mehrpour M. A promising new approach to cancer therapy: Targeting iron metabolism in cancer stem cells. Semin Cancer Biol. 2018;53:125-38.
[215] Schonberg DL, Miller TE, Wu Q, Flavahan WA, Das NK, Hale JS, et al. Preferential Iron Trafficking Characterizes Glioblastoma Stem-like Cells. Cancer Cell. 2015;28:441-55.
[216] Mai TT, Hamai A, Hienzsch A, Caneque T, Muller S, Wicinski J, et al. Salinomycin kills cancer stem cells by sequestering iron in lysosomes. Nat Chem. 2017;9:1025-33.
[217] Miller LD, Coffman LG, Chou JW, Black MA, Bergh J, D'Agostino R, Jr., et al. An iron regulatory gene signature predicts outcome in breast cancer. Cancer Res. 2011;71:6728-37.
[218] Alkhateeb AA, Connor JR. The significance of ferritin in cancer: anti-oxidation, inflammation and tumorigenesis. Biochim Biophys Acta. 2013;1836:245-54.
[219] Shpyleva SI, Tryndyak VP, Kovalchuk O, Starlard-Davenport A, Chekhun VF, Beland FA, et al. Role of ferritin alterations in human breast cancer cells. Breast Cancer Res Treat. 2011;126:63-71.
[220] Orino K, Lehman L, Tsuji Y, Ayaki H, Torti SV, Torti FM. Ferritin and the response to oxidative stress. Biochem J. 2001;357:241-7.
[221] Geller SA, de Campos FP. Hereditary hemochromatosis. Autops Case Rep. 2015;5:7-10.
[222] Agudo A, Bonet C, Sala N, Munoz X, Aranda N, Fonseca-Nunes A, et al. Hemochromatosis (HFE) gene mutations and risk of gastric cancer in the European Prospective Investigation into Cancer and Nutrition (EPIC) study. Carcinogenesis. 2013;34:1244-50.
[223] Kallianpur AR, Hall LD, Yadav M, Christman BW, Dittus RS, Haines JL, et al. Increased prevalence of the HFE C282Y hemochromatosis allele in women with breast cancer. Cancer Epidemiol Biomarkers Prev. 2004;13:205-12.
[224] Shaheen NJ, Silverman LM, Keku T, Lawrence LB, Rohlfs EM, Martin CF, et al. Association between hemochromatosis (HFE) gene mutation carrier status and the risk of colon cancer. J Natl Cancer Inst. 2003;95:154-9.
[225] Feder JN. The hereditary hemochromatosis gene (HFE): a MHC class I-like gene that functions in the regulation of iron homeostasis. Immunol Res. 1999;20:175-85.
[226] Chen Y, Zhang S, Wang X, Guo W, Wang L, Zhang D, et al. Disordered signaling governing ferroportin transcription favors breast cancer growth. Cell Signal. 2015;27:168-76.
[227] Pinnix ZK, Miller LD, Wang W, D'Agostino R, Jr., Kute T, Willingham MC, et al. Ferroportin and iron regulation in breast cancer progression and prognosis. Sci Transl Med. 2010;2:43ra56.
[228] Wang YF, Zhang J, Su Y, Shen YY, Jiang DX, Hou YY, et al. G9a regulates breast cancer growth by modulating iron homeostasis through the repression of ferroxidase hephaestin. Nat Commun. 2017;8:274.
[229] Li H, Liu Y, Shang L, Cai J, Wu J, Zhang W, et al. Iron regulatory protein 2 modulates the switch from aerobic glycolysis to oxidative phosphorylation in mouse embryonic fibroblasts. Proc Natl Acad Sci U S A. 2019;116:9871-6.
[230] Huang BW, Miyazawa M, Tsuji Y. Distinct regulatory mechanisms of the human ferritin gene by hypoxia and hypoxia mimetic cobalt chloride at the transcriptional and post-transcriptional levels. Cell Signal. 2014;26:2702-9.
[231] Hyde BB, Elorza AA, Mikkola HK, Schlaeger TM, Shirihai OS. ABC-Me (ABCB10) Is Required for Erythroid Development in the Mouse Embryo and Is Protective against Mitochondrial Oxidative Stress. Blood. 2008;112:529-.
[232] Hyde BB, Liesa M, Elorza AA, Qiu W, Haigh SE, Richey L, et al. The mitochondrial transporter ABC-me (ABCB10), a downstream target of GATA-1, is essential for erythropoiesis in vivo. Cell Death Differ. 2012;19:1117-26.

[233] Liesa M, Luptak I, Qin F, Hyde BB, Sahin E, Siwik DA, et al. Mitochondrial transporter ATP binding cassette mitochondrial erythroid is a novel gene required for cardiac recovery after ischemia/reperfusion. Circulation. 2011;124:806-13.
[234] Davis MR, Shawron KM, Rendina E, Peterson SK, Lucas EA, Smith BJ, et al. Hypoxia inducible factor-2 alpha is translationally repressed in response to dietary iron deficiency in Sprague-Dawley rats. J Nutr. 2011;141:1590-6.
[235] Yan Y, Liu F, Han L, Zhao L, Chen J, Olopade OI, et al. HIF-2alpha promotes conversion to a stem cell phenotype and induces chemoresistance in breast cancer cells by activating Wnt and Notch pathways. J Exp Clin Cancer Res. 2018;37:256.
[236] Isono T, Chano T, Yoshida T, Kageyama S, Kawauchi A, Suzaki M, et al. Hydroxyl-HIF2-alpha is potential therapeutic target for renal cell carcinomas. Am J Cancer Res. 2016;6:2263-76.
[237] Zhang Q, Lou Y, Zhang J, Fu Q, Wei T, Sun X, et al. Hypoxia-inducible factor-2alpha promotes tumor progression and has crosstalk with Wnt/beta-catenin signaling in pancreatic cancer. Mol Cancer. 2017;16:119.
[238] Anderson ER, Taylor M, Xue X, Ramakrishnan SK, Martin A, Xie L, et al. Intestinal HIF2alpha promotes tissue-iron accumulation in disorders of iron overload with anemia. Proc Natl Acad Sci U S A. 2013;110:E4922-30.
[239] Shi CY, Fan Y, Liu B, Lou WH. HIF1 contributes to hypoxia-induced pancreatic cancer cells invasion via promoting QSOX1 expression. Cell Physiol Biochem. 2013;32:561-8.
[240] Das P, Siegers GM, Postovit LM. Illuminating luminal B: QSOX1 as a subtype-specific biomarker. Breast Cancer Res. 2013;15:104.
[241] Wilkens S. Structure and mechanism of ABC transporters. F1000Prime Rep. 2015;7:14.
[242] Rees DC, Johnson E, Lewinson O. ABC transporters: the power to change. Nat Rev Mol Cell Biol. 2009;10:218-27.
[243] ter Beek J, Guskov A, Slotboom DJ. Structural diversity of ABC transporters. J Gen Physiol. 2014;143:419-35.
[244] Jones PM, George AM. The ABC transporter structure and mechanism: perspectives on recent research. Cell Mol Life Sci. 2004;61:682-99.
[245] Linton KJ. Structure and function of ABC transporters. Physiology (Bethesda). 2007;22:122-30.
[246] Dermauw W, Van Leeuwen T. The ABC gene family in arthropods: comparative genomics and role in insecticide transport and resistance. Insect Biochem Mol Biol. 2014;45:89-110.
[247] Vasiliou V, Vasiliou K, Nebert DW. Human ATP-binding cassette (ABC) transporter family. Hum Genomics. 2009;3:281-90.
[248] Prochazka L, Koudelka S, Dong LF, Stursa J, Goodwin J, Neca J, et al. Mitochondrial targeting overcomes ABCA1-dependent resistance of lung carcinoma to alpha-tocopheryl succinate. Apoptosis. 2013;18:286-99.
[249] Kralova J, Kolar M, Kahle M, Truksa J, Lettlova S, Balusikova K, et al. Glycol porphyrin derivatives and temoporfin elicit resistance to photodynamic therapy by different mechanisms. Sci Rep. 2017;7:44497.
[250] Fu D. Where is it and How Does it Get There - Intracellular Localization and Traffic of P-glycoprotein. Front Oncol. 2013;3:321.
[251] Schaedler TA, Faust B, Shintre CA, Carpenter EP, Srinivasan V, van Veen HW, et al. Structures and functions of mitochondrial ABC transporters. Biochem Soc Trans. 2015;43:943-51.
[252] Minami K, Kamijo Y, Nishizawa Y, Tabata S, Horikuchi F, Yamamoto M, et al. Expression of ABCB6 is related to resistance to 5-FU, SN-38 and vincristine. Anticancer Res. 2014;34:4767-73.
[253] Park S, Shimizu C, Shimoyama T, Takeda M, Ando M, Kohno T, et al. Gene expression profiling of ATP-binding cassette (ABC) transporters as a predictor of the pathologic response to neoadjuvant chemotherapy in breast cancer patients. Breast Cancer Res Treat. 2006;99:9-17.
[254] Kim JY, Kim JK, Kim H. ABCB7 simultaneously regulates apoptotic and non-apoptotic cell death by modulating mitochondrial ROS and HIF1alpha-driven NFkappaB signaling. Oncogene. 2020;39:1969-82.
[255] Elliott AM, Al-Hajj MA. ABCB8 mediates doxorubicin resistance in melanoma cells by protecting the mitochondrial genome. Mol Cancer Res. 2009;7:79-87.

[256] Oiso S, Takayama Y, Nakazaki R, Matsunaga N, Motooka C, Yamamura A, et al. Factors involved in the cisplatin resistance of KCP4 human epidermoid carcinoma cells. Oncol Rep. 2014;31:719-26.
[257] Sodani K, Patel A, Kathawala RJ, Chen ZS. Multidrug resistance associated proteins in multidrug resistance. Chin J Cancer. 2012;31:58-72.
[258] Gadsby DC, Vergani P, Csanady L. The ABC protein turned chloride channel whose failure causes cystic fibrosis. Nature. 2006;440:477-83.
[259] Bryan J, Munoz A, Zhang X, Dufer M, Drews G, Krippeit-Drews P, et al. ABCC8 and ABCC9: ABC transporters that regulate K+ channels. Pflugers Arch. 2007;453:703-18.
[260] Annilo T, Dean M. Degeneration of an ATP-binding cassette transporter gene, ABCC13, in different mammalian lineages. Genomics. 2004;84:34-46.
[261] Baker A, Carrier DJ, Schaedler T, Waterham HR, van Roermund CW, Theodoulou FL. Peroxisomal ABC transporters: functions and mechanism. Biochem Soc Trans. 2015;43:959-65.
[262] Coelho D, Kim JC, Miousse IR, Fung S, du Moulin M, Buers I, et al. Mutations in ABCD4 cause a new inborn error of vitamin B12 metabolism. Nat Genet. 2012;44:1152-5.
[263] Barthelme D, Dinkelaker S, Albers SV, Londei P, Ermler U, Tampe R. Ribosome recycling depends on a mechanistic link between the FeS cluster domain and a conformational switch of the twin-ATPase ABCE1. Proc Natl Acad Sci U S A. 2011;108:3228-33.
[264] Kusuhara H, Sugiyama Y. ATP-binding cassette, subfamily G (ABCG family). Pflugers Arch. 2007;453:735-44.
[265] Masereeuw R, Russel FG. Regulatory pathways for ATP-binding cassette transport proteins in kidney proximal tubules. AAPS J. 2012;14:883-94.
[266] Miller DS. Regulation of ABC transporters at the blood-brain barrier. Clin Pharmacol Ther. 2015;97:395-403.
[267] Choi CH. ABC transporters as multidrug resistance mechanisms and the development of chemosensitizers for their reversal. Cancer Cell Int. 2005;5:30.
[268] Fletcher JI, Williams RT, Henderson MJ, Norris MD, Haber M. ABC transporters as mediators of drug resistance and contributors to cancer cell biology. Drug Resist Updat. 2016;26:1-9.
[269] Katayama K, Noguchi K, Sugimoto Y. Regulations of P-Glycoprotein/ABCB1/MDR1 in Human Cancer Cells. New Journal of Science. 2014;2014:10.
[270] Cole SP, Bhardwaj G, Gerlach JH, Mackie JE, Grant CE, Almquist KC, et al. Overexpression of a transporter gene in a multidrug-resistant human lung cancer cell line. Science. 1992;258:1650-4.
[271] Munoz M, Henderson M, Haber M, Norris M. Role of the MRP1/ABCC1 multidrug transporter protein in cancer. IUBMB Life. 2007;59:752-7.
[272] Li XQ, Li J, Shi SB, Chen P, Yu LC, Bao QL. Expression of MRP1, BCRP, LRP and ERCC1 as prognostic factors in non-small cell lung cancer patients receiving postoperative cisplatin-based chemotherapy. Int J Biol Markers. 2009;24:230-7.
[273] Filipits M, Pohl G, Rudas M, Dietze O, Lax S, Grill R, et al. Clinical role of multidrug resistance protein 1 expression in chemotherapy resistance in early-stage breast cancer: the Austrian Breast and Colorectal Cancer Study Group. J Clin Oncol. 2005;23:1161-8.
[274] Haber M, Smith J, Bordow SB, Flemming C, Cohn SL, London WB, et al. Association of high-level MRP1 expression with poor clinical outcome in a large prospective study of primary neuroblastoma. J Clin Oncol. 2006;24:1546-53.
[275] Doyle LA, Yang W, Abruzzo LV, Krogmann T, Gao Y, Rishi AK, et al. A multidrug resistance transporter from human MCF-7 breast cancer cells. Proc Natl Acad Sci U S A. 1998;95:15665-70.
[276] Westover D, Li F. New trends for overcoming ABCG2/BCRP-mediated resistance to cancer therapies. J Exp Clin Cancer Res. 2015;34:159.
[277] Mao Q, Unadkat JD. Role of the breast cancer resistance protein (BCRP/ABCG2) in drug transport--an update. AAPS J. 2015;17:65-82.
[278] Zhou S, Schuetz JD, Bunting KD, Colapietro AM, Sampath J, Morris JJ, et al. The ABC transporter Bcrp1/ABCG2 is expressed in a wide variety of stem cells and is a molecular determinant of the side-population phenotype. Nat Med. 2001;7:1028-34.

[279] Ding XW, Wu JH, Jiang CP. ABCG2: a potential marker of stem cells and novel target in stem cell and cancer therapy. Life Sci. 2010;86:631-7.
[280] Haraguchi N, Utsunomiya T, Inoue H, Tanaka F, Mimori K, Barnard GF, et al. Characterization of a side population of cancer cells from human gastrointestinal system. Stem Cells. 2006;24:506-13.
[281] Hirschmann-Jax C, Foster AE, Wulf GG, Nuchtern JG, Jax TW, Gobel U, et al. A distinct "side population" of cells with high drug efflux capacity in human tumor cells. Proc Natl Acad Sci U S A. 2004;101:14228-33.
[282] Ho MM, Ng AV, Lam S, Hung JY. Side population in human lung cancer cell lines and tumors is enriched with stem-like cancer cells. Cancer Res. 2007;67:4827-33.
[283] Kruger JA, Kaplan CD, Luo Y, Zhou H, Markowitz D, Xiang R, et al. Characterization of stem cell-like cancer cells in immune-competent mice. Blood. 2006;108:3906-12.
[284] Fletcher JI, Haber M, Henderson MJ, Norris MD. ABC transporters in cancer: more than just drug efflux pumps. Nat Rev Cancer. 2010;10:147-56.
[285] Eyre R, Harvey I, Stemke-Hale K, Lennard TW, Tyson-Capper A, Meeson AP. Reversing paclitaxel resistance in ovarian cancer cells via inhibition of the ABCB1 expressing side population. Tumour Biol. 2014;35:9879-92.
[286] Keshet GI, Goldstein I, Itzhaki O, Cesarkas K, Shenhav L, Yakirevitch A, et al. MDR1 expression identifies human melanoma stem cells. Biochem Biophys Res Commun. 2008;368:930-6.
[287] Saxena M, Stephens MA, Pathak H, Rangarajan A. Transcription factors that mediate epithelial-mesenchymal transition lead to multidrug resistance by upregulating ABC transporters. Cell Death Dis. 2011;2:e179.
[288] Jiang ZS, Sun YZ, Wang SM, Ruan JS. Epithelial-mesenchymal transition: potential regulator of ABC transporters in tumor progression. J Cancer. 2017;8:2319-27.
[289] Teft WA, Mansell SE, Kim RB. Endoxifen, the active metabolite of tamoxifen, is a substrate of the efflux transporter P-glycoprotein (multidrug resistance 1). Drug Metab Dispos. 2011;39:558-62.
[290] Iusuf D, Teunissen SF, Wagenaar E, Rosing H, Beijnen JH, Schinkel AH. P-glycoprotein (ABCB1) transports the primary active tamoxifen metabolites endoxifen and 4-hydroxytamoxifen and restricts their brain penetration. J Pharmacol Exp Ther. 2011;337:710-7.
[291] Krisnamurti DG, Louisa M, Anggraeni E, Wanandi SI. Drug Efflux Transporters Are Overexpressed in Short-Term Tamoxifen-Induced MCF7 Breast Cancer Cells. Adv Pharmacol Sci. 2016;2016:6702424.
[292] Stefan SM. Multi-target ABC transporter modulators: what next and where to go? Future Med Chem. 2019;11:2353-8.
[293] Crawford RR, Potukuchi PK, Schuetz EG, Schuetz JD. Beyond Competitive Inhibition: Regulation of ABC Transporters by Kinases and Protein-Protein Interactions as Potential Mechanisms of Drug-Drug Interactions. Drug Metab Dispos. 2018;46:567-80.
[294] Stolarczyk EI, Reiling CJ, Paumi CM. Regulation of ABC transporter function via phosphorylation by protein kinases. Curr Pharm Biotechnol. 2011;12:621-35.
[295] Perego P, Gatti L, Beretta GL. The ABC of glycosylation. Nat Rev Cancer. 2010;10:523.
[296] Aryal B, Laurent C, Geisler M. Correction: Learning from each other: ABC transporter regulation by protein phosphorylation in plant and mammalian systems. Biochem Soc Trans. 2016;44:663-73.
[297] Jedlitschky G, Burchell B, Keppler D. The multidrug resistance protein 5 functions as an ATP-dependent export pump for cyclic nucleotides. J Biol Chem. 2000;275:30069-74.
[298] Wijnholds J, Mol CA, van Deemter L, de Haas M, Scheffer GL, Baas F, et al. Multidrug-resistance protein 5 is a multispecific organic anion transporter able to transport nucleotide analogs. Proc Natl Acad Sci U S A. 2000;97:7476-81.
[299] Hou Y, Zhu Q, Li Z, Peng Y, Yu X, Yuan B, et al. The FOXM1-ABCC5 axis contributes to paclitaxel resistance in nasopharyngeal carcinoma cells. Cell Death Dis. 2017;8:e2659.
[300] Wielinga P, Hooijberg JH, Gunnarsdottir S, Kathmann I, Reid G, Zelcer N, et al. The human multidrug resistance protein MRP5 transports folates and can mediate cellular resistance against antifolates. Cancer Res. 2005;65:4425-30.

[301] Pratt S, Shepard RL, Kandasamy RA, Johnston PA, Perry W, 3rd, Dantzig AH. The multidrug resistance protein 5 (ABCC5) confers resistance to 5-fluorouracil and transports its monophosphorylated metabolites. Mol Cancer Ther. 2005;4:855-63.
[302] Mourskaia AA, Amir E, Dong Z, Tiedemann K, Cory S, Omeroglu A, et al. ABCC5 supports osteoclast formation and promotes breast cancer metastasis to bone. Breast Cancer Res. 2012;14:R149.
[303] Korolnek T, Zhang J, Beardsley S, Scheffer GL, Hamza I. Control of metazoan heme homeostasis by a conserved multidrug resistance protein. Cell Metab. 2014;19:1008-19.
[304] Tarling EJ, Edwards PA. ATP binding cassette transporter G1 (ABCG1) is an intracellular sterol transporter. Proc Natl Acad Sci U S A. 2011;108:19719-24.
[305] Namba Y, Sogawa C, Okusha Y, Kawai H, Itagaki M, Ono K, et al. Depletion of Lipid Efflux Pump ABCG1 Triggers the Intracellular Accumulation of Extracellular Vesicles and Reduces Aggregation and Tumorigenesis of Metastatic Cancer Cells. Front Oncol. 2018;8:376.
[306] Chen YH, Cimino PJ, Luo J, Dahiya S, Gutmann DH. ABCG1 maintains high-grade glioma survival in vitro and in vivo. Oncotarget. 2016;7:23416-24.
[307] Chen YH, McGowan LD, Cimino PJ, Dahiya S, Leonard JR, Lee DY, et al. Mouse low-grade gliomas contain cancer stem cells with unique molecular and functional properties. Cell Rep. 2015;10:1899-912.
[308] Ding X, Zhang W, Li S, Yang H. The role of cholesterol metabolism in cancer. Am J Cancer Res. 2019;9:219-27.
[309] Ehmsen S, Pedersen MH, Wang G, Terp MG, Arslanagic A, Hood BL, et al. Increased Cholesterol Biosynthesis Is a Key Characteristic of Breast Cancer Stem Cells Influencing Patient Outcome. Cell Rep. 2019;27:3927-38 e6.
[310] Yasui K, Mihara S, Zhao C, Okamoto H, Saito-Ohara F, Tomida A, et al. Alteration in copy numbers of genes as a mechanism for acquired drug resistance. Cancer Res. 2004;64:1403-10.
[311] Bao L, Wu J, Dodson M, Rojo de la Vega EM, Ning Y, Zhang Z, et al. ABCF2, an Nrf2 target gene, contributes to cisplatin resistance in ovarian cancer cells. Mol Carcinog. 2017;56:1543-53.
[312] Ogawa Y, Tsuda H, Hai E, Tsuji N, Yamagata S, Tokunaga S, et al. Clinical role of ABCF2 expression in breast cancer. Anticancer Res. 2006;26:1809-14.
[313] Russel FG, Koenderink JB, Masereeuw R. Multidrug resistance protein 4 (MRP4/ABCC4): a versatile efflux transporter for drugs and signalling molecules. Trends Pharmacol Sci. 2008;29:200-7.
[314] Kochel TJ, Reader JC, Ma X, Kundu N, Fulton AM. Multiple drug resistance-associated protein (MRP4) exports prostaglandin E2 (PGE2) and contributes to metastasis in basal/triple negative breast cancer. Oncotarget. 2017;8:6540-54.
[315] Pondarre C, Antiochos BB, Campagna DR, Clarke SL, Greer EL, Deck KM, et al. The mitochondrial ATP-binding cassette transporter Abcb7 is essential in mice and participates in cytosolic iron-sulfur cluster biogenesis. Hum Mol Genet. 2006;15:953-64.
[316] Maio N, Kim KS, Holmes-Hampton G, Singh A, Rouault TA. Dimeric ferrochelatase bridges ABCB7 and ABCB10 homodimers in an architecturally defined molecular complex required for heme biosynthesis. Haematologica. 2019;104:1756-67.
[317] Kim JY, Kim JK, Kim H. ABCB7 simultaneously regulates apoptotic and non-apoptotic cell death by modulating mitochondrial ROS and HIF1alpha-driven NFkappaB signaling. Oncogene. 2019.
[318] Kispal G, Csere P, Guiard B, Lill R. The ABC transporter Atm1p is required for mitochondrial iron homeostasis. FEBS Lett. 1997;418:346-50.
[319] Choi HK, Yang JW, Roh SH, Han CY, Kang KW. Induction of multidrug resistance associated protein 2 in tamoxifen-resistant breast cancer cells. Endocr Relat Cancer. 2007;14:293-303.
[320] Bekele RT, Venkatraman G, Liu RZ, Tang X, Mi S, Benesch MG, et al. Oxidative stress contributes to the tamoxifen-induced killing of breast cancer cells: implications for tamoxifen therapy and resistance. Sci Rep. 2016;6:21164.

Supplement

Supplementary Table 1. List of used antibodies.

Protein	Supplier	Catalogue no.	Dillution	Host
BNE antibodies				
ATP5B (complex V)	Sigma-Aldrich	HPA001520	1:2500	rabbit
mtCO2 (complex IV)	Abcam	ab110258	1:2500	mouse
NDUFA9 (complex I)	Abcam	ab14713	1:7000	mouse
SDHA (complex II)	Abcam	ab14715	1:10000	mouse
UQCRC2 (complex III)	Abcam	ab14745	1:10000	mouse
VDAC1	Abcam	ab15895	1:5000	rabbit
SDS-PAGE antibodies				
ABCB10	ThermoFisher Scientific	PA5-30468	1:1000	rabbit
ABCB7	ThermoFisher Scientific	PA530219	1:1000	rabbit
ABCC1	Cell Signaling Technology	#14685S	1:1000	rabbit
ABCC4	Cell Signaling Technology	#12705S	1:1000	rabbit
ABCC5	Santa Cruz Biotechnology	sc-376965	1:1000	mouse
ABCC6	Abcam	ab134913	1:2000	rabbit
ABCF2	Santa Cruz Biotechnology	sc-390496	1:250	mouse
ABCG1	Abcam	ab52617	1:1000	rabbit
ABCG2	Cell Signaling Technology	#4477S	1:1000	rabbit
ACO1	ThermoFisher Scientific	PA527824	1:1000	rabbit
ACO2	Cell Signaling Technology	#6571S	1:1000	rabbit
β-actin HRP	Santa Cruz Biotechnology	sc-47778	1:10000	--
β-actin HRP	ThermoFisher Scientific	MA5-15739	1:2000	--
AMPKα	Cell Signaling Technology	#2532S	1:1000	rabbit
Catalase	Abcam	ab1877	1:1000	rabbit
CYBRD1	Bioss	bs-8297R	1:1000	rabbit
DMT1	Cell Signaling Technology	#15083	1:1000	rabbit
DRP1	Santa Cruz Biotechnology	sc-101270	1:1000	mouse
HIF2α	Santa Cruz Biotechnology	sc-46691	1:1000	mouse

Ferritin	Abcam	ab75973	1:1000	rabbit
FPN	Bioss	bs-4906R	1:1000	rabbit
GLRX5	Bioss	bs-13395R	1:1000	rabbit
GLUT-1	Abcam	ab15309	1:1000	rabbit
GPX1	Abcam	ab108427	1:5000	rabbit
HEPH	Santa Cruz Biotechnology	sc-365365	1:1000	rabbit
HFE	Bioss	bs-12335R	1:1000	rabbit
HKII	Santa Cruz Biotechnology	sc-374091	1:500	rabbit
IRP2	ThermoFisher Scientific	PA116544	1:500	rabbit
LDH-A	Santa Cruz Biotechnology	sc-137243	1:1000	mouse
LDH-B	Santa Cruz Biotechnology	sc-100775	1:500	mouse
MFRN1	Bioss	bs-9523R	1:1000	rabbit
PDK1	Santa Cruz Biotechnology	sc-293160	1:500	mouse
PFK2	Santa Cruz Biotechnology	sc-377416	1:500	mouse
Phospho-AMPK Substrate Motif [LXRXX(pS/pT)]	Cell Signaling Technology	#5759S	1:1000	rabbit
Phospho-AMPK α-1,2 (Ser485, Ser491)	ThermoFisher Scientific	PA5-17543	1:1000	rabbit
Phospho-AMPKα (Thr172)	Cell Signaling Technology	#2535S	1:1000	rabbit
Phospho-DRP1 (Ser616)	Cell Signaling Technology	#4494S	1:1000	rabbit
Phospho-DRP1 (Ser637)	Cell Signaling Technology	#6319S	1:1000	rabbit
QSOX1	ThermoFisher Scientific	PA5-66006	1:1000	rabbit
SIRT3	Cell Signaling Technology	#5490P	1:1000	rabbit
SOD2	Acris Antibodies	AP03024PU-N	1:10000	rabbit
TfR1	ThermoFisher Scientific	13-6800	1:2500	mouse
ZIP14	Abcam	ab191199	1:2000	rabbit
Secondary antibodies				
anti-mouse HRP	Invitrogen	31439	1:10000	goat
anti-rabbit HRP	Merck	AP132P	1:10000	goat

Supplementary Table 2. List of used primers

Gene	Sequence 5´ → 3´
Reference genes	
RPLP0	F: ATCACAGAGGAAACTCTGCATTCTCG
	R: GATAGAATGGGGTACTGATGCAACAGTT
GAPDH	F: GGGAAGGTGAAGGTCGGAGTCA
	R: TTGATGGCAACAATATCCACTTTACCAGA
TBP	F: TGTATCCACAGTGAATCTTGGTTGTAAA
	R: CGTGGCTCTCTTATCCTCATGATTAC
POLR2A	F: TGCTCCGTATTCGCATCATGAACA
	R: ATCTGTCAGCATGTTGGACTCGATG
HPRT1	F: GACACTGGCAAAACAATGCAGA
	R: CGTGGGGTCCTTTTCACCAG
PPIA	F: AACGTGGTATAAAAGGGGCGGG
	R: GTCGAAGAACACGGTGGGGTT
OAZ1	F: GGATCCTCAATAGCCACTGC
	R: TACAGCAGTGGAGGGAGACC
CSC markers	
SOX2	F: CAGAGAAGAGAGTGTTTGCAAAAGGGG
	R: GGCTTAAGCCTGGGGCTCAAA
CXCR4	F: TTGATGTGTGTCTAGGCAGGA
	R: GATTCACTACACGCTCTGGAATG
CDH2	F: GCGGAGATCCTACTGGACGGTT
	R: TTTCAAAGTCGATTGGTTTGACCACGG
CD44	F: GCTGACCTCTGCAAGGCTTTCAATAG
	R: CTTCTTCGACTGTTGACTGCAATGCA
ABCG2	F: TCGTTATTAGATGTCTTAGCTGCAA
	R: TTGTACCACGTAACCTGAATTACA
ABC transporters	
ABCA1	F: AGCCTGGAACTTCAGCCCTGGATGTACA
	R: GCCAGGGTCTTTGGTGAGGGCGTTTAA
ABCA2	F: ATCATGGTGAACGGTCGCCTG
	R: GGTCCGCACCGTGATCATGTAG
ABCA3	F: ACCTACATCCCCTGATGGCGGAGAAC
	R: TACTCCATGATGGCCCGGTCCACA
ABCA4	F: ACAGCAGACTGAAAGTCATGACCTCC
	R: GTTCCTTTCTGGCTGCAGGAACG
ABCA5	F: TTATCATGCTCACACTTAATAGTA
	R: ATAAAGATGATCTCCGTAAGC
ABCA6	F: CTATAAGCTGCCCGTGGCAGAC
	R: GTGCACTGAGAAAGGCTGTATTCTTCC

ABCA7	F: CTGTATGGCTGGTCGATCACAC
	R: TTTATGCAGGTGAGCACCACATAG
ABCA8	F: TCTTCGGGATTCAGCGTTCT
	R: AACAAGTGCCAAGAAAAGGGC
ABCA9	F: TGCCCTCAGGAGAATGCGCTGT
	R: TAACCGTGTGATGGCGATCATTGCGTC
ABCA10	F: ATGTCCACCCTCTATCTCGGGC
	R: CTGCTCCAAGGTAGCCTGAGAGA
ABCA12	F: ATGGTATGATCCAGAAGGCTATCACTCC
	R: TACATGATGATGCCATGTCGGGC
ABCA13	F: CAATAATGAAGGAGGTTCGGGAA
	R: CATTTGAAGCTGCCGTTAACC
ABCB1	F: AAAGCGACTGAATGTTCAGTGGCTCCGAG
	R: ACCCGGCTGTTGTCTCCATAGGCAA
ABCB2	F: ATCCTGGATGATGCCACCAGT
	R: GAGAAGCACTGAGCGGGAGTA
ABCB3	F: CCTCAGCGCTGAAGCAGAAGTC
	R: ACAGTAAAGCCGCGTCCACCA
ABCB4	F: AGGCGGCAAAGAACGGAACAG
	R: AATACTCCAATCATTTTCACTGTCTTCGT
ABCB5	F: GCAAGGGAAGCAAATGCGTA
	R: TGCGATCCTCTGTTTCTGCC
ABCB6	F: GCTCTGGCTGCATCCGAATA
	R: TTGGGGCACAACTCCAATGT
ABCB7	F: ATCCGGCCTTTAGTCTCTGTTAGCGG
	R: CTCTGGAATCTGCTGGTAGGCTCGAG
ABCB8	F: GTGCATTTATTTCGGGTCGGG
	R: CTGCGGTAGCCATCAGAGTA
ABCB9	F: GCCTCCTTCTTCCTCATCGTG
	R: TTTCTGGATGACGATGCCATCAA
ABCB10	F: ATCATTGCTGTAATTTATGGGCG
	R: ATTTCCAATACGTTCCTCAGCTA
ABCB11	F: GCTACCAGGATAGTTTAAGGGCTTC
	R: GATCTACAACAGCTAATGGAGGTTCG
ABCC1	F: TCTCAGATCGCTCACCCCTGTTCTCG
	R: CTGTGATCCACCAGAAGGTGATCCTCGAC
ABCC2	F: TTGTGAACAGGTTTGCCGGCGATA
	R: TGGCCATGCAGATCATGACAAGGG
ABCC3	F: GGAGAAGGACCTCTGGTCCCTAAAGGAA
	R: CCTTGTGTCGTGCCGTCTGCTTTTC
ABCC4	F: CAAGATGCTGCCCGTGTACCA
	R: AATTTTAAACAAGGGATTGAGCCACCAGA
ABCC5	F: ATCATCCCCAGTCCTGGGTATAG

	R: CAAGGCATCTTGGCATTCCAAC
ABCC6	F: ACAAGTGTGCTGACCGAGGCGA
	R: ATGAGGATCTGGGTCTTCCGGAGAAGG
ABCC7	F: ACTGGTGCATACTCTAATCACAG
	R: TATTAAGAATCCCACCTGCTTTCA
ABCC8	F: TTCATCCAGAAGTACTTCCGGG
	R: TGAGTCCTTCTACGGTTTCGG
ABCC9	F: ATGATTGTGGGCCAAGTAGGA
	R: TTACATTGCTCCAGTGAACTTTTCC
ABCC10	F: GGGAGAAGGGTGTCACCCTTAG
	R: CCAGAGGGTCATCGAGGAGATAGA
ABCC11	F: TGGATCGTCAGCGGGAACATC
	R: CAGAAGTTCCAGGTCCCGATTCAG
ABCC12	F: TCCTTTGCAGAAAGATATGACCC
	R: GAAAATGTGGCGAAGGAGAGTA
ABCC13	F: ATCAAGAAACCATCTCTACTCTATGC
	R: CTTCATTATGAGTGGGCTAGTGAA
ABCD1	F: CCAGCGCATGTTCTACATCCCGCAGAG
	R: CTTTGCATGTCCTCCACTGAGTCCGGGTA
ABCD2	F: AAATGTTCCCATAATTACACCAGCAGG
	R: AAGAGAGAACTTTTCCCACAACCATTG
ABCD3	F: CTTCAGCAAGTACTTGACGGCGCGAAAC
	R: GGTTTTCCACTTTTCTTACCGTGCAGGCC
ABCD4	F: GAAGTCACAGGACTGCGAGA
	R: GAGATGGAGACCCGCTCAAG
ABCE1	F: TAGGACCACGCTCGACGTCGGAGAAAAG
	R: TTGTTCAACGCCGTTGGCGAAGCC
ABCF1	F: AATGCAGACCTGTACATTGTAGCCGGCCG
	R: GATGCTCAGGGCTCGGTTGGCAATGTG
ABCF2	F: AATTGACCTTGACACACGAGTGGCTC
	R: TTTCGGATCATGCCATCTGTGGGTAGTA
ABCF3	F: TTCGCTACAATGCCAACAGG
	R: TTCCTTGTCCACAGGCTTCAG
ABCG1	F: GAAGGTGTCCTGCTACATCATGC
	R: AAGCTTCAGATGTGCCGACAC
ABCG2	F: TCGTTATTAGATGTCTTAGCTGCAA
	R: TTGTACCACGTAACCTGAATTACA
ABCG4	F: CTGGTACAGCCTCAAAGCGT
	R: GCCCGTCATCCAGTACACAA
ABCG5	F: TGCTTCTCCTACGTCCTGCAGA
	R: CTTCTGGAAGGAGCCGGGATTG
ABCG8	F: AGAGGAGAGAGGGCTGCCGAAA
	R: AGGTGAAGTACAGGCTGTTGTCACTTTCA

Iron metabolism-related genes	
ACO1	F: TGCCATTACTAGCTGCACAAACA
	R: GACAGGCTAGTTTTGATGTAAGGCA
CYBRD1	F: AGTGATTGCAACAGCACTTATGGG
	R: AGGATCAGAAGGCCAAGCGTA
EPAS1	F: CGCCATCATCTCTCTGGATTTCGGGAATC
	R: TCTGGGTGCTGTGGCTCCTCAA
GLRX5	F: AAGAAGGACAAGGTGGTGGTCTTCCTCAA
	R: TTGTAGGCCGCGTAATCGCGGA
HEPH	F: GTGCATGCTCATGGAGTGCTA
	R: CCAGACCTCTCTGGGATGTTC
HFE	F: AAGGAAGAGGCAGGGTTCAAGA
	R: TTTGTCTCCTTCCCACAGTGAGT
IREB2	F: AAATGACAGTTCACATAAGAAGTTCTTCG
	R: AGCTTCCAACAAGACCCGTAT
QSOX1	F: AGTCCCATCATGACACGTGGC
	R: GCCAGGTACTCTTCGTTATTTCTCGC
SLC11A2	F: TGCACCATGAGGAAGAAGCA
	R: GGTGGATACCTGAGTGGCTG
SLC39A14	F: ACTTCATCGCCCTGTCCATT
	R: GGTCCTTCTTGGAGGGAAGC
SLC40A1	F: CTACTGCAATCACAATCCAAAGGGA
	R: GGCTAAGATGTTGGTTAACTGGTCAA
TFRC	F: GACGCGCTAGTGTTCTTCTGTGTGGC
	R: CGAGCCAGGCTGAACCGGGTATATGA